Searches for Charged-Lepton Flavor Violation Experimental Status and Prospects

Doug Glenzinski
Fermilab
May 2016

Outline

- Introduction
- Searches using muons
- Searches using taus
- Comparisons with collider searches
- Summary

Introduction

Rare decays can be incisive probes of underlying physics

- $K^0 \rightarrow \mu^+\mu^-$, $K \rightarrow \pi\nu\nu$
- $B^0 \rightarrow \mu^+\mu^-$, $B \rightarrow s\gamma$
- $\mu^+ \rightarrow e^+\gamma$, $\mu^+ \rightarrow e^+e^+e^-$, $\mu^-N \rightarrow e^-N$
- $\tau \rightarrow e\gamma$, $\tau \rightarrow \mu\gamma$, $\tau \rightarrow eee$, $\tau \rightarrow \mu\mu\mu$, $\tau \rightarrow e\mu\mu$,…

Introduction

Rare decays can be incisive probes of underlying physics

- $K^0 \rightarrow \mu^+\mu^-$, $K \rightarrow \pi\nu\nu$
- $B^0 \rightarrow \mu^+\mu^-$, $B \rightarrow s\gamma$
- $\mu^+ \rightarrow e^+\gamma$, $\mu^+ \rightarrow e^+e^+e^-$, $\mu^-N \rightarrow e^-N$
- $\tau \rightarrow e\gamma$, $\tau \rightarrow \mu\gamma$, $\tau \rightarrow eee$, $\tau \rightarrow \mu\mu\mu$, $\tau \rightarrow e\mu\mu$,…

Observations and Limits *both* provide important information

Introduction

Rare decays can be incisive probes of underlying physics

- $K^0 \rightarrow \mu^+\mu^-$, $K \rightarrow \pi\nu\nu$
- $B^0 \rightarrow \mu^+\mu^-$, $B \rightarrow s\gamma$
- $\mu^+ \rightarrow e^+\gamma$, $\mu^+ \rightarrow e^+e^+e^-$, $\mu^-N \rightarrow e^-N$
- $\tau \rightarrow e\gamma$, $\tau \rightarrow \mu\gamma$, $\tau \rightarrow eee$, $\tau \rightarrow \mu\mu\mu$, $\tau \rightarrow e\mu\mu$,…

Focus of this talk
Charged-Lepton Flavor Violation (cLFV)

Why cLFV?

- Quarks mix, ν mix… what about l^+?
- Hints that something may be awry ($h \rightarrow \tau\mu$, $B \rightarrow D\tau\nu / D\mu\nu$, $B \rightarrow K\mu\mu / Kee$, …)
- cLFV offers opportunity to probe Λ_{NP} ~ O(10^3 -10^4) TeV >> TeV

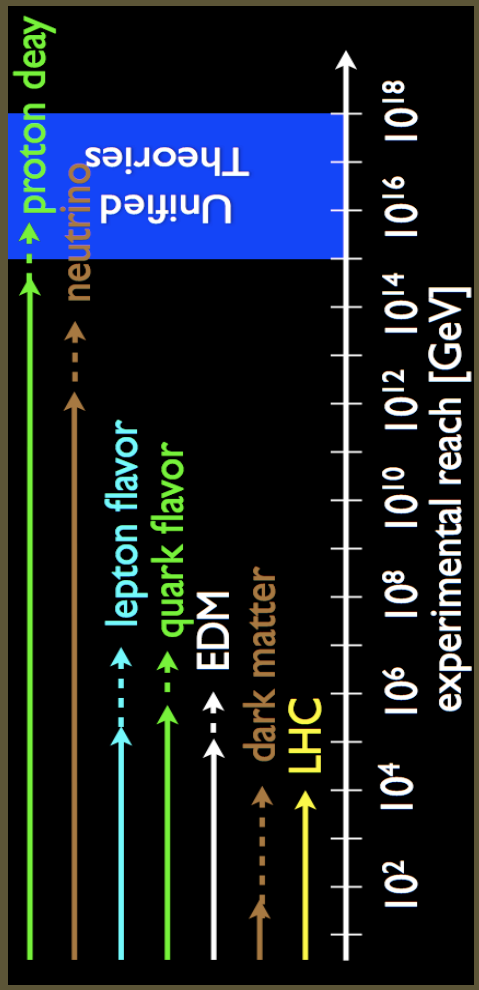

Some cLFV Processes

Process	Current Limit	Next Generation exp
$\tau \rightarrow \mu\eta$	BR < 6.5 E-8	
$\tau \rightarrow \mu\gamma$	BR < 6.8 E-8	10^{-9} - 10^{-10} (Belle II, LHCb)
$\tau \rightarrow \mu\mu\mu$	BR < 3.2 E-8	
$\tau \rightarrow eee$	BR < 3.6 E-8	
$K_L \rightarrow e\mu$	BR < 4.7 E-12	
$K^+ \rightarrow \pi^+ e^- \mu^+$	BR < 1.3 E-11	
$B^0 \rightarrow e\mu$	BR < 7.8 E-8	
$B^+ \rightarrow K^+ e\mu$	BR < 9.1 E-8	
$\mu^+ \rightarrow e^+\gamma$	BR < 5.7 E-13	10^{-14} (MEG)
$\mu^+ \rightarrow e^+e^+e^-$	BR < 1.0 E-12	10^{-16} (PSI)
$\mu^- N \rightarrow e^- N$	$R_{\mu e}$ < 7.0 E-13	10^{-17} (Mu2e, COMET)

(current limits from the PDG)

- Expect significant progress in near future in μ, τ

cLFV in the ν-Standard Model

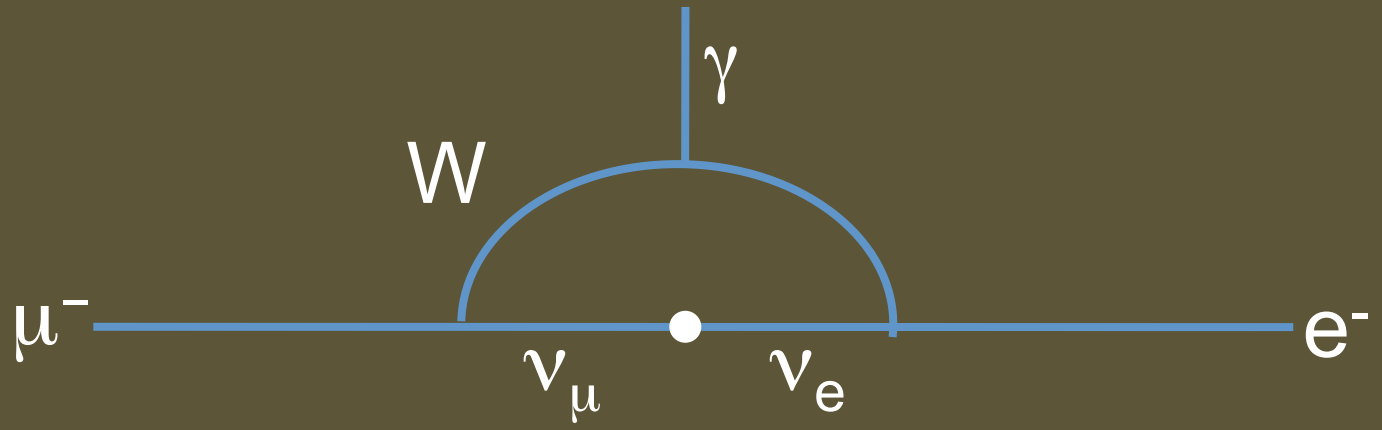

- Extremely suppressed
  (rate ~ $\Delta m_\nu^4 / M_w^4 < 10^{-50}$)
- Many NP models predict rates observable at next generation cLFV experiments
- Observation is unambiguously BSM NP

NP Contributions to cLFV

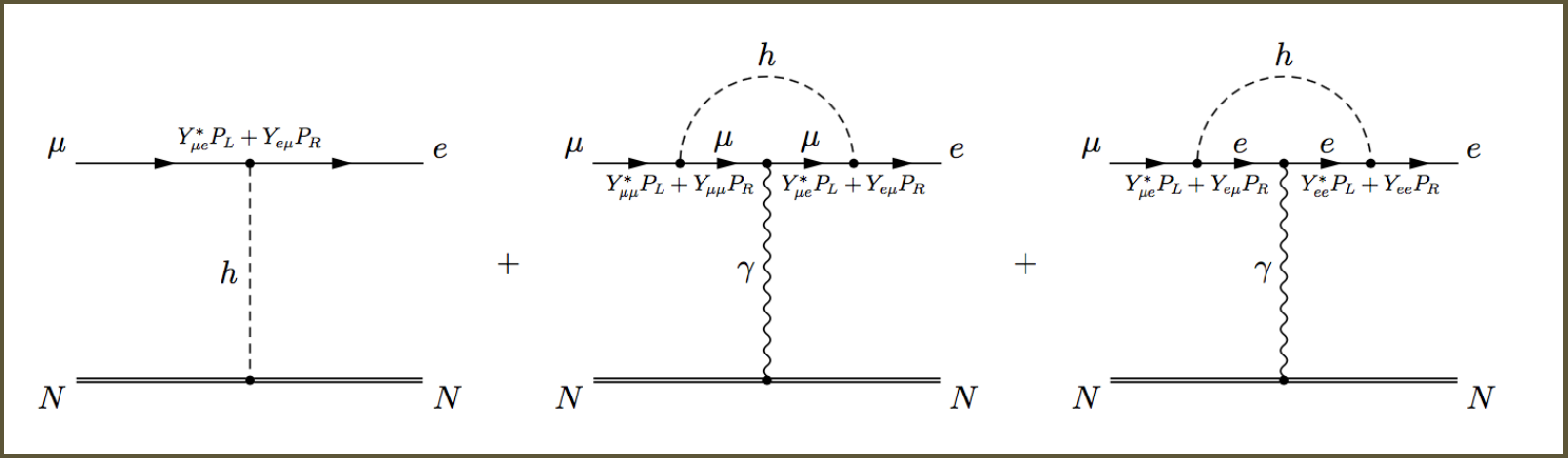

- As has been discussed, LFV higgs couplings will contribute

NP Contributions to cLFV

Loops

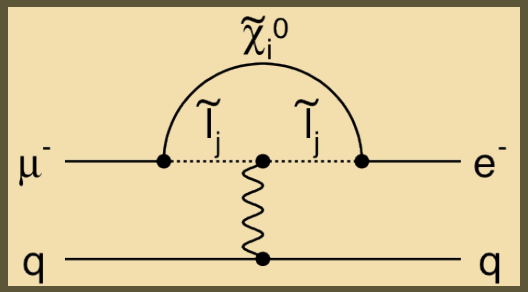

Supersymmetry

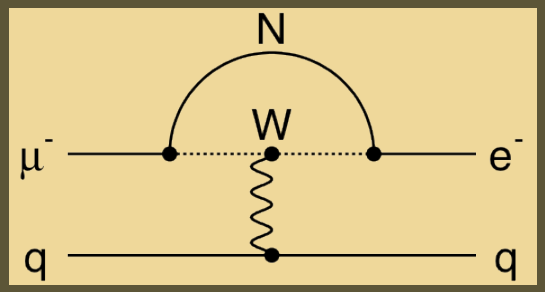

Heavy Neutrinos

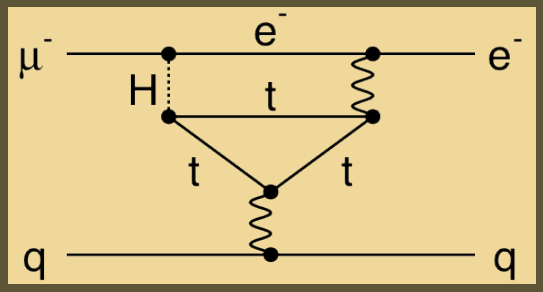

Two Higgs Doublets

Contact Terms

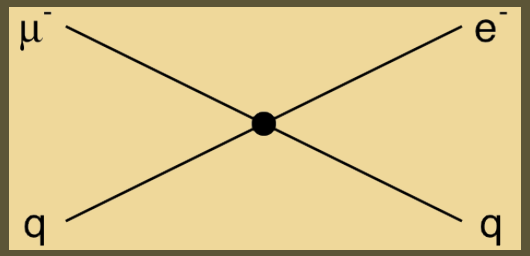

Compositeness

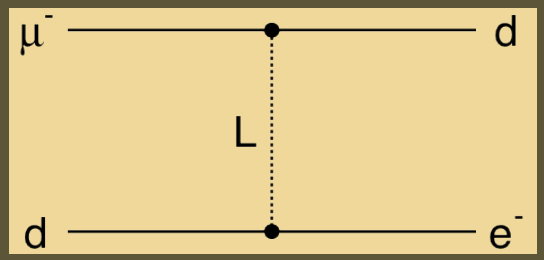

Leptoquarks

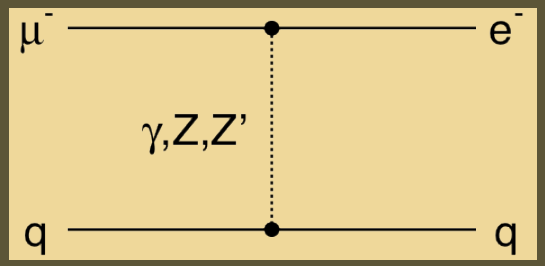

New Heavy Bosons / Anomalous Couplings

Sensitive to broad array of NP: SUSY, 2HDM, LQ, LHT, ED, …

cLFV Predictions

$\mu^+ \rightarrow e^+\gamma$ $\mu^-N \rightarrow e^-N$ $\mu^+ \rightarrow e^+e^+e^-$

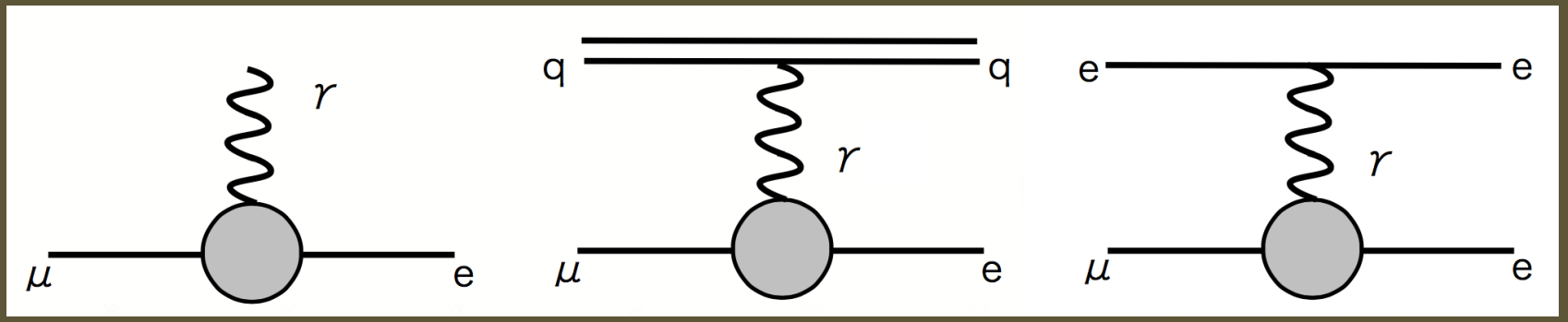

cLFV rates and ratios are sensitive probes of underlying model

cLFV Predictions

$\mu^+ \rightarrow e^+\gamma$ $\mu^-N \rightarrow e^-N$ $\mu^+ \rightarrow e^+e^+e^-$

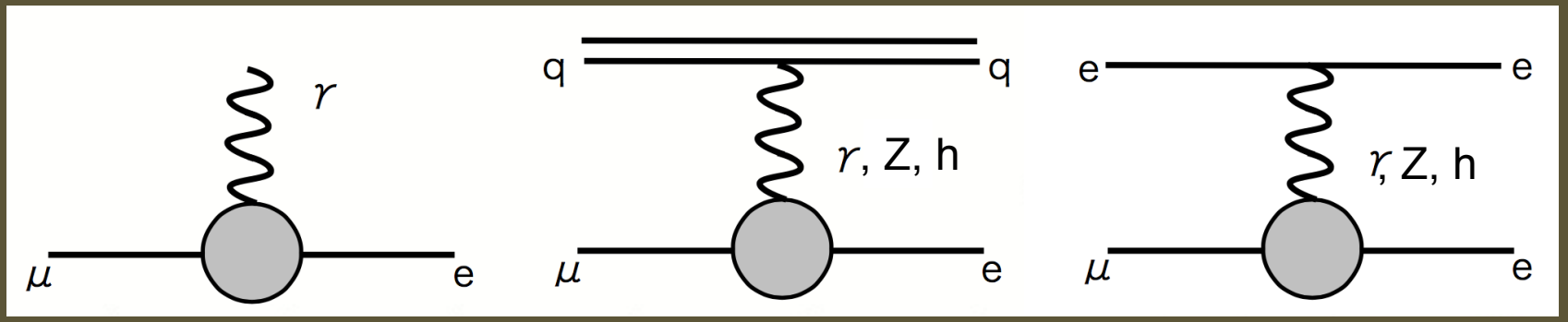

cLFV rates and ratios are sensitive probes of underlying model

cLFV Predictions

$\mu^+ \rightarrow e^+\gamma$ $\mu^-N \rightarrow e^-N$ $\mu^+ \rightarrow e^+e^+e^-$

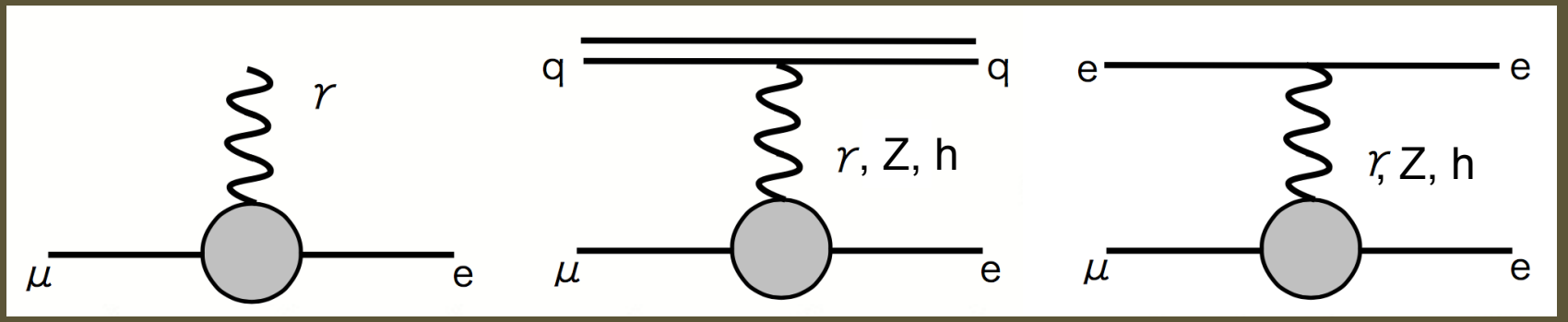

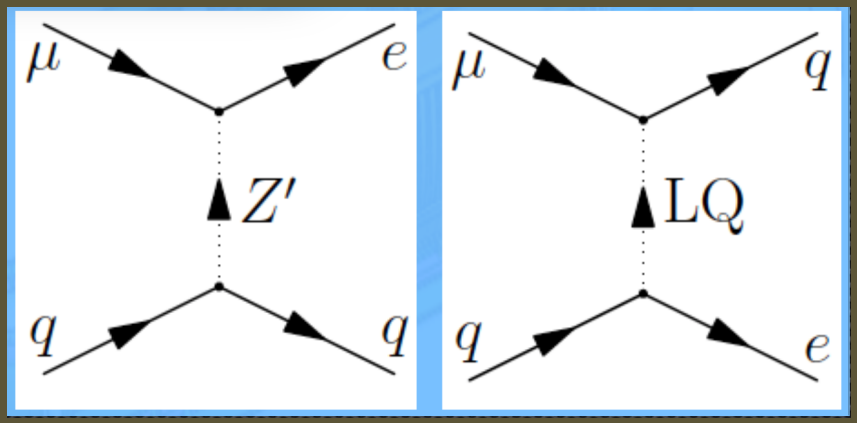

cLFV rates and ratios are sensitive probes of underlying model

cLFV Sensitivity

★★★ = Discovery Sensitivity

W. Altmannshofer, A.J.Buras, S.Gori, P.Paradisi, D.M.Straub

arXiv:0909.1333[hep-ph]

	AC	RVV2	AKM	δLL	FBMSSM	LHT	RS
$D^0 - \bar{D}^0$	★★★	★	★	★	★	★★★	?
ϵ_K	★	★★★	★★★	★	★	★★	★★★
$S_{\psi\phi}$	★★★	★★★	★★★	★	★	★★★	★★★
$S_{\phi K_S}$	★★★	★★	★	★★★	★★★	★	?
$A_{\rm CP}\,(B \to X_s\gamma)$	★	★	★	★★★	★★★	★	?
$A_{7,8}(B \to K^*\mu^+\mu^-)$	★	★	★	★★★	★★★	★★	?
$A_9(B \to K^*\mu^+\mu^-)$	★	★	★	★	★	★	?
$B \to K^{(*)}\nu\bar{\nu}$	★	★	★	★	★	★	★
$B_s \to \mu^+\mu^-$	★★★	★★★	★★★	★★★	★★★	★	★
$K^+ \to \pi^+\nu\bar{\nu}$	★	★	★	★	★	★★★	★★★
$K_L \to \pi^0\nu\bar{\nu}$	★	★	★	★	★	★★★	★★★
$\mu \to e\gamma$	★★★	★★★	★★★	★★★	★★★	★★★	★★★
$\tau \to \mu\gamma$	★★★	★★★	★	★★★	★★★	★★★	★★★
$\mu + N \to e + N$	★★★	★★★	★★★	★★★	★★★	★★★	★★★
d_n	★★★	★★★	★★★	★★	★★★	★	★★★
d_e	★★★	★★★	★★	★	★★★	★	★★★
$(g-2)_\mu$	★★★	★★★	★★	★★★	★★★	★	?

Table 8: "DNA" of flavour physics effects for the most interesting observables in a selection of SUSY and non-SUSY models ★★★ signals large effects, ★★ visible but small effects and ★ implies that the given model does not predict sizable effects in that observable.

cLFV Sensitivity

★★★ = Discovery Sensitivity

W. Altmannshofer, A.J.Buras, S.Gori, P.Paradisi, D.M.Straub

	AC	RVV2	AKM	δLL	FBMSSM	LHT	RS
$D^0 - \bar{D}^0$	★★★	★	★	★	★	★★★	?
ϵ_K	★	★★★	★★★	★	★	★★	★★★
$S_{\psi\phi}$	★★★	★★★	★★★	★	★	★★★	★★★
$S_{\phi K_S}$	★★★	★★	★	★★★	★★★	★	?
$A_{\rm CP}(B \to X_s\gamma)$	★	★	★	★★★	★★★	★	?
$A_{7,8}(B \to K^*\mu^+\mu^-)$	★	★	★	★★★	★★★	★★	?
$A_9(B \to K^*\mu^+\mu^-)$	★	★	★	★	★	★	?
$B \to K^{(*)}\nu\bar{\nu}$	★	★	★	★	★	★	★
$B_s \to \mu^+\mu^-$	★★★	★★★	★★★	★★★	★★★	★	★
$K^+ \to \pi^+\nu\bar{\nu}$	★	★	★	★	★	★★★	★★★
$K_L \to \pi^0\nu\bar{\nu}$	★	★	★	★	★	★★★	★★★
$\mu \to e\gamma$	★★★	★★★	★★★	★★★	★★★	★★★	★★★
$\tau \to \mu\gamma$	★★★	★★★	★	★★★	★★★	★★★	★★★
$\mu + N \to e + N$	★★★	★★★	★★★	★★★	★★★	★★★	★★★
d_n	★★★	★★★	★★★	★★	★★★	★	★★★
d_e	★★★	★★★	★★	★	★★★	★	★★★
$(g-2)_\mu$	★★★	★★★	★★	★★★	★★★	★	?

Table 8: "DNA" of flavour physics effects for the most interesting observables in a selection of SUSY and non-SUSY models ★★★ signals large effects, ★★ visible but small effects and ★ implies that the given model does not predict sizable effects in that observable.

arXiv:0909.1333[hep-ph]

- The sensitivity of these experiments is **relevant and compelling**

Using cLFV to Determine NP

Can use ratio of rates to determine dominant operator contribution

- multiple ratios can determine multiple operators and the ratio of their couplings

e.g. ($\mu \rightarrow e\gamma$) / ($\mu N \rightarrow eN$)

e.g. $\mu N \rightarrow eN$ with different nuclei

- Also information in angular distributions
  - $\mu \rightarrow e\gamma$, eee, τ chnls

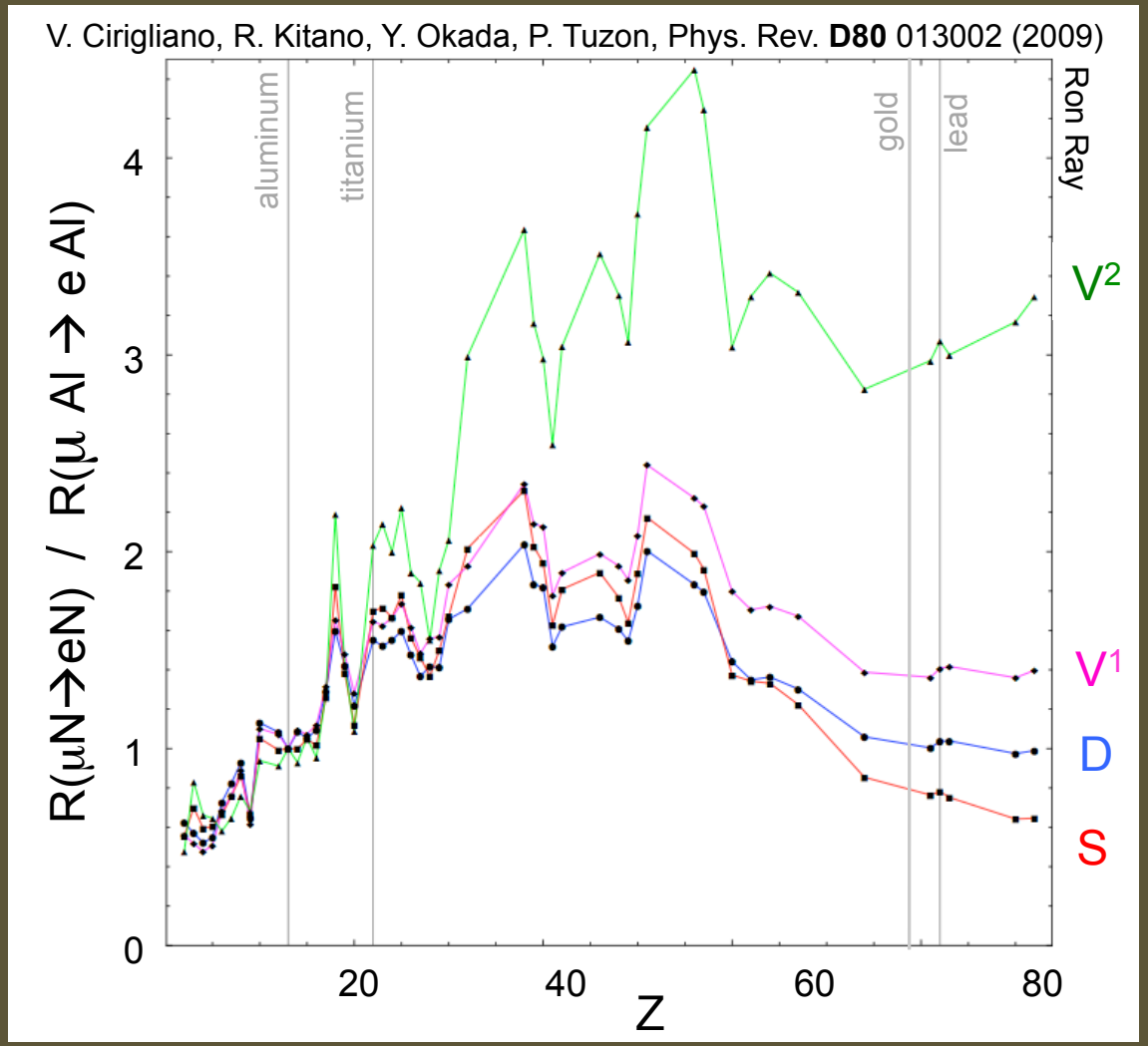

Using cLFV to Determine NP

M.Blanke, A.J.Buras, B.Duling, S.Recksiegel, C.Tarantino

arXiv:0909.5454v2[hep-ph]

ratio	LHT	MSSM (dipole)	MSSM (Higgs)
$\frac{Br(\mu^-\to e^-e^+e^-)}{Br(\mu\to e\gamma)}$	$0.02\ldots1$	$\sim 6\cdot10^{-3}$	$\sim 6\cdot10^{-3}$
$\frac{Br(\tau^-\to e^-e^+e^-)}{Br(\tau\to e\gamma)}$	$0.04\ldots0.4$	$\sim 1\cdot10^{-2}$	$\sim 1\cdot10^{-2}$
$\frac{Br(\tau^-\to \mu^-\mu^+\mu^-)}{Br(\tau\to \mu\gamma)}$	$0.04\ldots0.4$	$\sim 2\cdot10^{-3}$	$0.06\ldots0.1$
$\frac{Br(\tau^-\to e^-\mu^+\mu^-)}{Br(\tau\to e\gamma)}$	$0.04\ldots0.3$	$\sim 2\cdot10^{-3}$	$0.02\ldots0.04$
$\frac{Br(\tau^-\to \mu^-e^+e^-)}{Br(\tau\to \mu\gamma)}$	$0.04\ldots0.3$	$\sim 1\cdot10^{-2}$	$\sim 1\cdot10^{-2}$
$\frac{Br(\tau^-\to e^-e^+e^-)}{Br(\tau^-\to e^-\mu^+\mu^-)}$	$0.8\ldots2.0$	~ 5	$0.3\ldots0.5$
$\frac{Br(\tau^-\to \mu^-\mu^+\mu^-)}{Br(\tau^-\to \mu^-e^+e^-)}$	$0.7\ldots1.6$	~ 0.2	$5\ldots10$
$\frac{R(\mu\mathrm{Ti}\to e\mathrm{Ti})}{Br(\mu\to e\gamma)}$	$10^{-3}\ldots10^{2}$	$\sim 5\cdot10^{-3}$	$0.08\ldots0.15$

Table 3: *Comparison of various ratios of branching ratios in the LHT model ($f = 1$ TeV) and in the MSSM without [92, 93] and with [96, 97] significant Higgs contributions.*

- Relative rates model dependent
- Measure >1 to pin-down theory details

cLFV using muons

cLFV Experiments using muons

	$\mu^+ \rightarrow e^+\gamma$	$\mu^-N \rightarrow e^-N$	$\mu^+ \rightarrow e^+e^+e^-$
	MEG (PSI)	Mu2e (FNAL) COMET (JPARC)	Mu3e (PSI)
Now:	4.2×10^{-13} *	6×10^{-13}	1×10^{-12}
Future:	4×10^{-14}	6×10^{-17}	1×10^{-14}
Timeframe:	2020	2023	2020

(@ 90% CL)

* Preliminary result using full data set, submitted for publication

Over the next 5-7y significant progress expected for these three processes

cLFV Experiments using muons

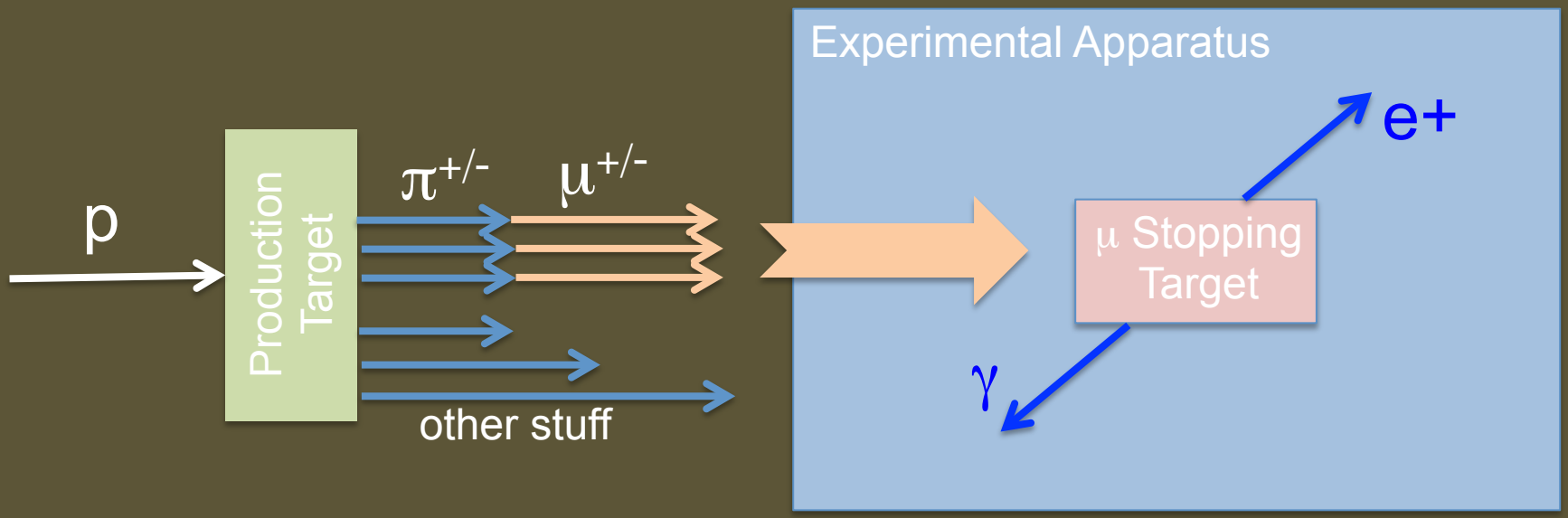

All 3 experiments use same basic principles

cLFV Experiments using muons

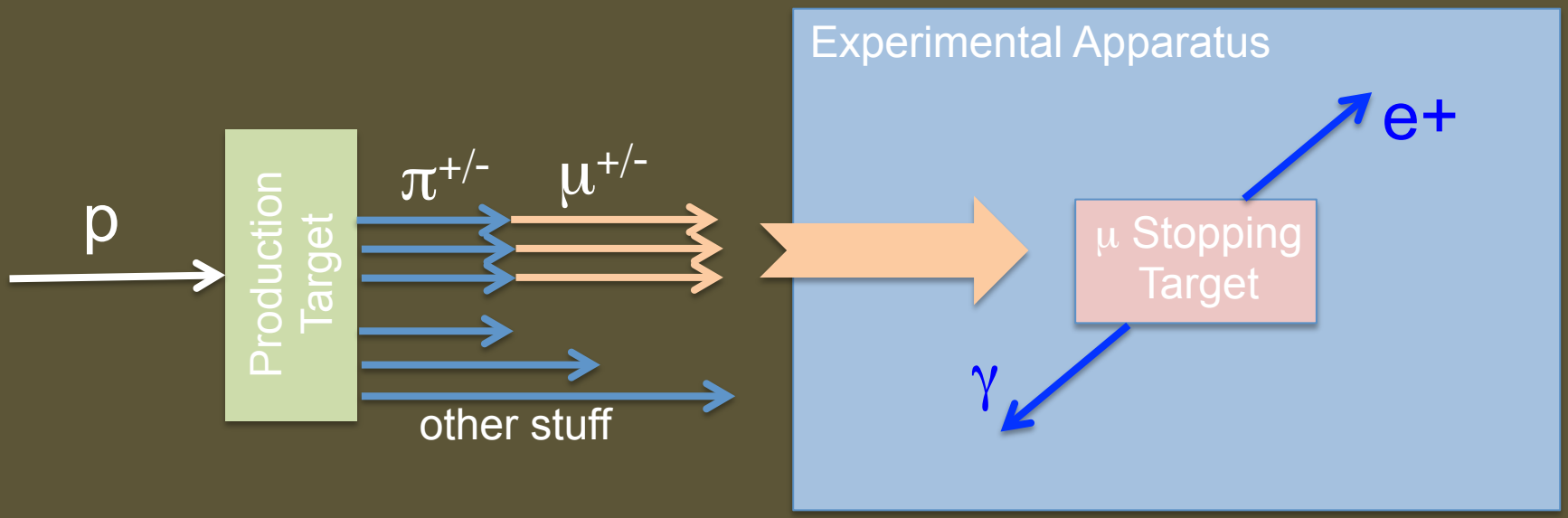

Require:

- High intensity, high purity μ source
- High μ stopping rate
- Detector to precisely measure particles consistent with having originated from stopping target

cLFV Experiments using muons

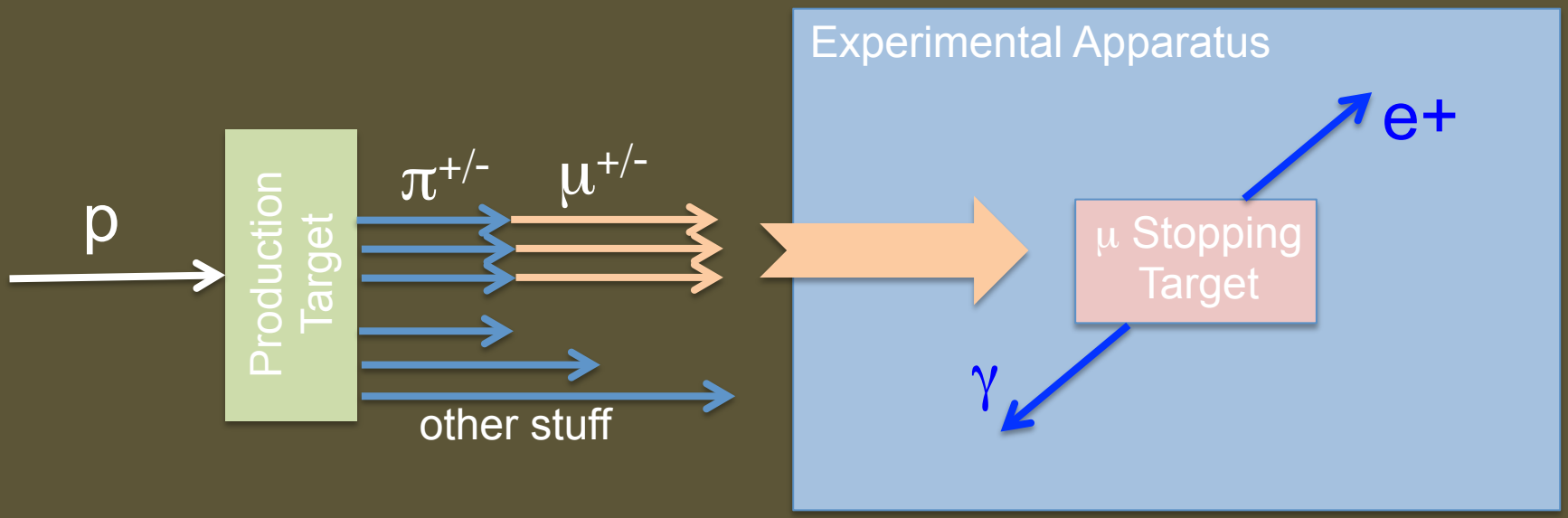

NB. In these experiments, 100 MeV/c is “high momentum”

	P (MeV/c)	E (MeV)	KE (MeV)
e :	100	100	100
μ :	100	145	40
π :	100	170	30
p :	100	1005	5

MEG Experiment ($\mu^+ \rightarrow e^+\gamma$)

Signal

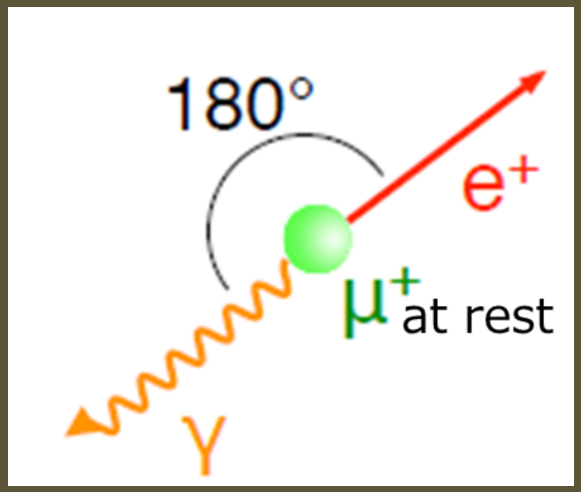

Back-to-back $e\gamma$

$E_e = E_\gamma = m_\mu/2$

Background

$\mu^+ \rightarrow e^+\nu\nu\gamma$
Radiative Muon Decay (RMD)

Accidentals (ACC)

MEG Experiment ($\mu^+ \rightarrow e^+\gamma$)

Signal

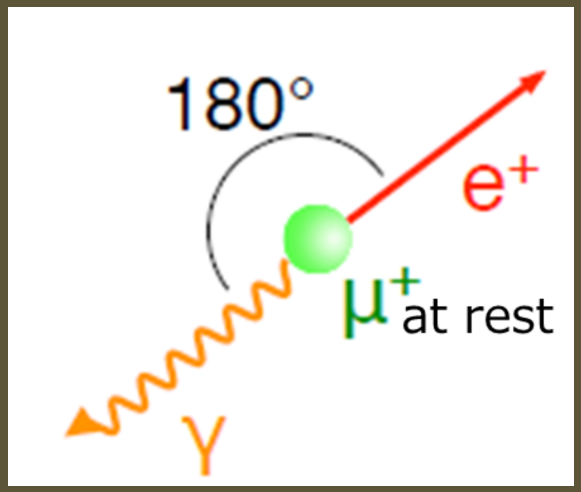

Background

$\mu^+ \rightarrow e^+\nu\nu\gamma$
Radiative Muon Decay (RMD)

Accidentals (ACC)

$$\mathcal{B}_{\text{Acc}} \propto \quad (\frac{R_\mu}{D})(\Delta t_{e\gamma})\frac{\Delta E_e}{m_\mu/2}\left(\frac{\Delta E_\gamma}{15m_\mu/2}\right)^2\left(\frac{\Delta\theta_{e\gamma}}{2}\right)^2$$

MEG beam

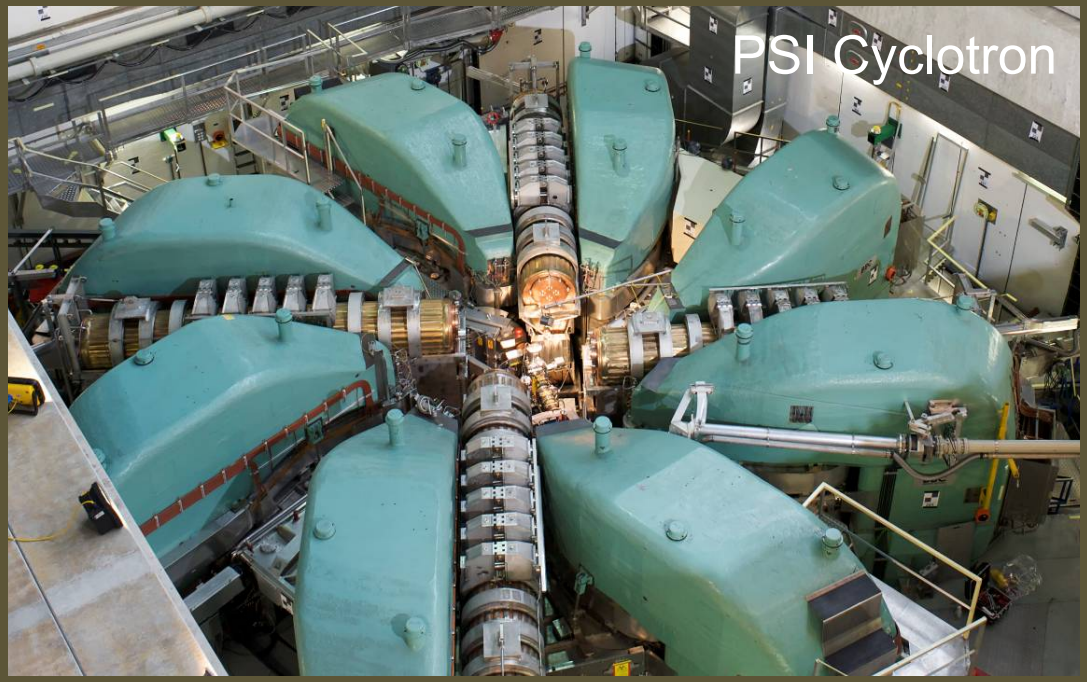

- 1.3 MW of 0.6 GeV protons
- “surface” muon beam, p_μ ~ 28 MeV/c
- MEG uses few 10^7 μ^+/s

MEG Detector

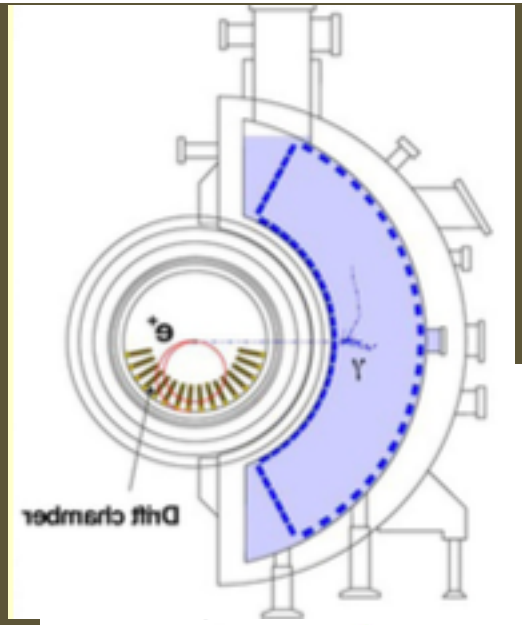

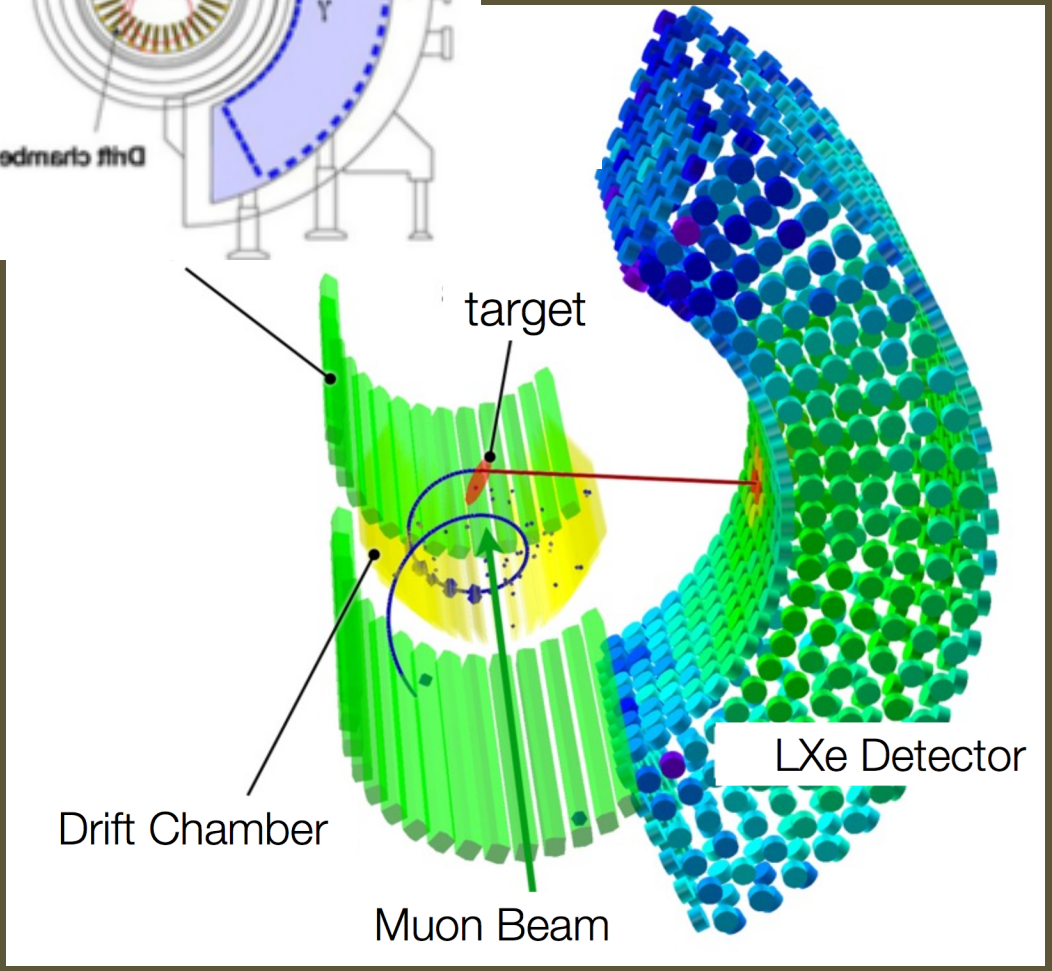

- Liquid Xe calorimeter
  - PMT readout
  - 11% of solid angle
- Drift Chamber (DC)
  - Radius : 19 - 28 cm
- Scintillator timing counters (TC)
- DC and TC inside graded solenoid field
- 205 μm polyethelene target

MEG Solenoid

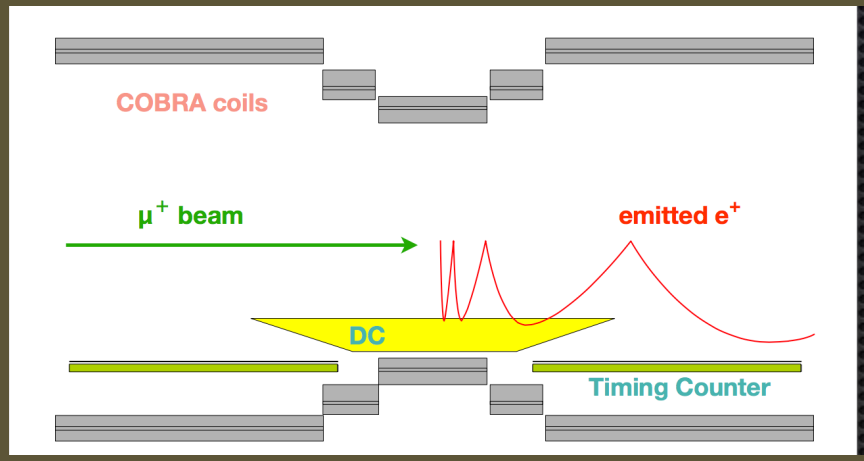

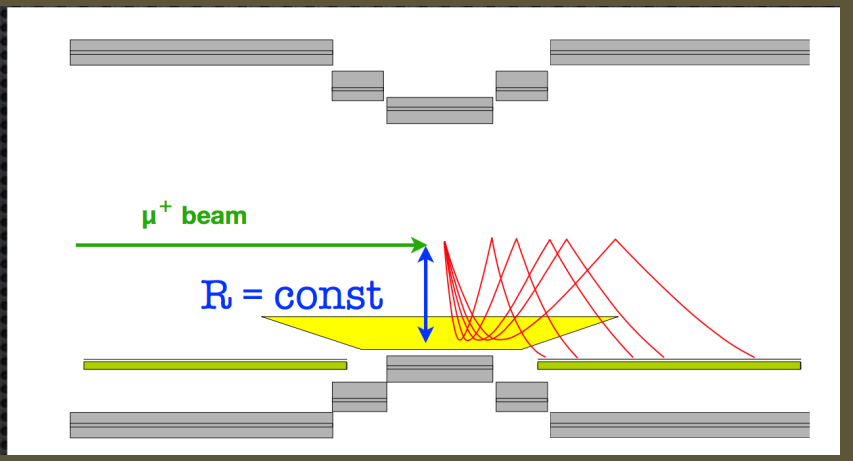

Sweeps e+ out of central region

Bending radius independent of pitch angle

COBRA = COnstant Bending Radius

- 1.3 T in central region
- 0.5 T in outer regions

MEG Analysis

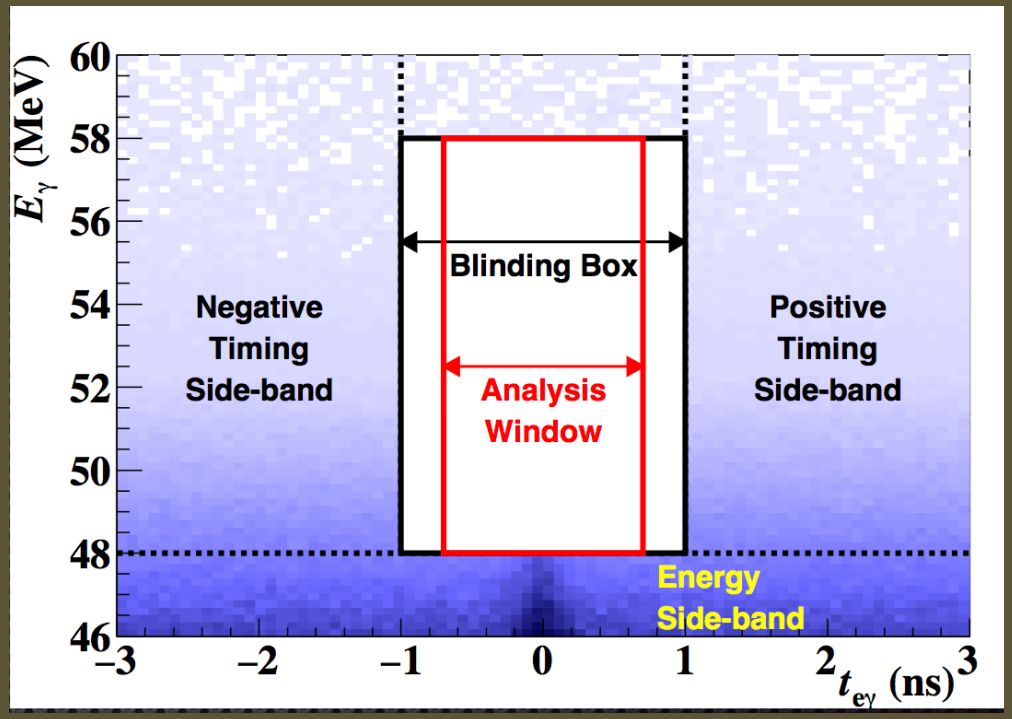

Utilizes 5 variables

- E_e, E_γ
- $t_{e\gamma} = t_e - t_\gamma$
- $\theta_{e\gamma}$
- $\phi_{e\gamma}$

Blind Analysis
Full Lhood fit to data

- Uses full data set (2009-2013)
  - ~7.5 x 10^{14} stopped μ^+

MEG Analysis

$$\mathcal{L}\left(N_{\rm sig}, N_{\rm RMD}, N_{\rm ACC}, \mathbf{t}\right) = \frac{e^{-N}}{N_{\rm obs}!} C(N_{\rm RMD}, N_{\rm ACC}, \mathbf{t}) \times \prod_{i=1}^{N_{\rm obs}} \left(N_{\rm sig} S(\mathbf{x}_i, \mathbf{t}) + N_{\rm RMD} R(\mathbf{x}_i) + N_{\rm ACC} A(\mathbf{x}_i)\right)$$

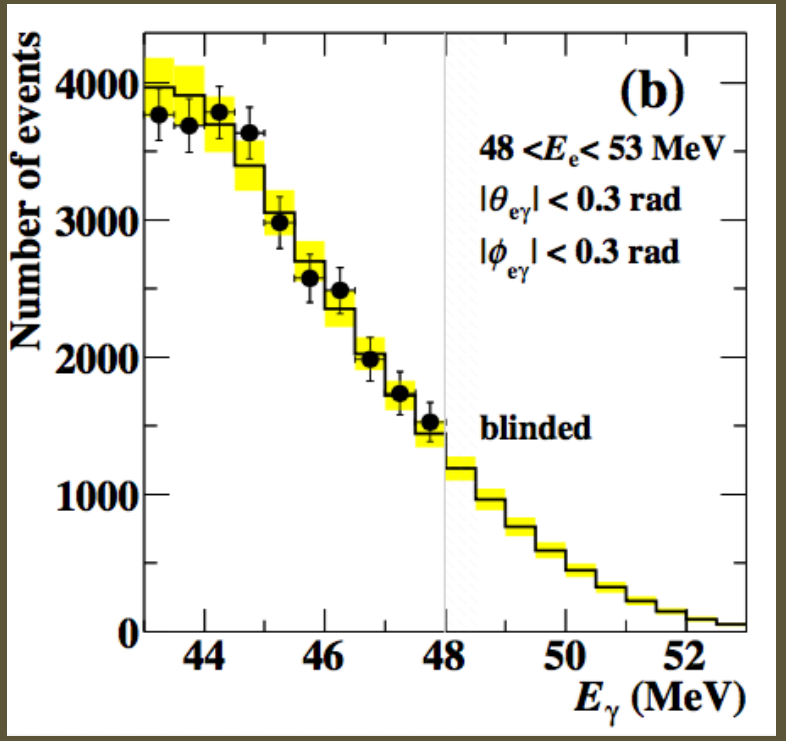

$x_i = (E_e , E_\gamma , t_{e\gamma} , \theta_{e\gamma} , \phi_{e\gamma})$

PDF_{ACC} : from sideband data

PDF_{SIG} & PDF_{RMD} : theory $\otimes$ resolution

MEG Calibrations

Table 1 The calibration tools of the MEG experiment.

Process		Energy	Main Purpose	Frequency
Cosmic rays	$\mu^{\pm}$ from atmospheric showers	Wide spectrum O(GeV)	LXe-DCH relative position	annually
			DCH alignment	
			TC energy and time offset calibration	
			LXe purity	on demand
Charge exchange	$\pi^- p \to \pi^0 n$ $\pi^0 \to \gamma\gamma$	55, 83, 129 MeV photons	LXe energy scale/resolution	annually
Radiative μ–decay	$\mu^+ \to e^+ \gamma\nu\bar{\nu}$	photons > 40 MeV,	LXe-TC relative timing	continuously
		positrons > 45 MeV	Normalisation	
Normal μ–decay	$\mu^+ \to e^+ \nu\bar{\nu}$	52.83 MeV end-point positrons	DCH energy scale/resolution	continuously
			DCH and target alignment	
			Normalisation	
Mott positrons	e^+ target $\to e^+$ target	$\approx$ 50 MeV positrons	DCH energy scale/resolution	annually
			DCH alignment	
Proton accelerator	^{7}Li(p, γ)^{8}Be	14.8, 17.6 MeV photons	LXe uniformity/purity	weekly
	^{11}B(p, γ)^{12}C	4.4, 11.6, 16.1 MeV photons	TC interbar/ LXe–TC timing	weekly
Neutron generator	^{58}Ni(n, γ)^{59}Ni	9 MeV photons	LXe energy scale	weekly
Radioactive source	^{241}Am(α, γ)^{237}Np	5.5 MeV α's, 56 keV photons	LXe PMT calibration/purity	weekly
Radioactive source	^{9}Be($\alpha_{^{241}\mathrm{Am}}$, n)^{12}C* ^{12}C$^\star(\gamma)^{12}$C	4.4 MeV photons	LXe energy scale	on demand
LED			LXe PMT calibration	continuously

from arXiv:1605.0508

Scale and resolutions determined with high degree of confidence

MEG Result : 2009-2013 data

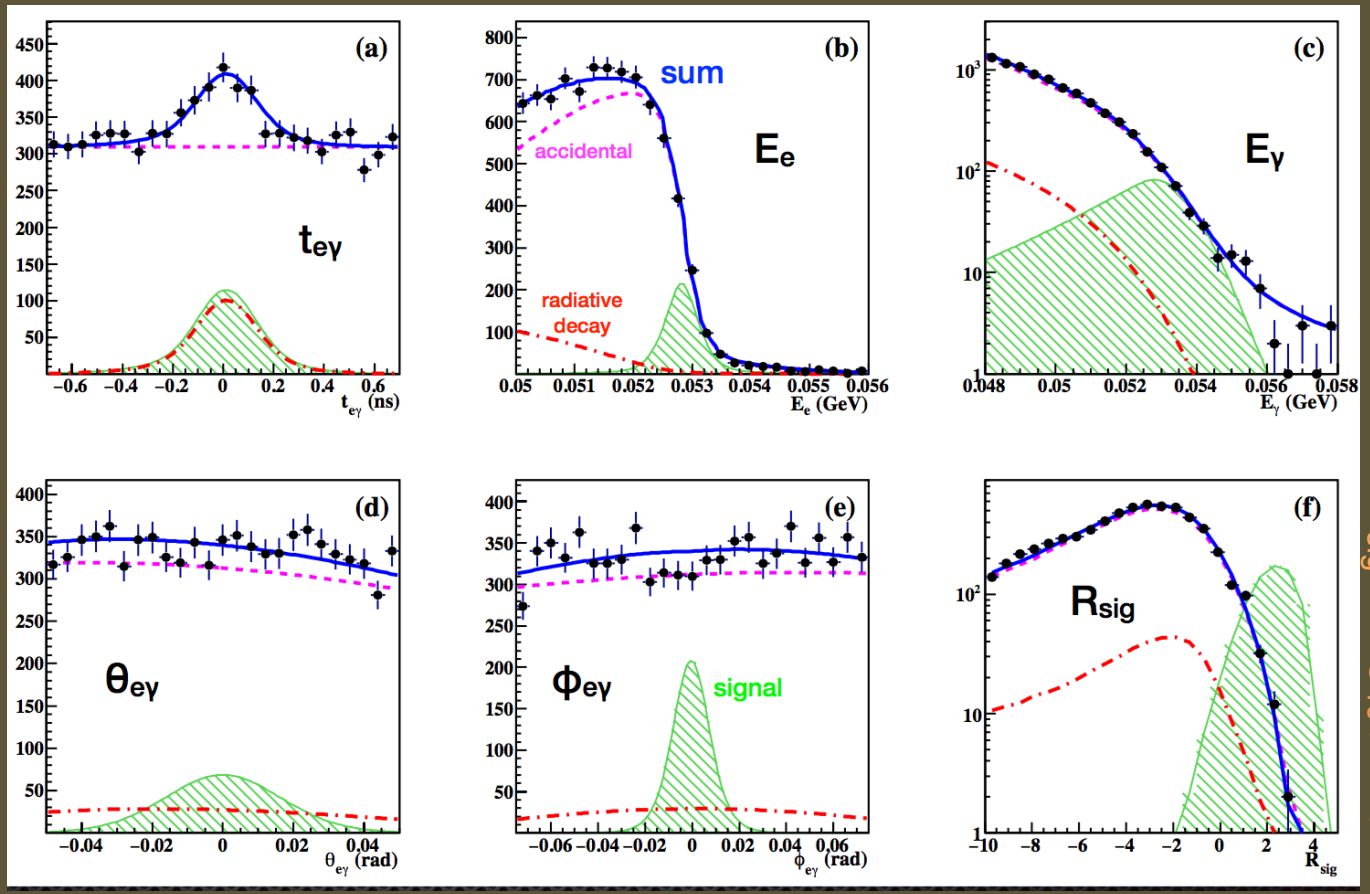

Best fit BR($\mu^+ \rightarrow e^+\gamma$) = -2.2×10^{-13}

BR($\mu^+ \rightarrow e^+\gamma$) < 4.2×10^{-13} @ 90% CL

(< 5.3×10^{-13} expected)

MEG-II Upgrade

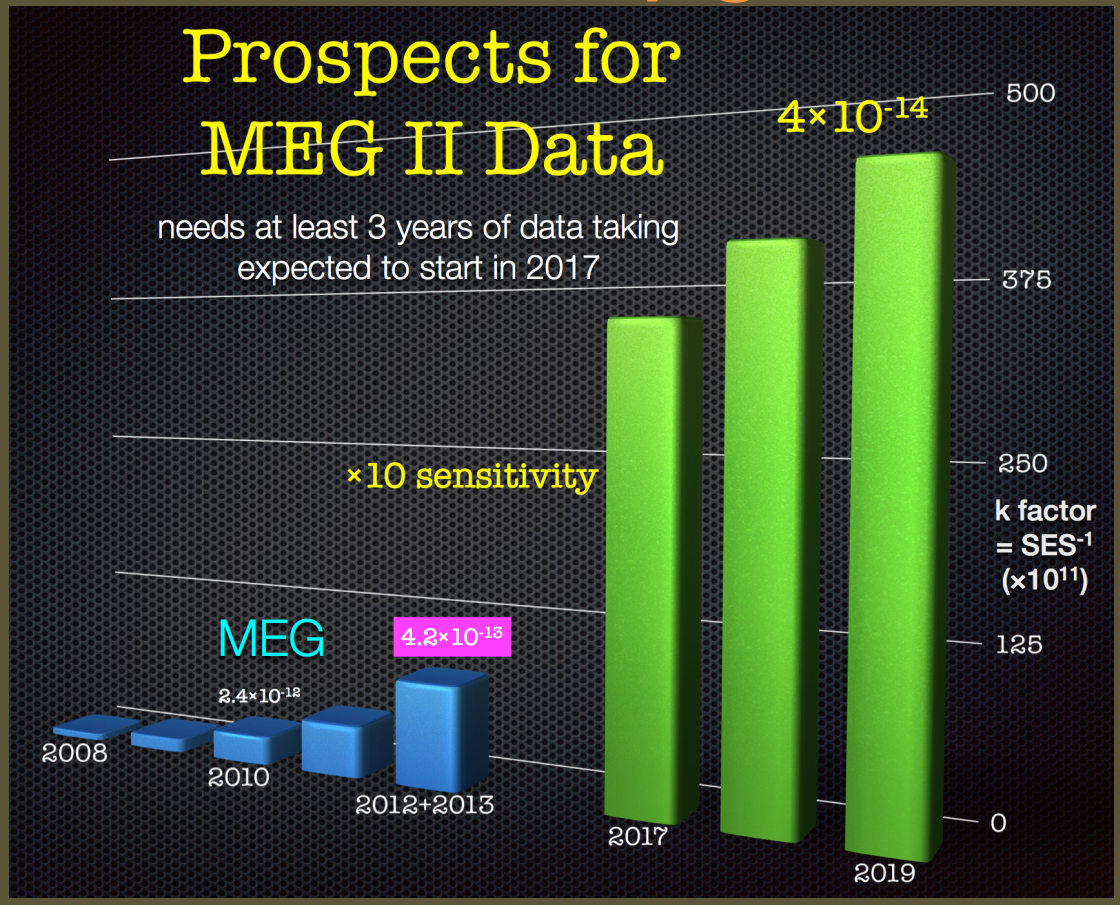

- Expect to begin 3y data taking in 2017
  - Aim to improve sensitivity by x10

MEG-II Upgrade

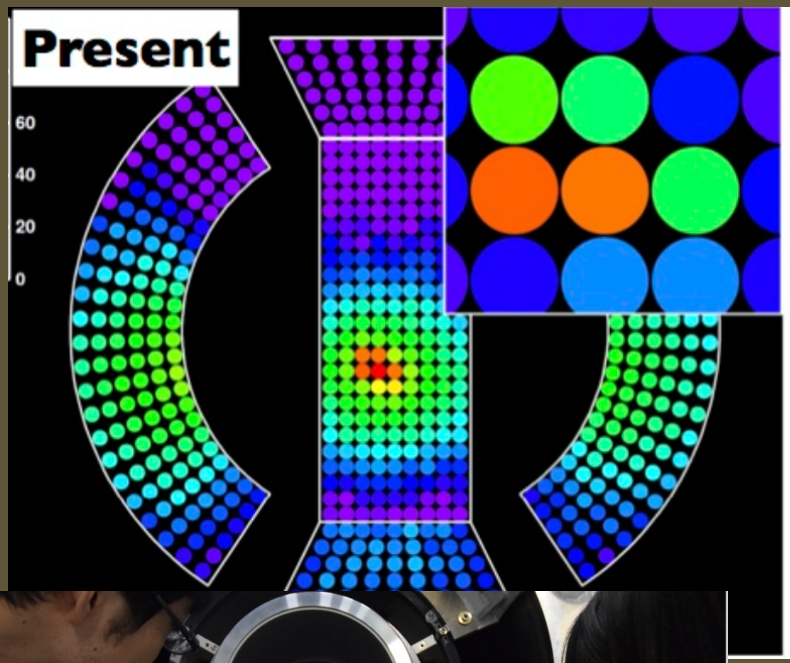

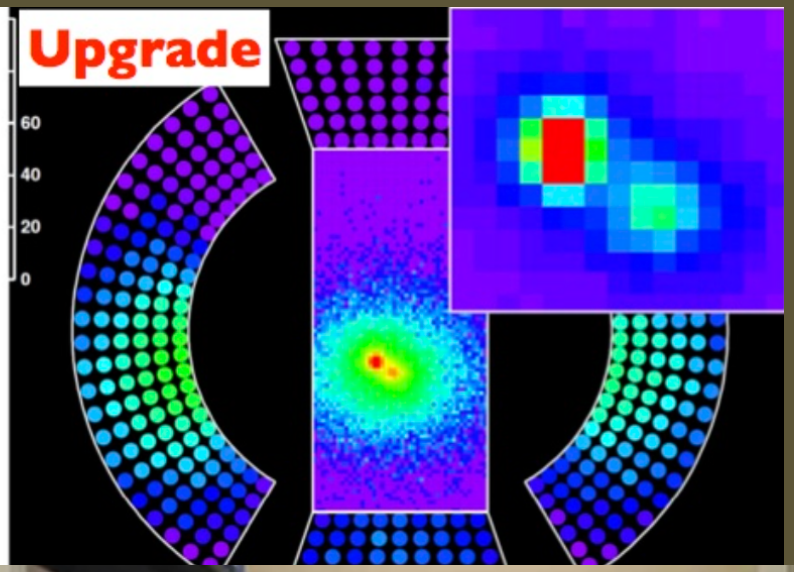

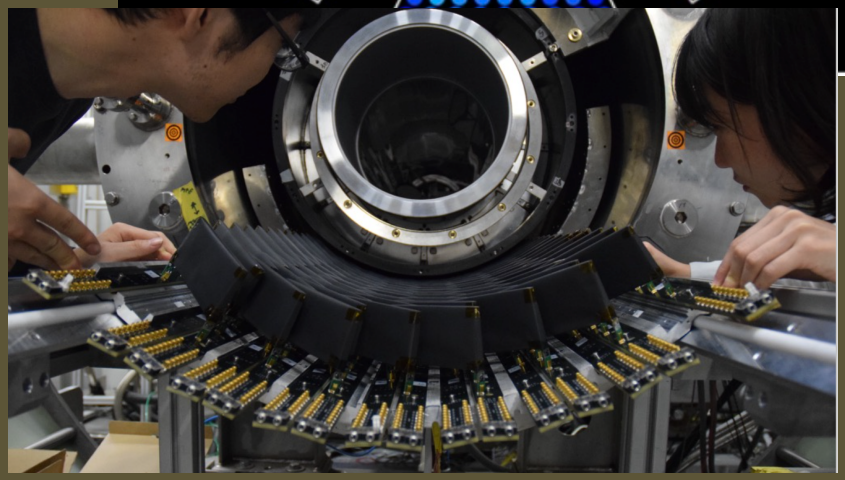

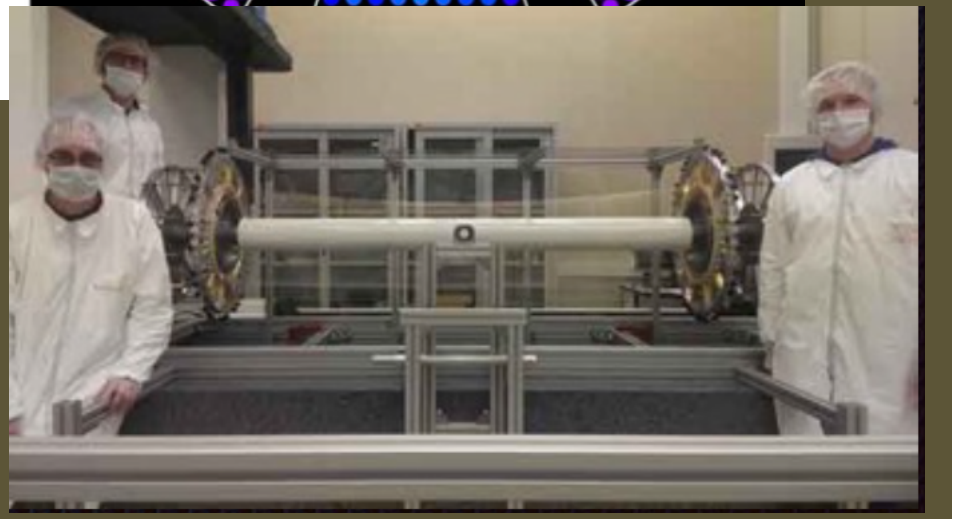

10^8 stop-μ^+/s, improved resolutions

Muon-to-electron Conversion

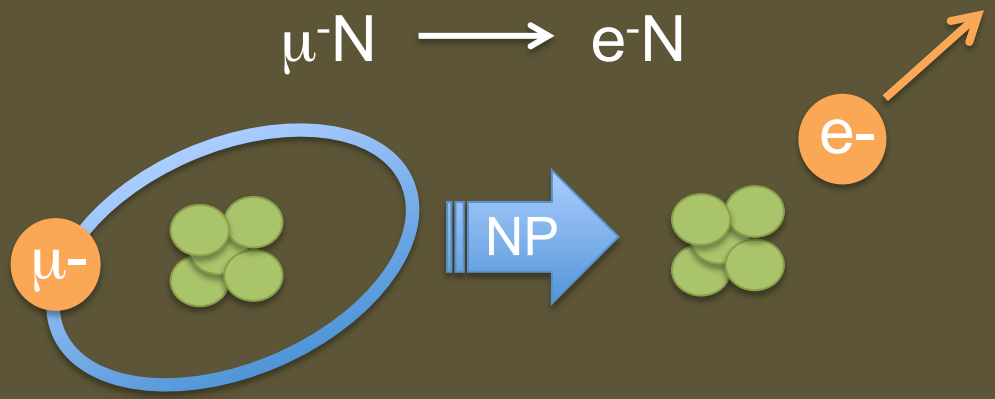

Current State-of-the-art (@ 90% CL) :

$$R_{\mu e} = \frac{\Gamma(\mu^- \text{ Au} \rightarrow e^- \text{ Au})}{\Gamma(\mu^- \text{ Au capture})} < 7 \times 10^{-13}$$

W. Bertl, et al. (SINDRUM-II) Eur.Phys.J. C47, 337 (2006).

Muon-to-electron Conversion

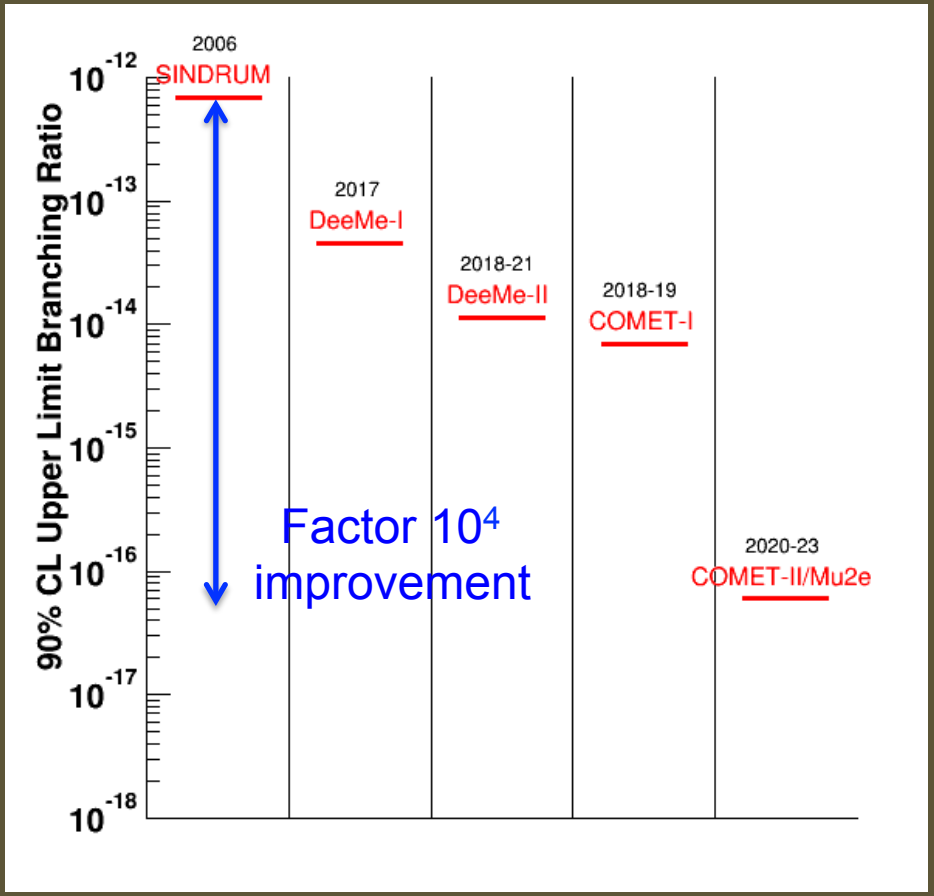

- Significant progress expected in near future

Mu2e and COMET ($\mu^-N \rightarrow e^-N$)

Signal

$\mu^-N \longrightarrow e^-N$

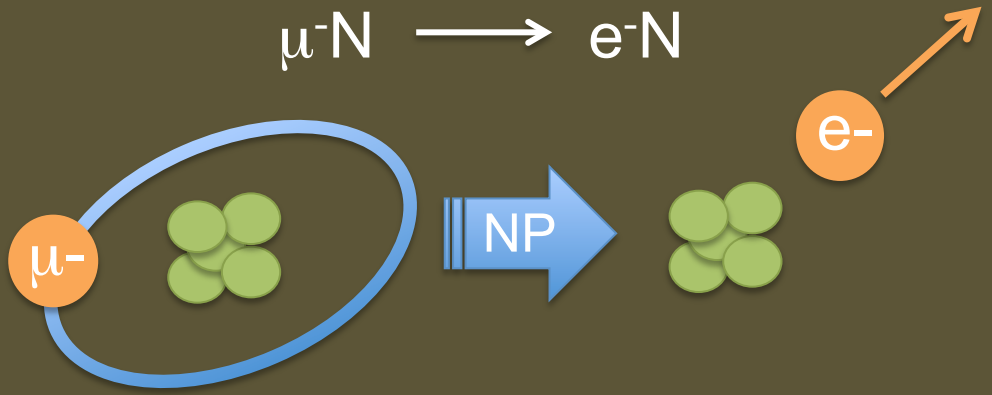

Mono-energetic electron

$E_{\mu e} = m_\mu - B(A,Z) - R(A,Z) \sim 105$ MeV

Coherent interaction with nucleus

Background

Decay in Orbit (DIO)
($\mu^-N \rightarrow e^-\nu\nu N$)

Radiative Pion Capture (RPC)
($\pi^-N \rightarrow \gamma N'$)

Cosmogenic

Decay in Orbit

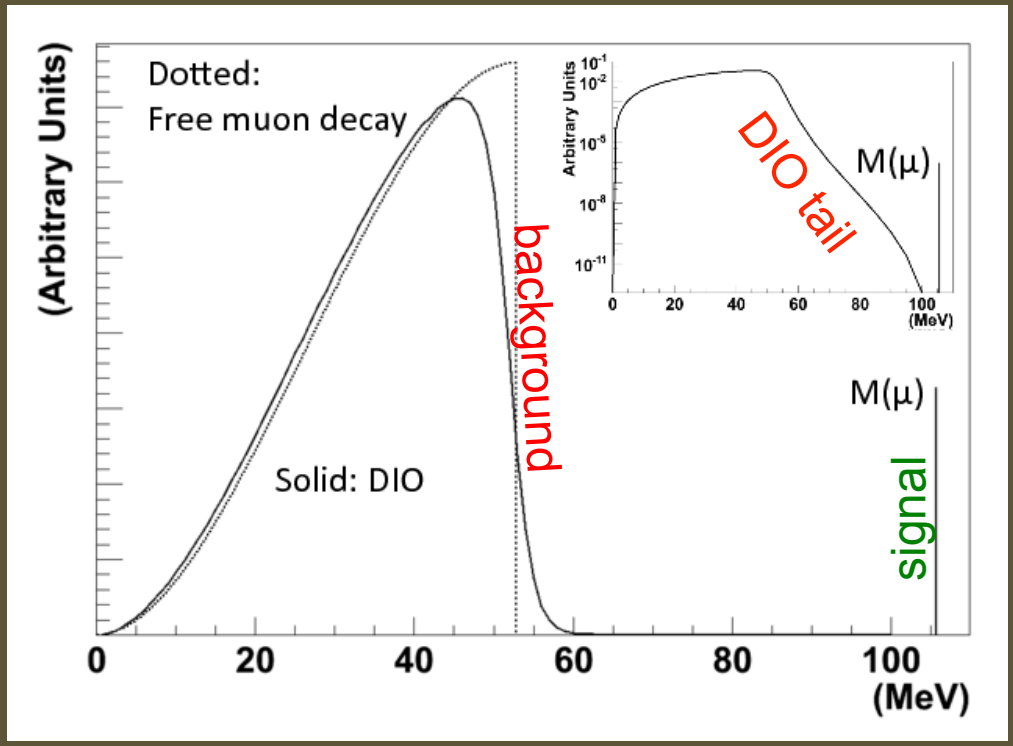

- E_e follows the Michel spectrum… but with a long tail from nuclear recoil $E_{max} = E_{\mu e}$
  - Requires excellent σ_p (<200 keV/c) to suppress

Radiative Pion Capture

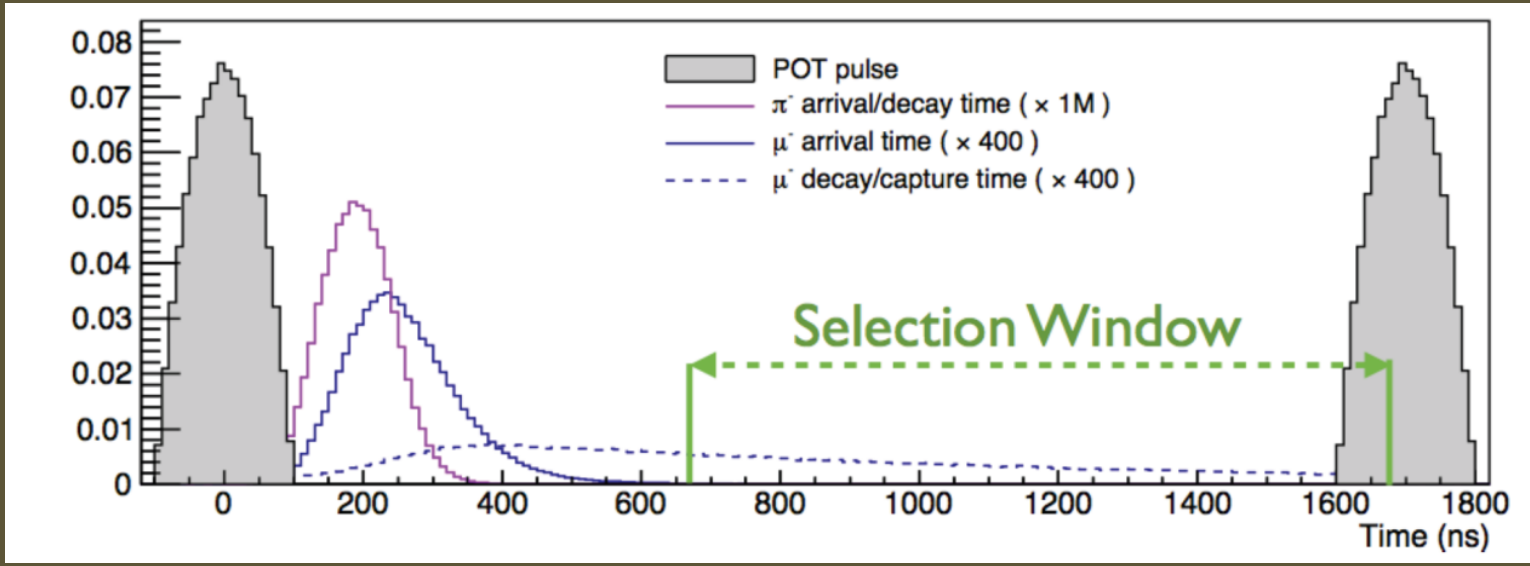

- Pion that survive to the stopping target are promptly captured on the nucleus
  - few% of the time, radiate γ with $E_\gamma \sim m_\mu$
  - Can suppress using pulsed beam and utilizing a delayed search window

Mu2e and COMET

Signal

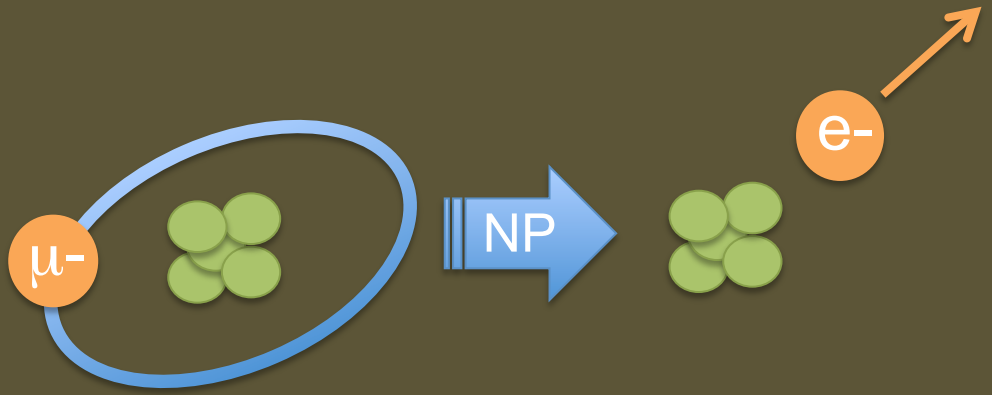

Background

Decay in Orbit (DIO)
($\mu^- N \rightarrow e^- \nu\nu N$)

Radiative Pion Capture (RPC)
($\pi^- N \rightarrow \gamma N'$)

Cosmogenic

Keys to success: excellent spectrometer resolution, pulsed proton beam, high efficiency cosmic veto

Aside : muonic atoms

- Stopped μ^- is captured in atomic orbit
  - Quickly (~fs) cascades to 1s state
- Bohr radius ~20 fm (for aluminum)
  - Significant overlap of μ^- and N wavefunctions
- Once in orbit, 3 things can happen
  - Decay : $\mu^- N(A,Z) \rightarrow e^- \nu\nu N(A,Z)$ (background)
  - Capture : $\mu^- N(A,Z) \rightarrow \nu N^*(A,Z-1)$ (normalization)
  - Conversion : $\mu^- N(A,Z) \rightarrow e^- N(A,Z)$ (signal)

Aside : muonic atoms

- Stopped μ^- is captured in atomic orbit
  - Quickly (~fs) cascades to 1s state
- Bohr radius ~20 fm (for aluminum)
  - Significant overlap of μ^- and N wavefunctions
- Once in orbit, 3 things can happen
  - Decay : $\mu^- N(A,Z) \rightarrow e^- \nu\nu N(A,Z)$ (39%)
  - Capture : $\mu^- N(A,Z) \rightarrow \nu N^*(A,Z-1)$ (61%)

For an aluminum stopping target

Aside : muonic atoms

- Stopped μ^- is captured in atomic orbit
  - Quickly (~fs) cascades to 1s state
- Bohr radius ~20 fm (for aluminum)
  - Significant overlap of μ^- and N wavefunctions
- Once in orbit, 3 things can happen
  - Decay : $\mu^- N(A,Z) \rightarrow e^- \nu\nu N(A,Z)$ (39%)
  - Capture : $\mu^- N(A,Z) \rightarrow \nu N^*(A,Z-1)$ (61%)

Produces 1n, 2γ, 0.1p per capture

For an aluminum stopping target

Detector view 500-1695 ns after proton pulse

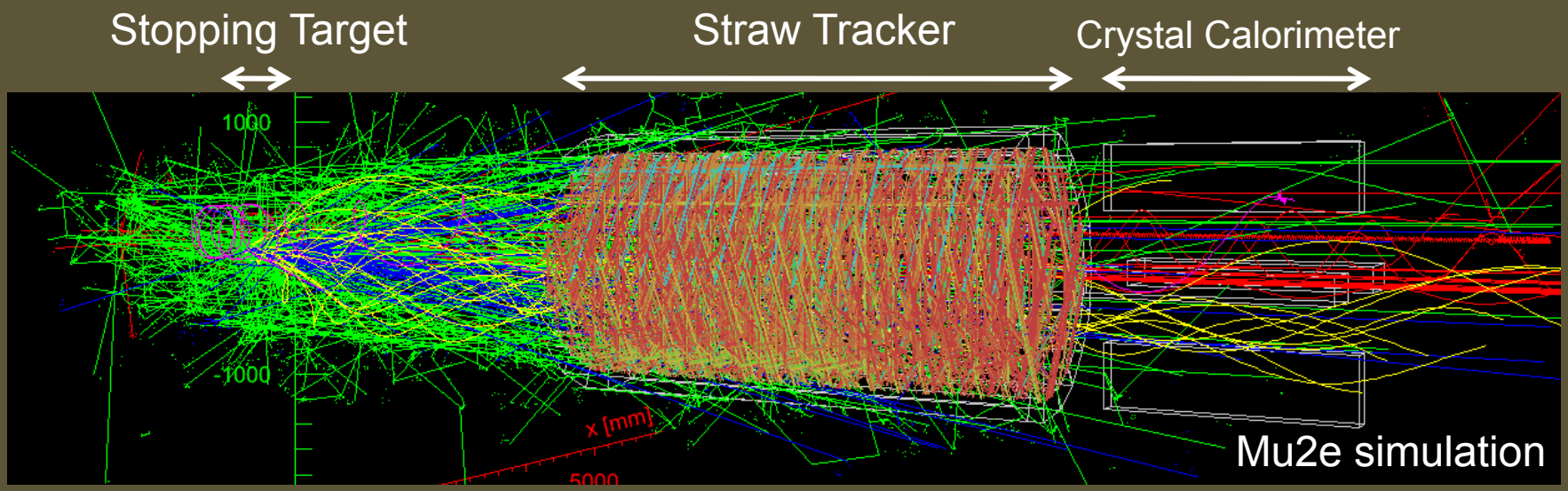

Timing information helps mitigate this

The Mu2e Proton Beam

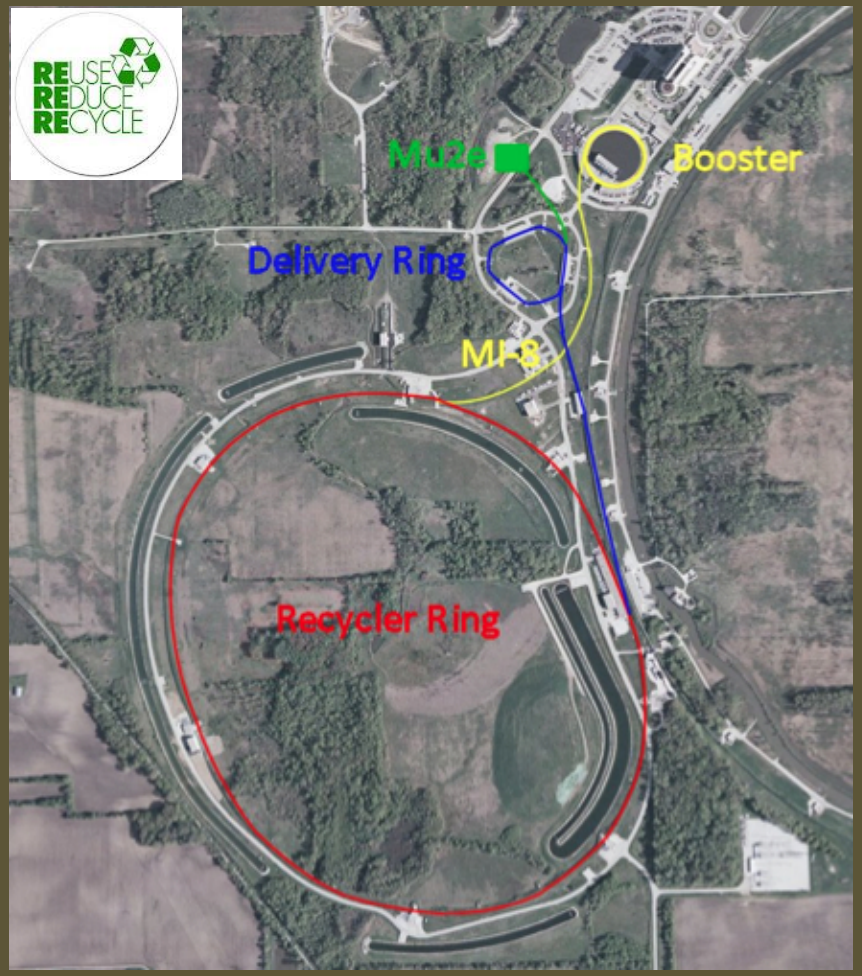

- 8kW of 8 GeV protons
  10^{10} stop μ^-/s
- Protons delivered in pulses of 4 x 10^7 ppp spaced by 1695 ns.
- Mu2e can (and will) run simultaneously with NOvA and short baseline neutrino experiments

The COMET-II Proton Beam

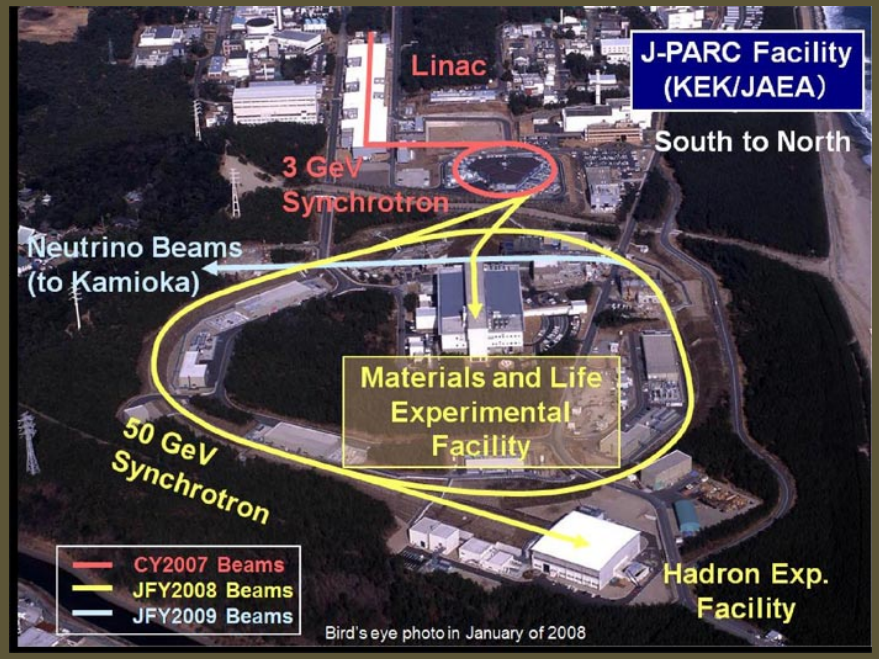

- 56kW of 8 GeV protons
  10^{11} stop μ^-/s
- Protons spaced by 1100 ns.
- COMET will share beam time with T2K, etc.

Mu2e Experimental Apparatus

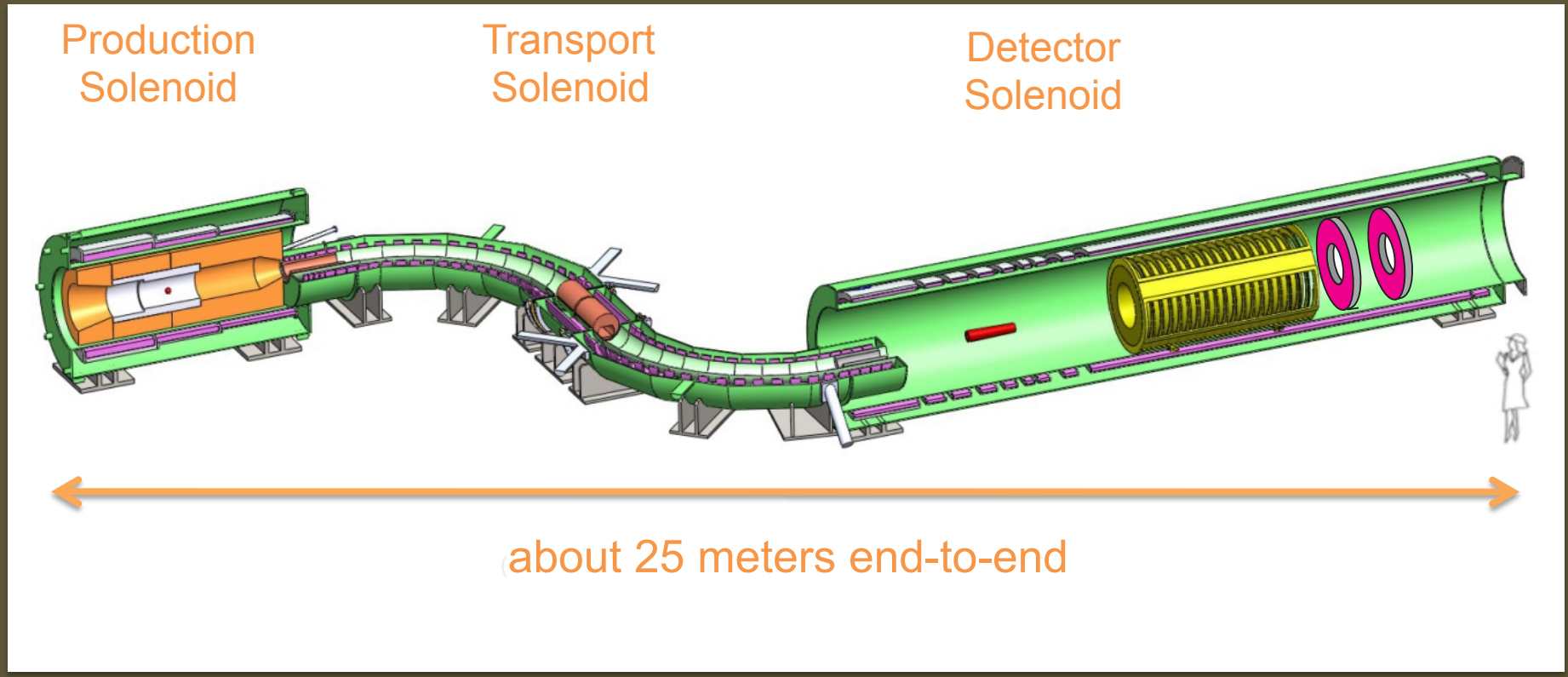

- Consists of 3 solenoid systems

Mu2e Experimental Apparatus

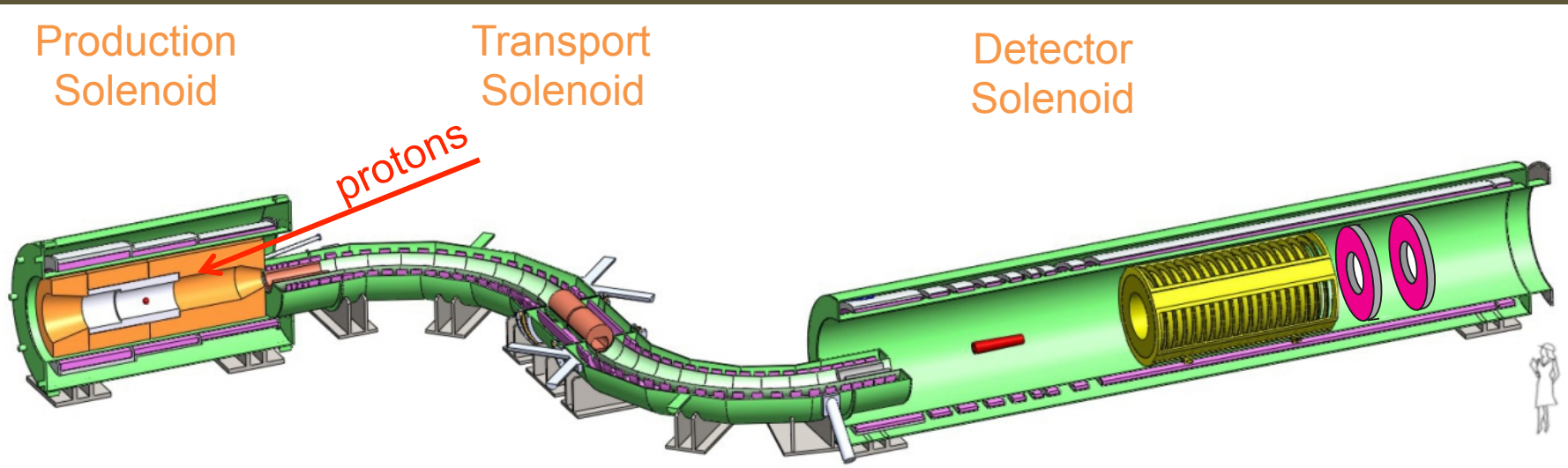

Production Solenoid:
8 GeV protons interact with a tungsten target to produce μ^- (from π^- decay)

- Consists of 3 solenoid systems

Mu2e Experimental Apparatus

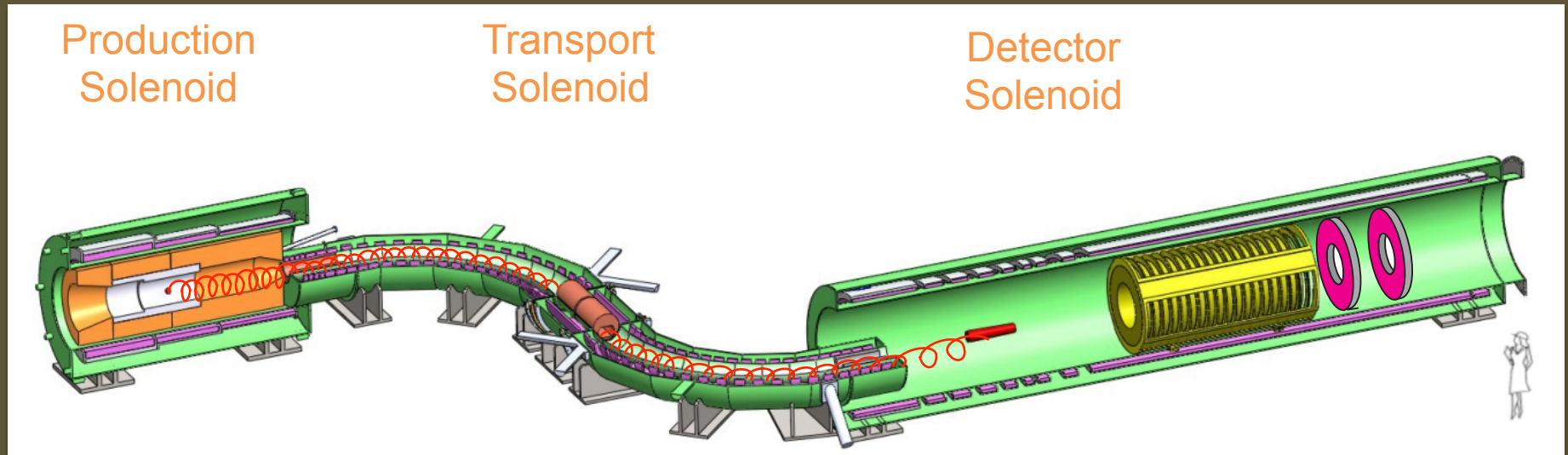

Transport Solenoid:
Captures π- and subsequent μ-; momentum- and sign-selects beam

- Consists of 3 solenoid systems

Mu2e Experimental Apparatus

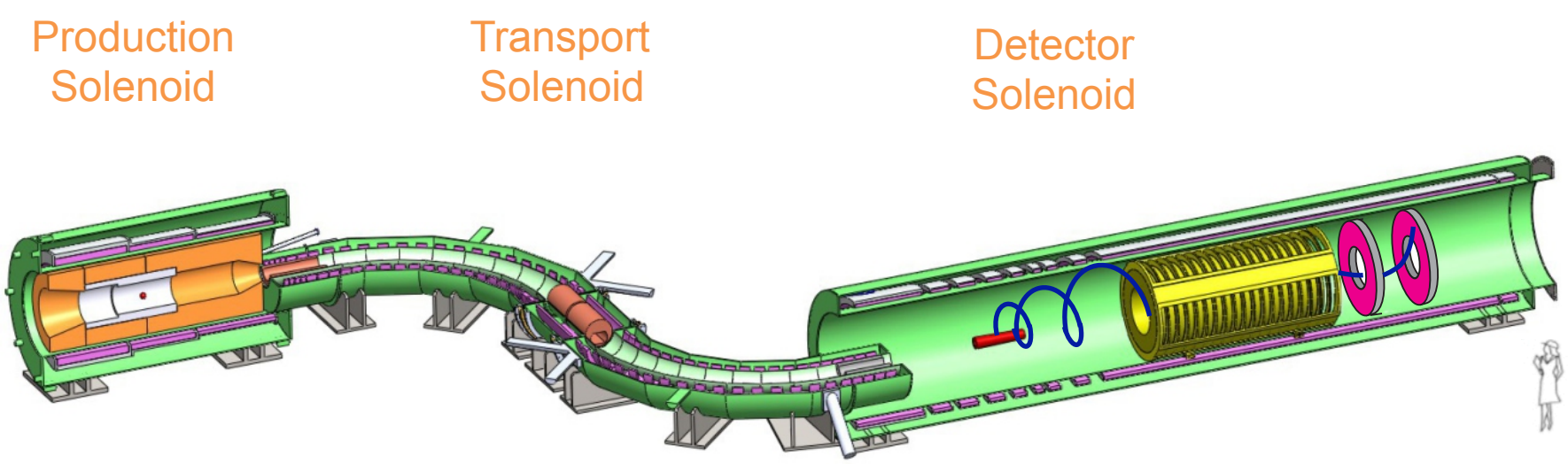

Detector Solenoid:
Upstream – Al. stopping target, Downstream – tracker, calorimeter
(not shown – cosmic ray veto system, extinction monitor, target monitor)

- Consists of 3 solenoid systems

Mu2e Experimental Apparatus

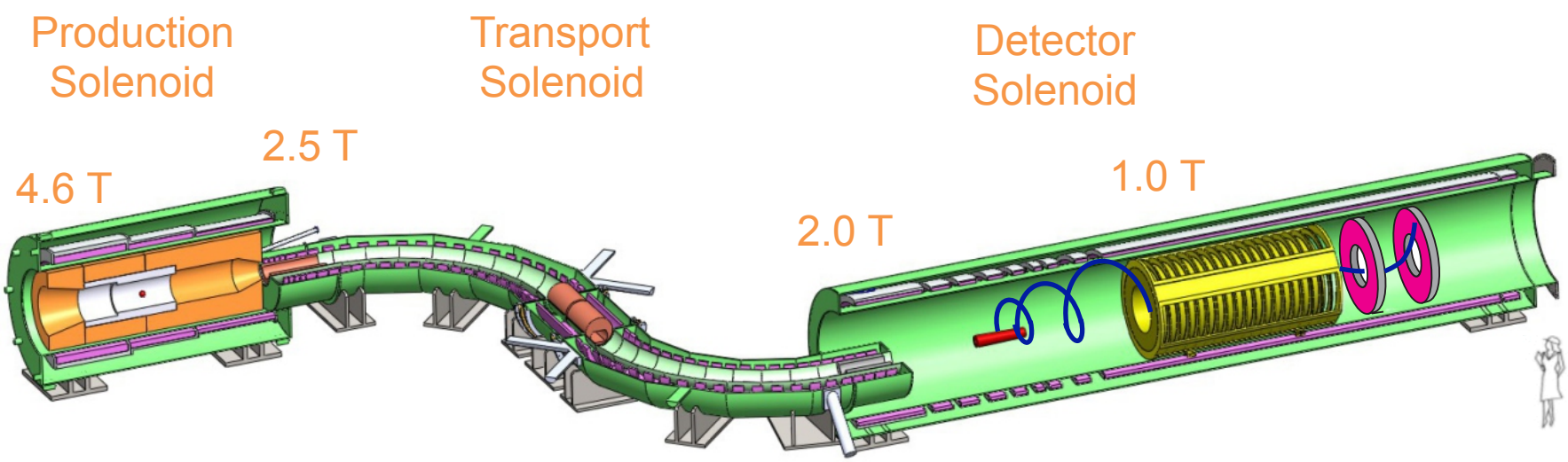

Graded fields important to suppress backgrounds, to increase muon yield, and to improve geometric acceptance for signal electrons

- Consists of 3 solenoid systems

Mu2e Experimental Apparatus

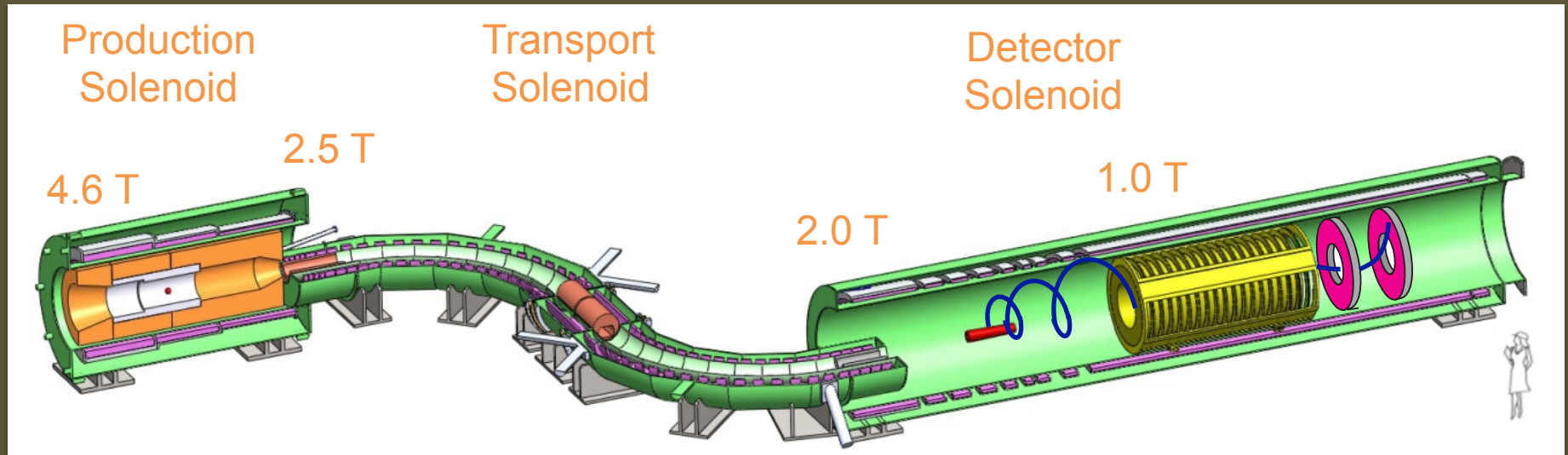

Graded fields important to suppress backgrounds, to increase muon yield, and to improve geometric acceptance for signal electrons

- Derived from MELC concept originated by Lobashev and Djilkibaev in 1989

COMET-II Apparatus

- Also inspired by Lobashev and Djilkibaev

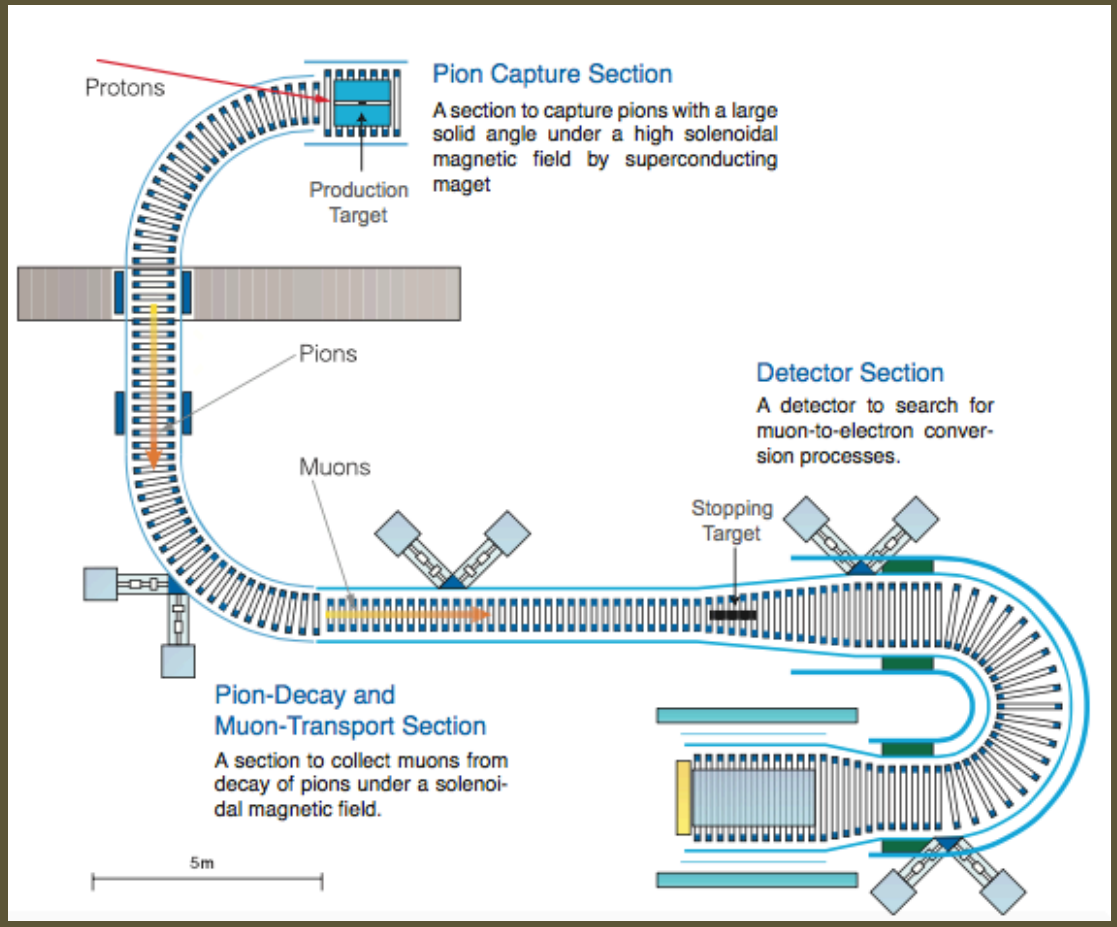

COMET Evolution

Phase I

Phase –II

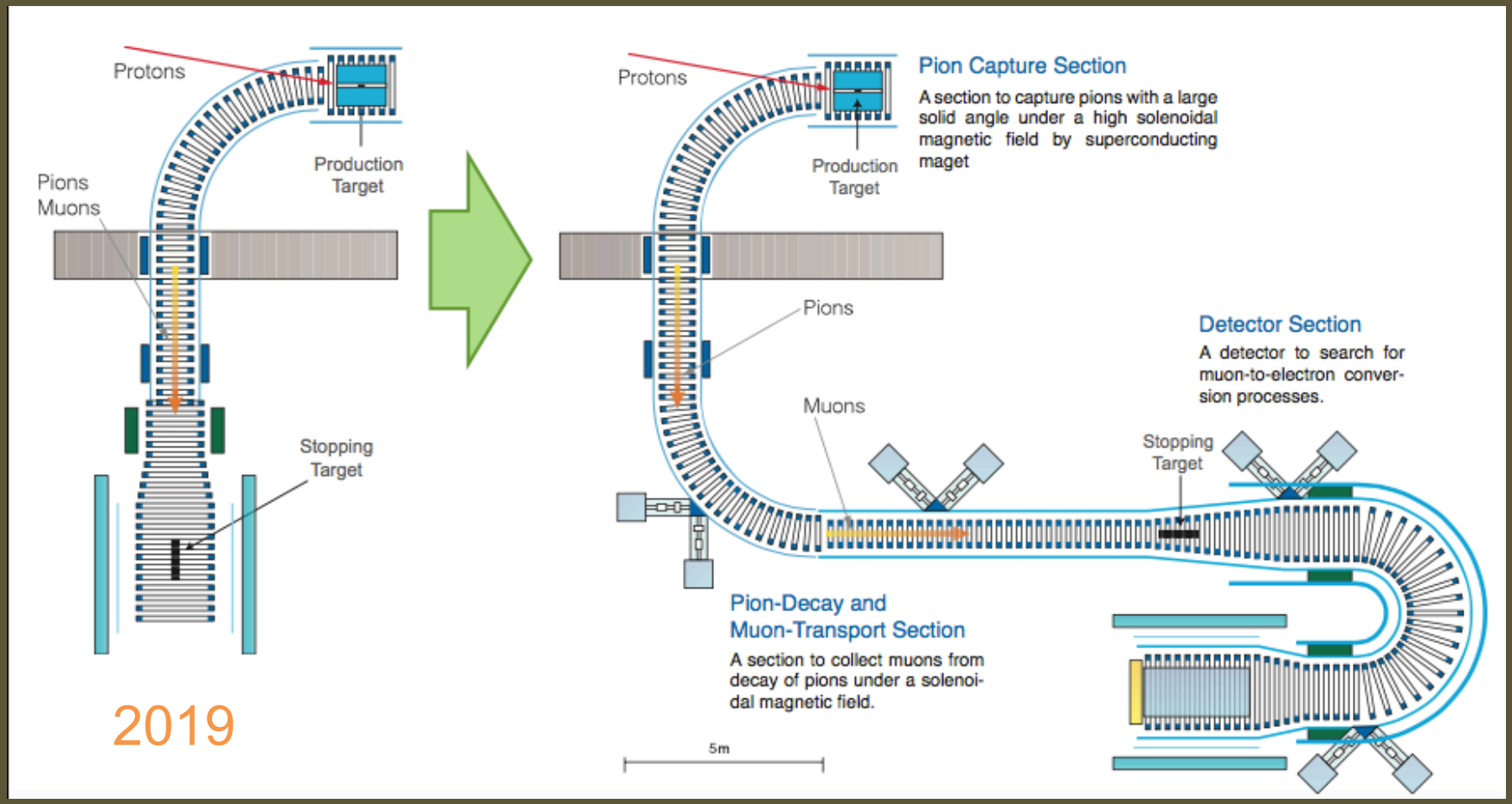

Construction well underway

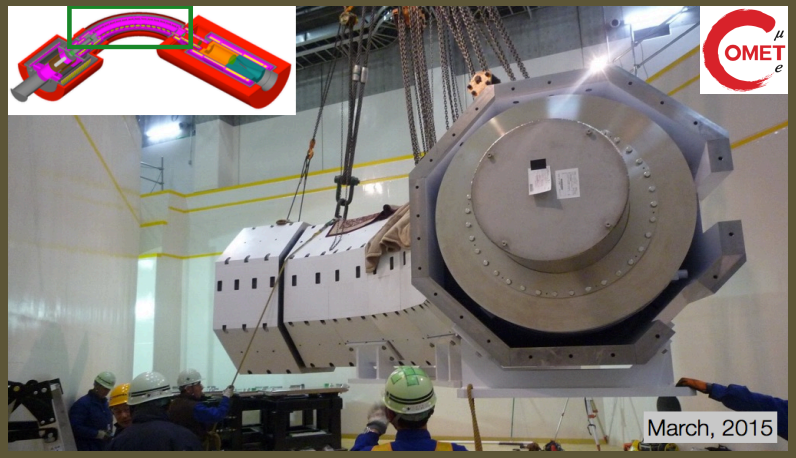

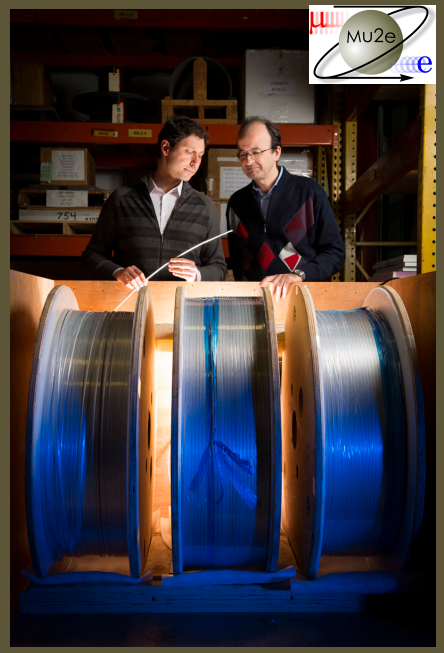

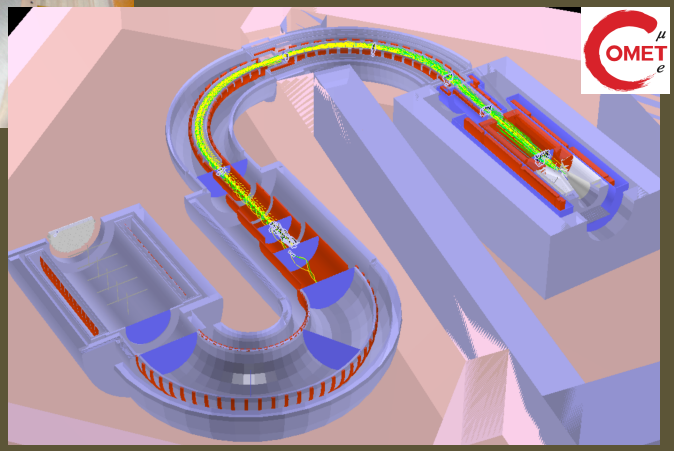

Sensitivity Comparison

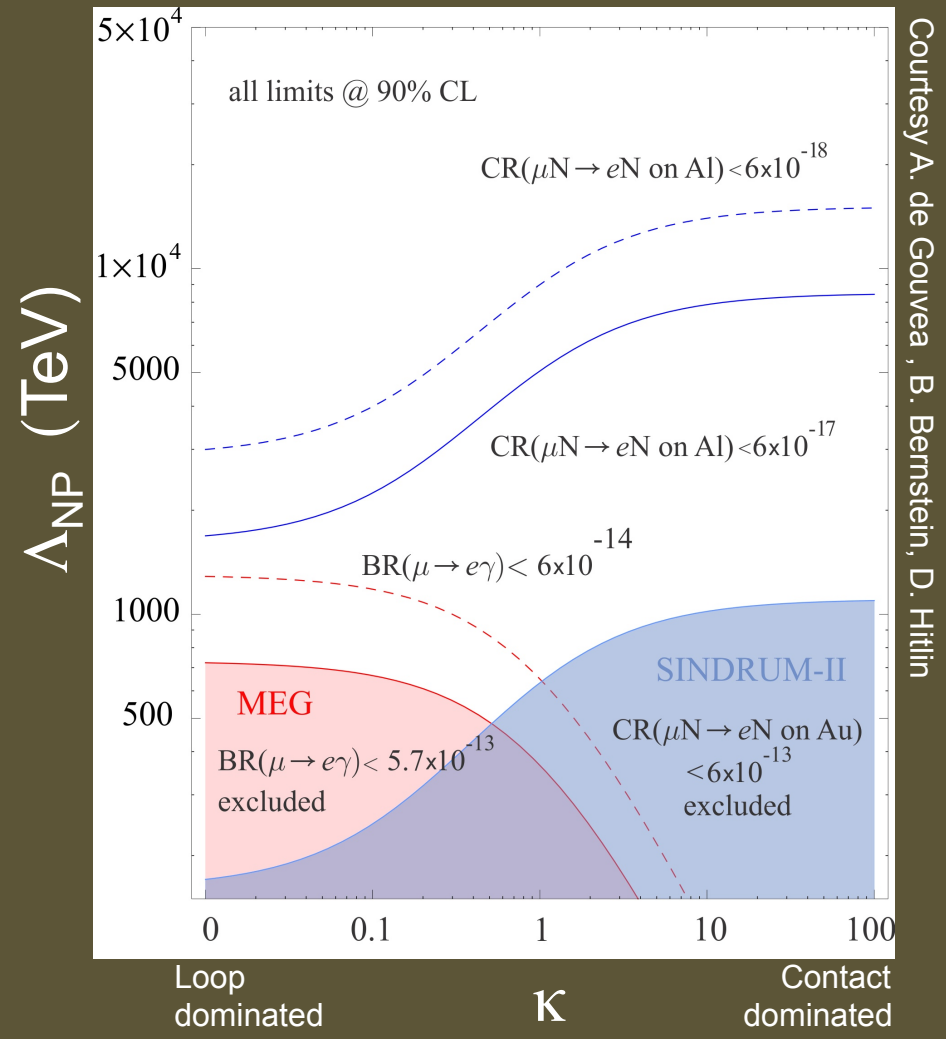

- Mu2e/COMET-II offer excellent sensitivity ~independent of NP scenario

Mu3e Experiment ($\mu^+ \rightarrow e^+e^+e^-$)

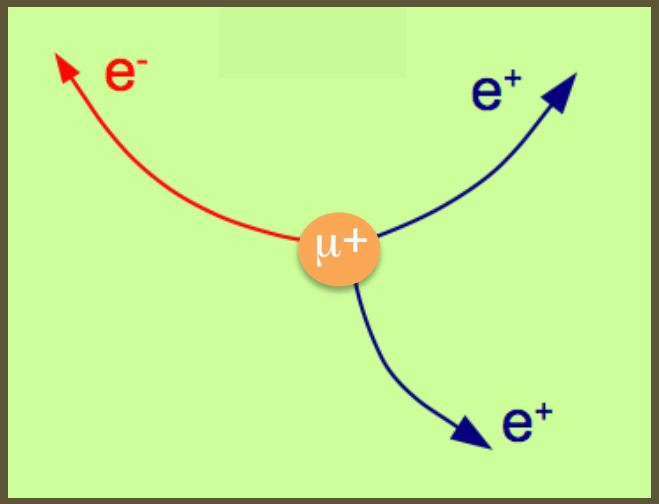

Current State-of-the-art (@ 90% CL) :

$$B(\mu^+ \rightarrow e^+e^+e^-) < 1 \times 10^{-12}$$

U. Bellgardt, et al. (SINDRUM) Nucl.Phys. B299, 1 (1988).

Mu3e Experiment ($\mu^+ \rightarrow e^+e^+e^-$)

Signal

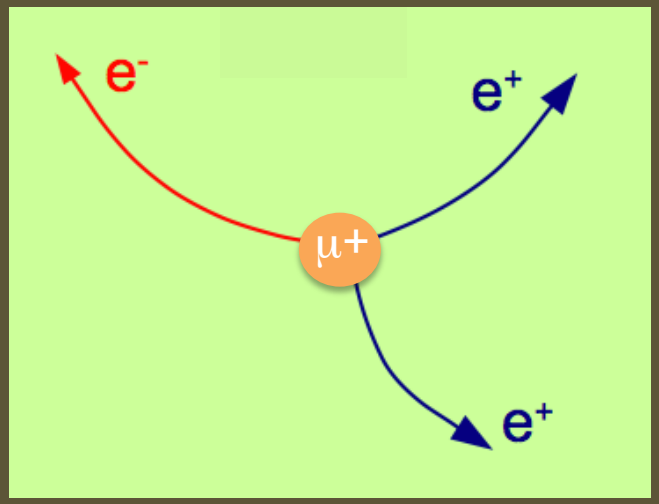

$\Sigma\, p = 0$

$E_e < m_\mu/2$

$\Sigma\, E_e = m_\mu$

Background

$\mu^+ \rightarrow e^+\nu\nu\gamma \rightarrow e^+\nu\nu e^+e^-$
Radiative Muon Decay (RMD)

Accidentals

Mu3e Experiment ($\mu^+ \rightarrow e^+e^+e^-$)

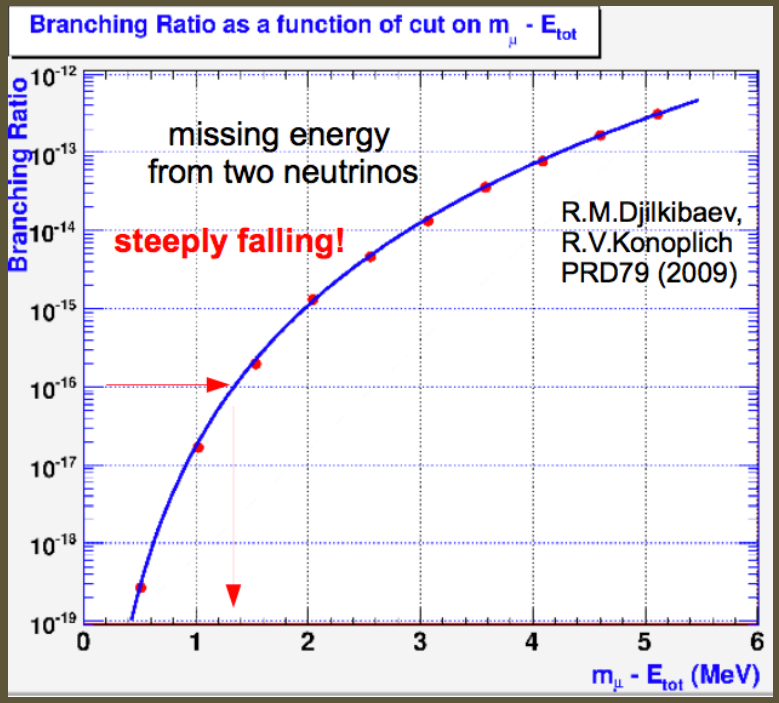

Background

$\mu^+ \rightarrow e^+\nu\nu\gamma \rightarrow e^+\nu\nu e^+e^-$
Radiative Muon Decay (RMD)

Accidentals

Keys to success: excellent momentum, timing, and vertex resolutions

Mu3e Experiment ($\mu^+ \rightarrow e^+e^+e^-$)

Phase-Ia

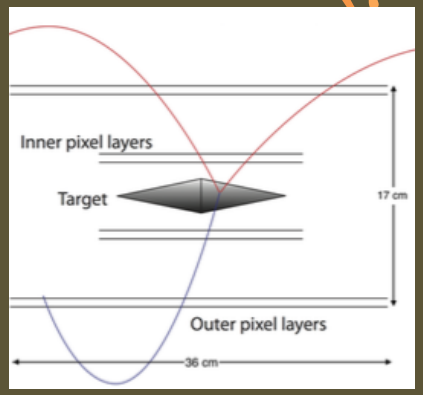

BR < 10^{-14}
10^7 μ^+/s
2019-2020

Phase-Ib

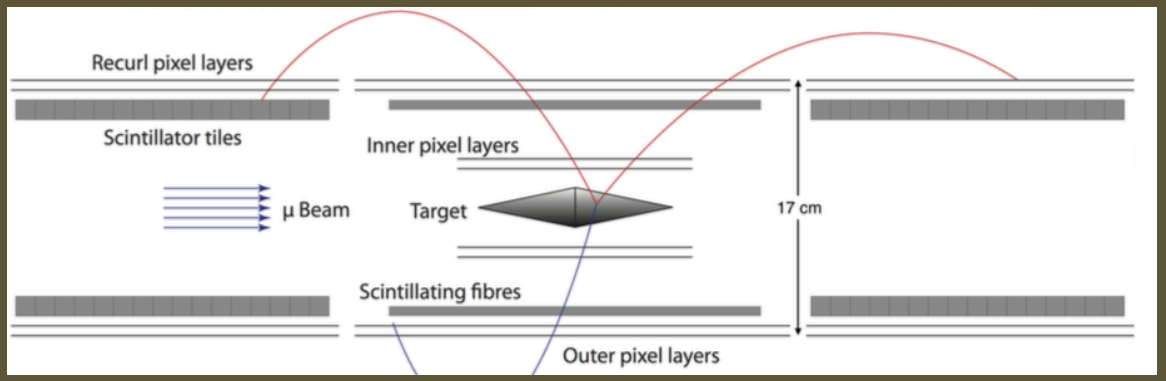

BR < 10^{-15}
10^8 μ^+/s
>2020

Phase-II

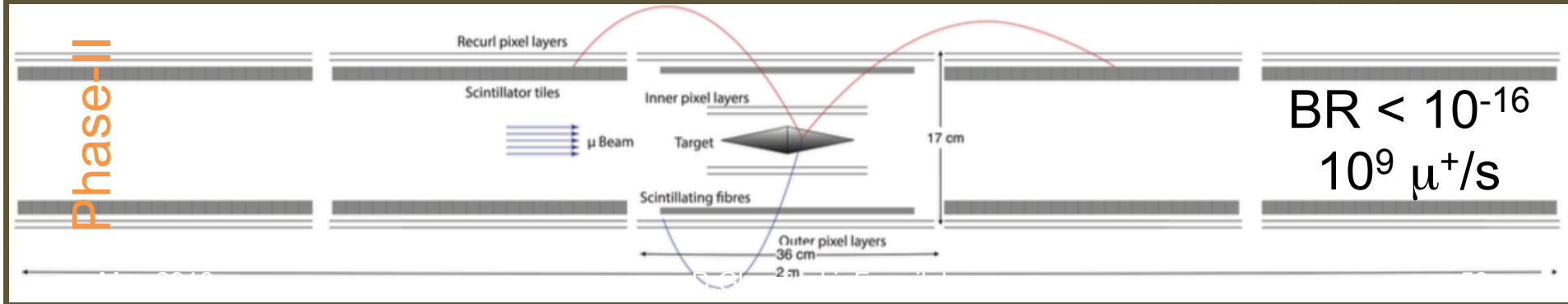

BR < 10^{-16}
10^9 μ^+/s

Mu3e (Phase-I) beam

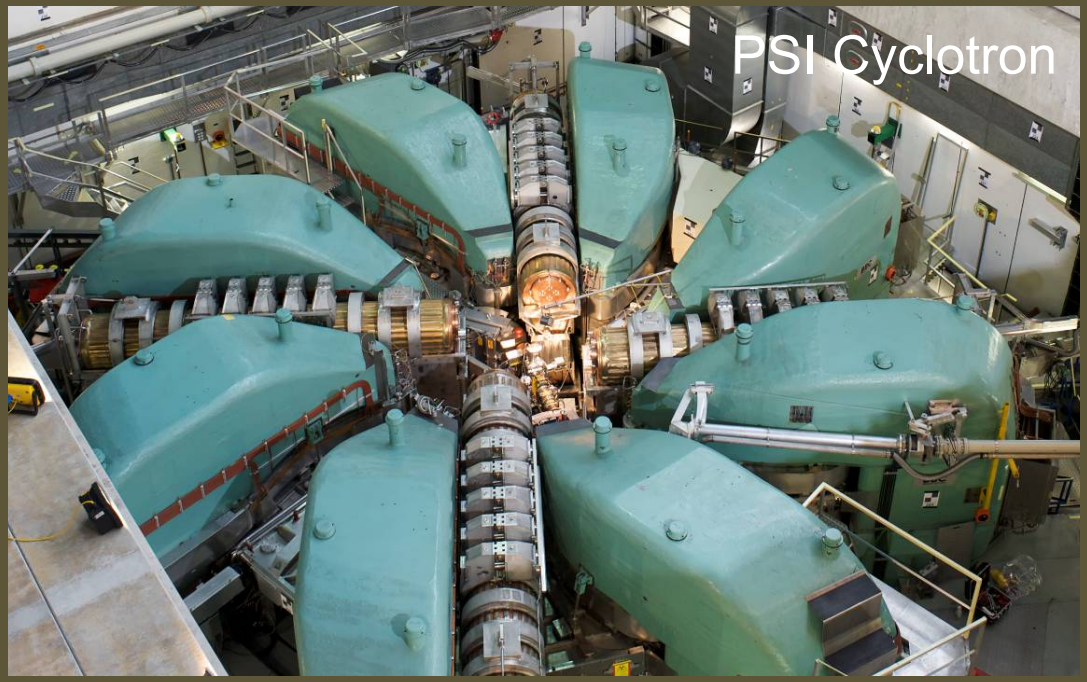

- 1.3 MW of 0.6 GeV protons
- “surface” muon beam, p_μ ~ 28 MeV/c
- Mu3e will use 10^7 – 10^8 μ^+/s

Mu3e (Phase-II) beam

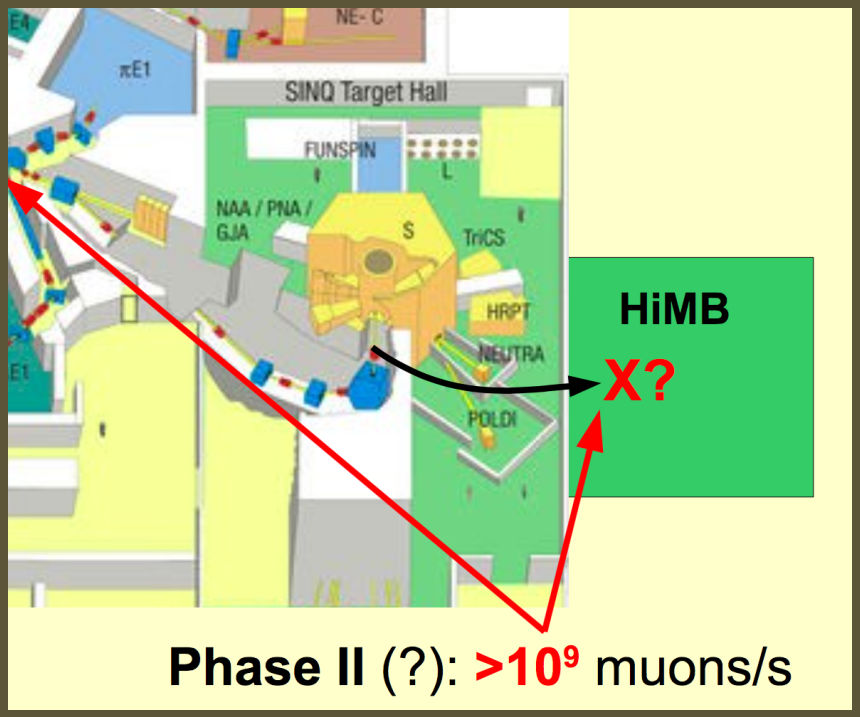

To achieve Phase-II sensitivity requires an upgraded facility at PSI: High Intensity Muon Source

- Currently under development
- Not (yet) approved

Mu3e Detector

25 μm Kapton, 50 μm silicon: 0.1% X_0

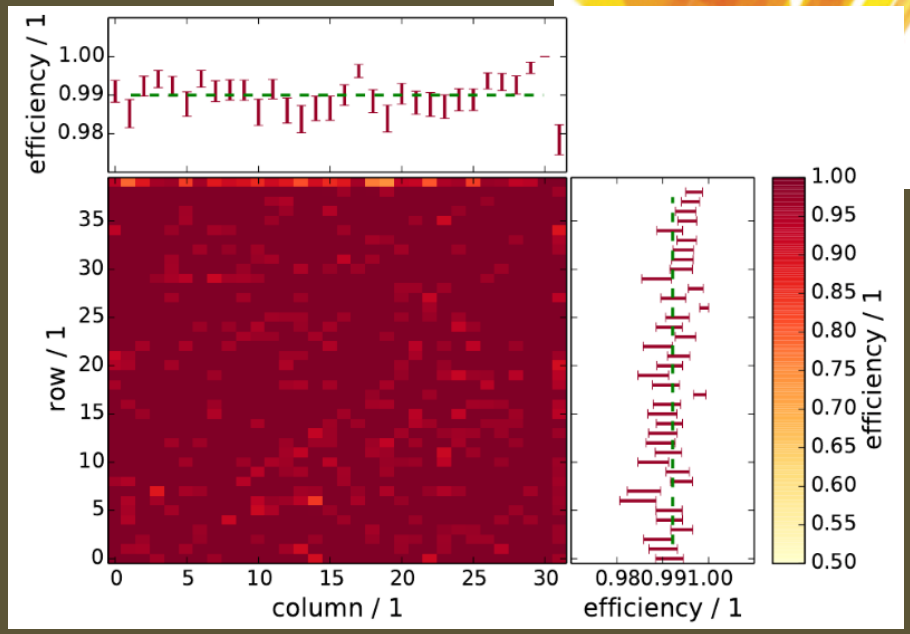

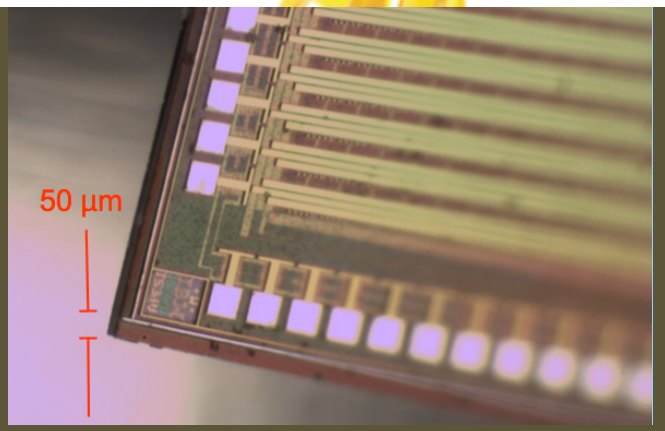

- Low mass pixel array (thinned to 50 μm)

Mu3e Detector

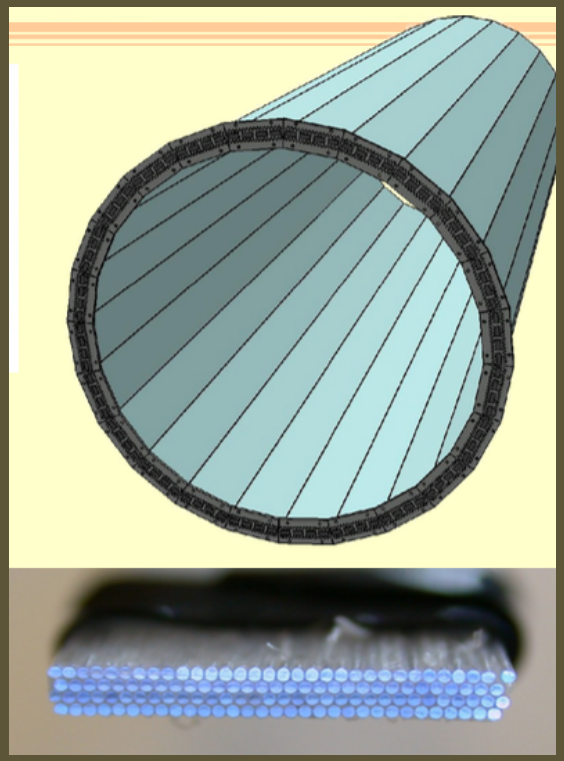

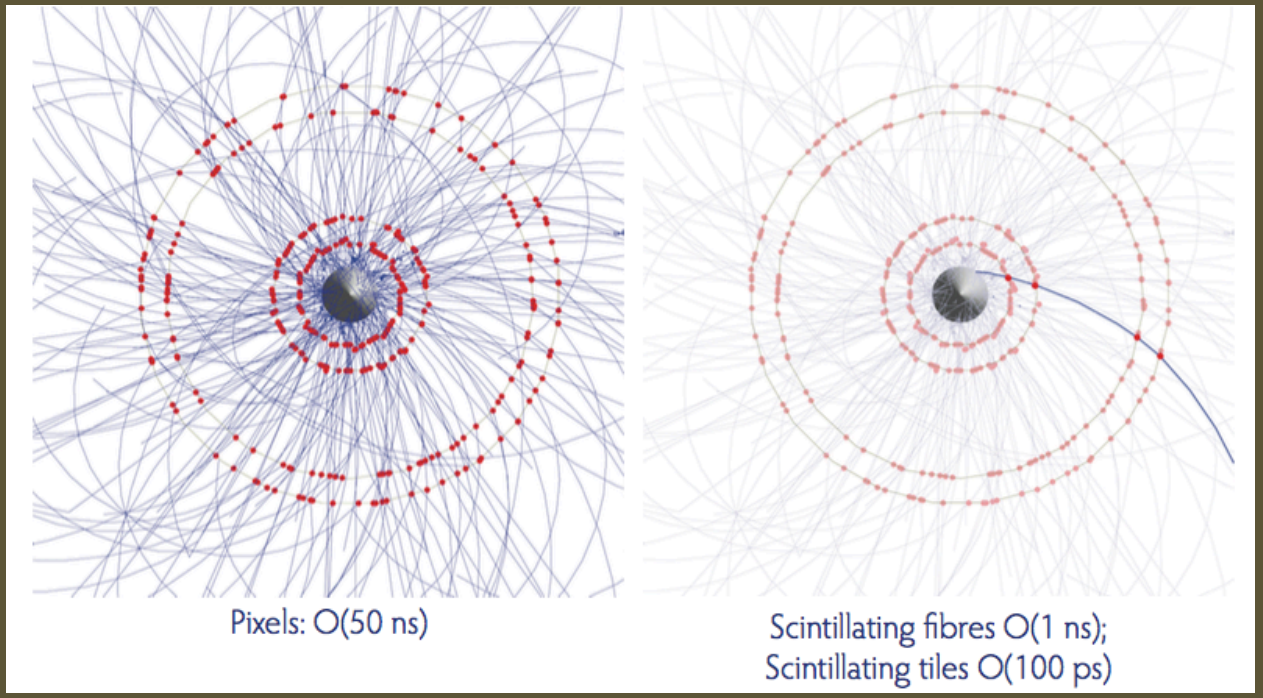

- Scintillating arrays for 100ps timing

Mu3e Sensitivity

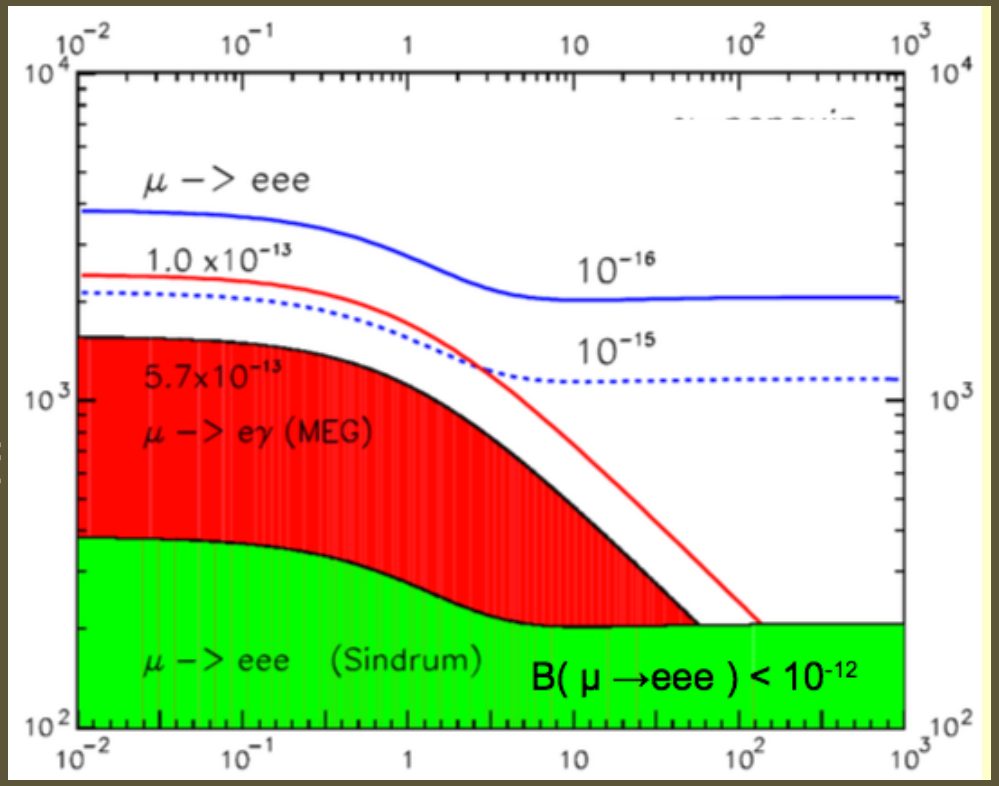

Mu3e offers compelling,complementary sensitivity

cLFV using taus

cLFV Experiments using taus

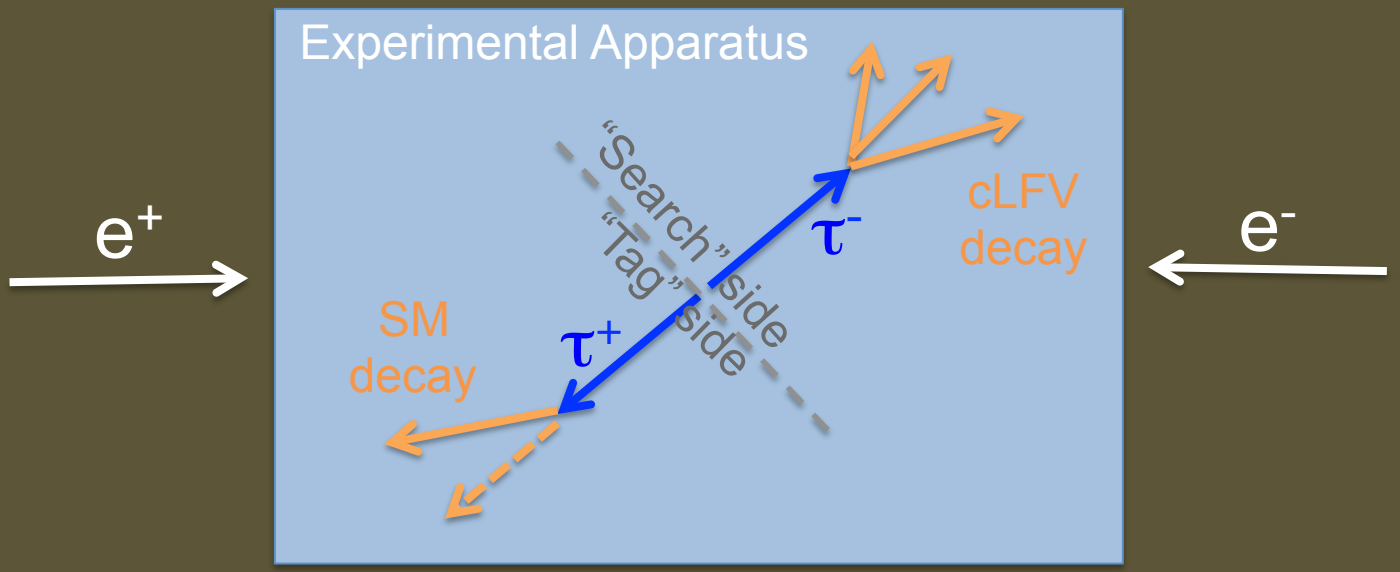

Sensitivity dominated by Belle & BaBar

cLFV Experiments using taus

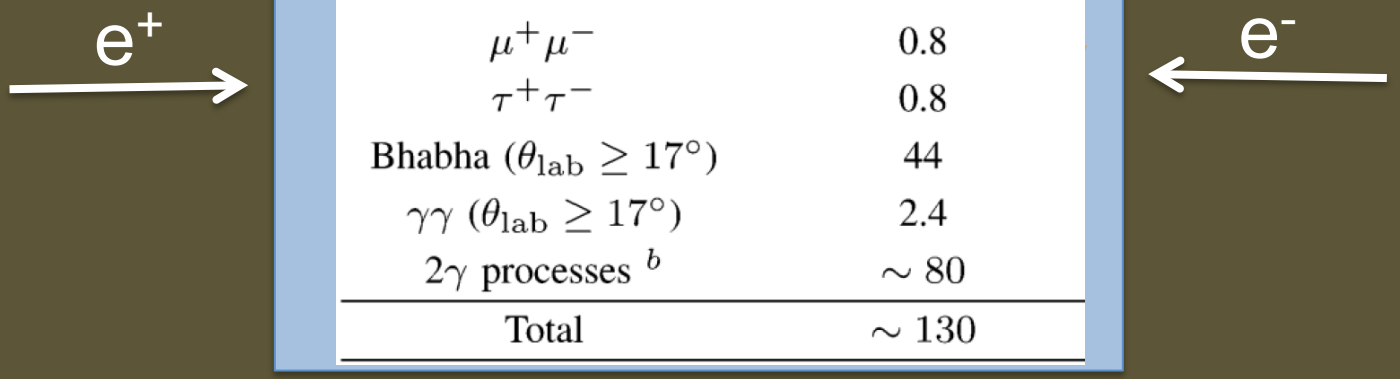

Physics process	Cross section (nb)
$\Upsilon(4S) \to B\bar{B}$	1.2
$e^+e^- \to$ continuum	2.8
$\mu^+\mu^-$	0.8
$\tau^+\tau^-$	0.8
Bhabha ($\theta_{\rm lab} \geq 17°$)	44
$\gamma\gamma$ ($\theta_{\rm lab} \geq 17°$)	2.4
2γ processes [b]	~ 80
Total	~ 130

$\tau^+\tau^-$ production cross section ~ 1 nb

Latest results use 500-800 fb^{-1} ~ 500-800M $\tau^+\tau^-$ pairs

cLFV Experiments using taus

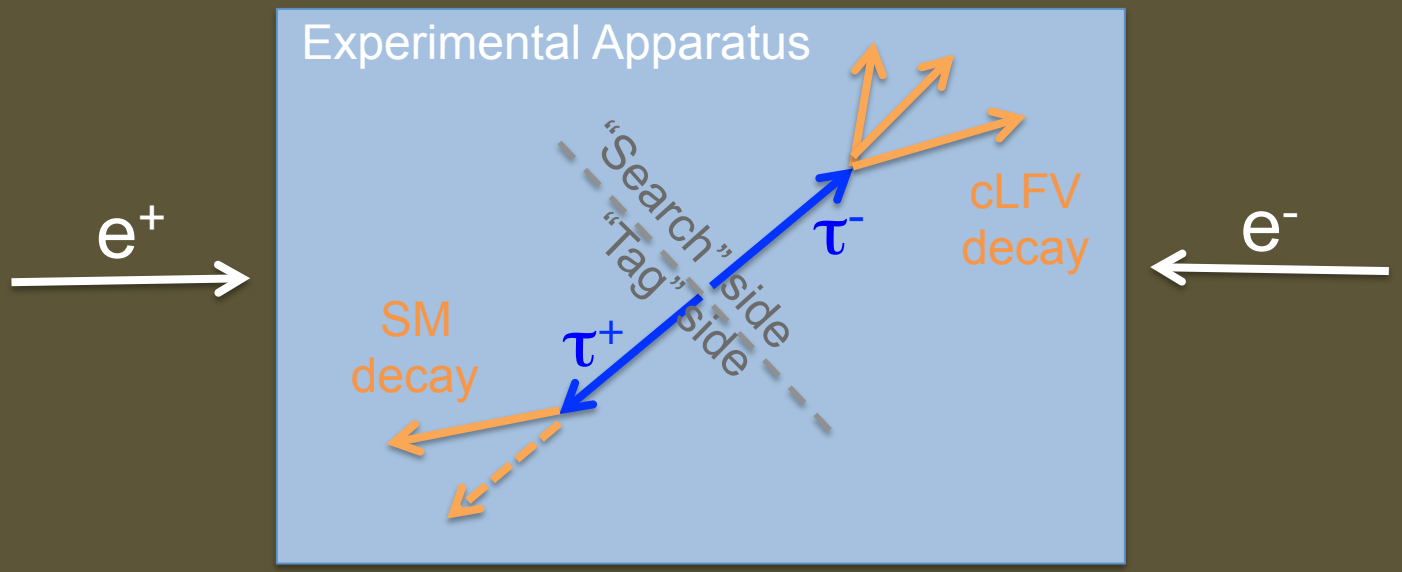

- Exploit (E,p) constraints available at e^+e^- collider
- On Search side: $m_{reco} = m_\tau$, $E_{reco} = E_{beam}$ (in CM)
- Employ excellent particle identification algorithms
- Additional requirements to suppress qq, μμ, ee, γγ

Some cLFV Results

Belle: $\tau \to \mu\gamma$

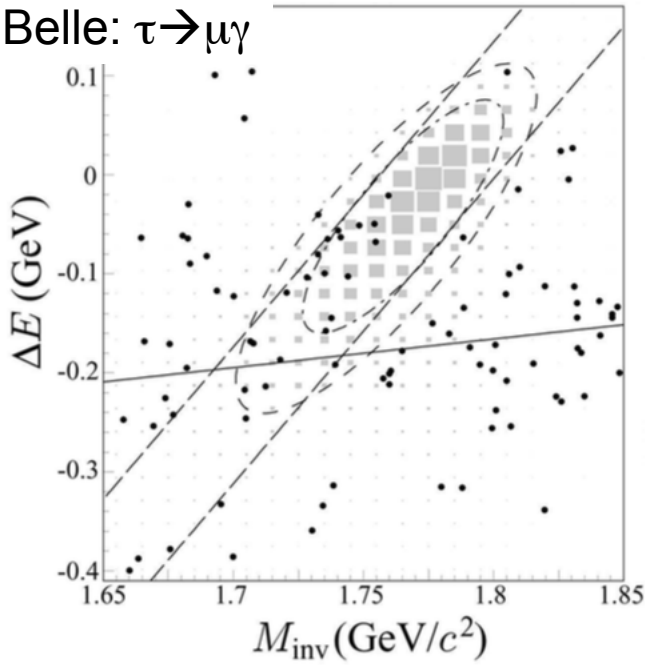

Belle: $\tau \to e\gamma$

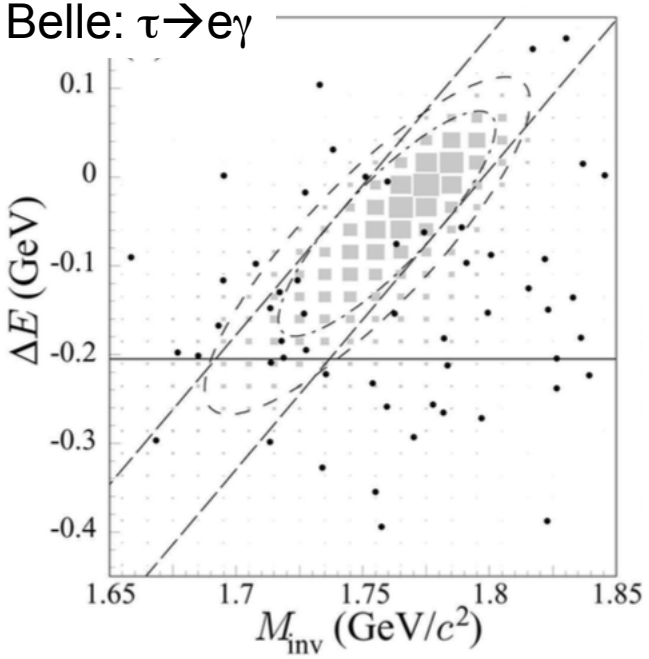

- Data Signal MC
  Inner (outer) ellipse : Signal (blinded) region

- No significant excess is observed
- $\tau \to e\gamma$, $\mu\gamma$ already observe background

Some cLFV Results

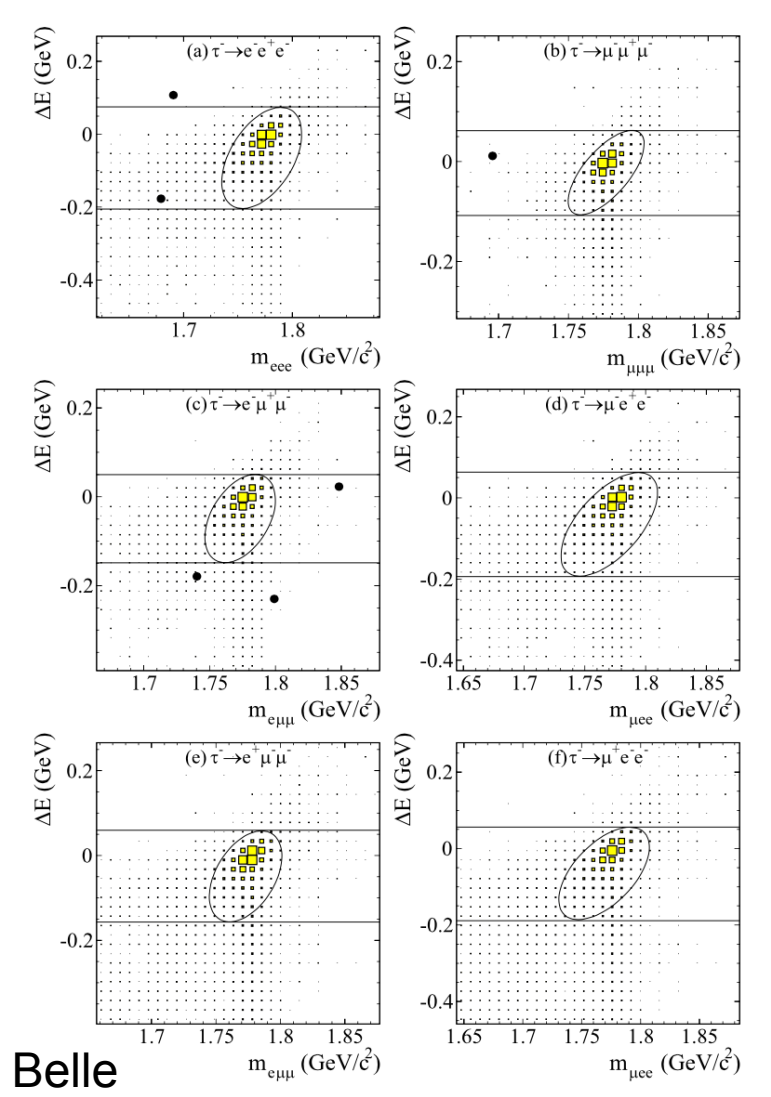

- Data
- Signal MC

  Ellipse = Signal Region
  Solid lines : m_{reco} sidebands

- $\tau \to$ 3 leptons very clean
- No events in signal region

cLFV tau decays at LHCb

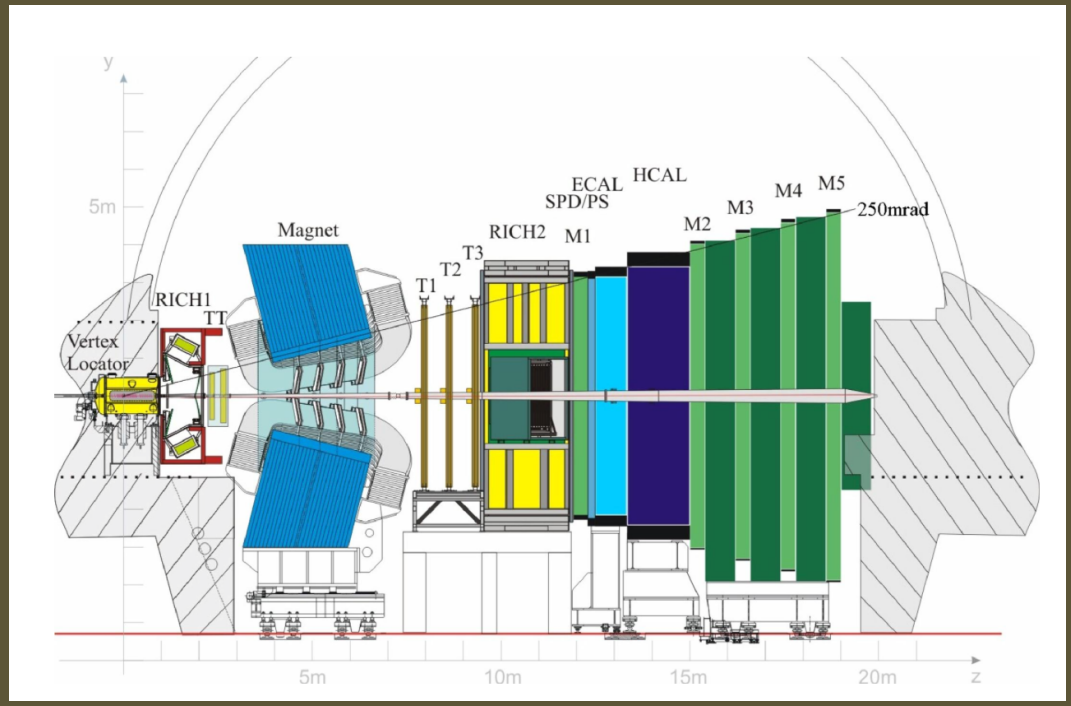

- Lots of τ from $b \rightarrow \tau\nu X$ and $c \rightarrow \tau\nu X$
- Effective cross section of 85 μb
- Competitive $\tau \rightarrow \mu\mu\mu$ sensitivity

cLFV Result

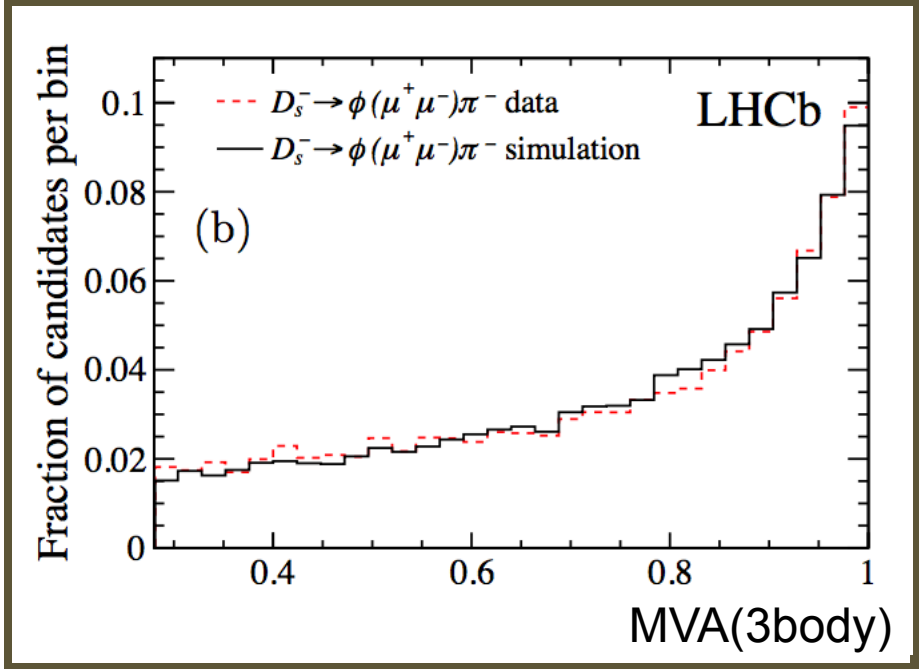

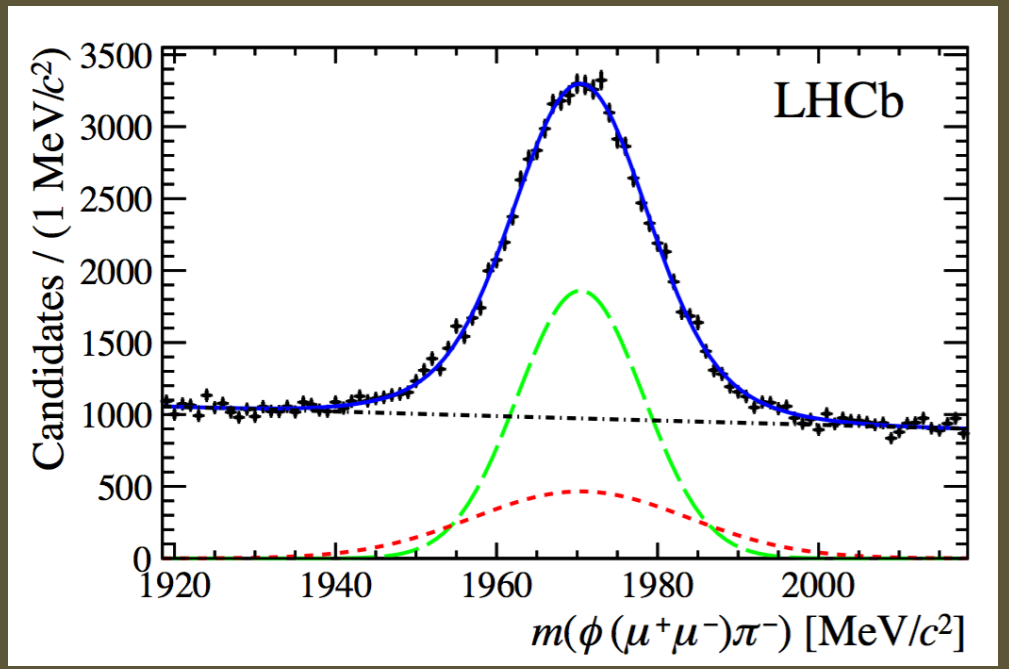

$$\mathcal{B}\left(\tau^- \to \mu^-\mu^+\mu^-\right) = \frac{\mathcal{B}\left(D_s^- \to \phi\left(\mu^+\mu^-\right)\pi^-\right)}{\mathcal{B}\left(D_s^- \to \tau^-\bar{\nu}_\tau\right)} \times f_\tau^{D_s} \times \frac{\epsilon_{\rm cal}^{\rm R}}{\epsilon_{\rm sig}^{\rm R}} \times \frac{\epsilon_{\rm cal}^{\rm T}}{\epsilon_{\rm sig}^{\rm T}} \times \frac{N_{\rm sig}}{N_{\rm cal}} \equiv \alpha N_{\rm sig},$$

- Normalized to $D_s \to \phi\pi \to (\mu\mu)\pi$

cLFV Result

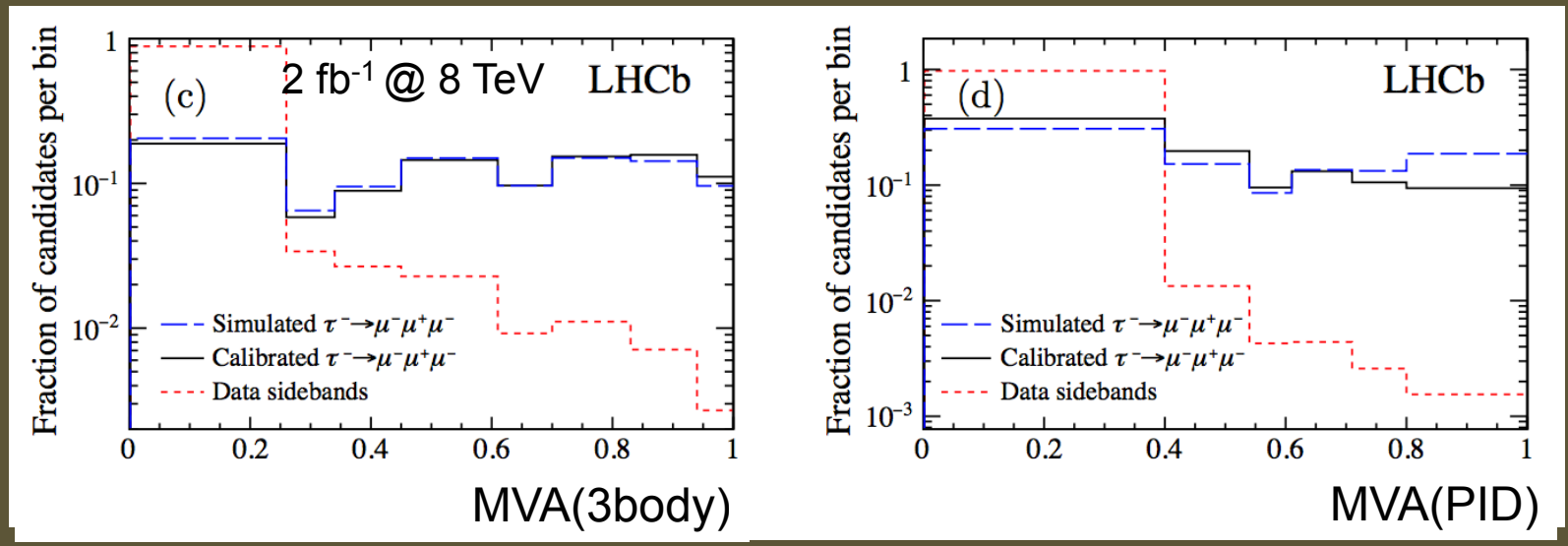

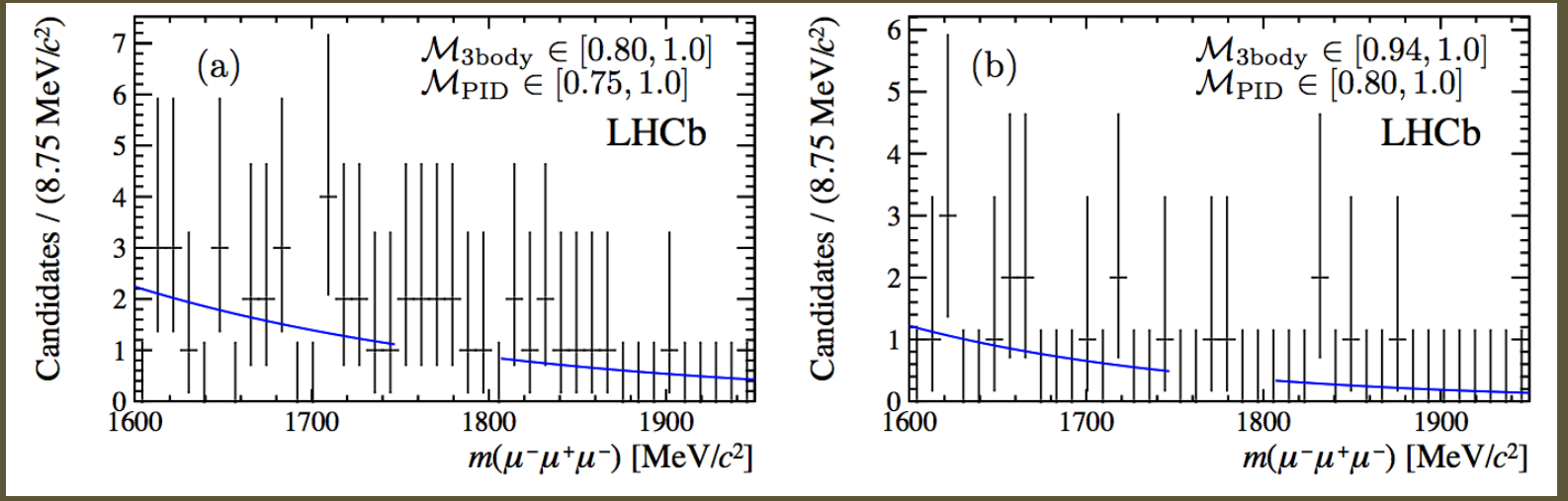

- 3D lhood fit ($M_{\mu\mu\mu}$, MVA_{3body}, MVA_{PID})

Most Recent HFAG Results

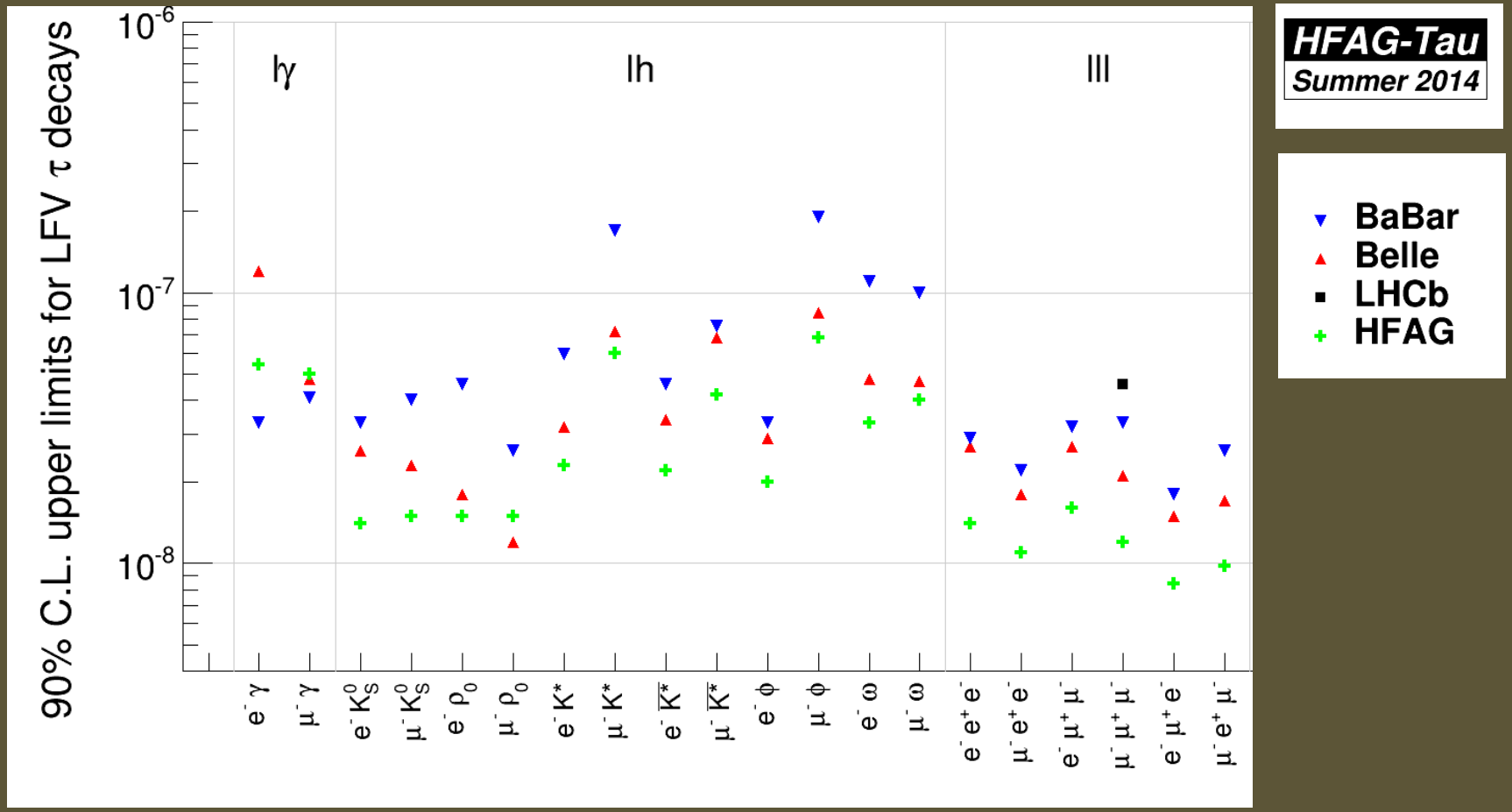

Future Sensitivity

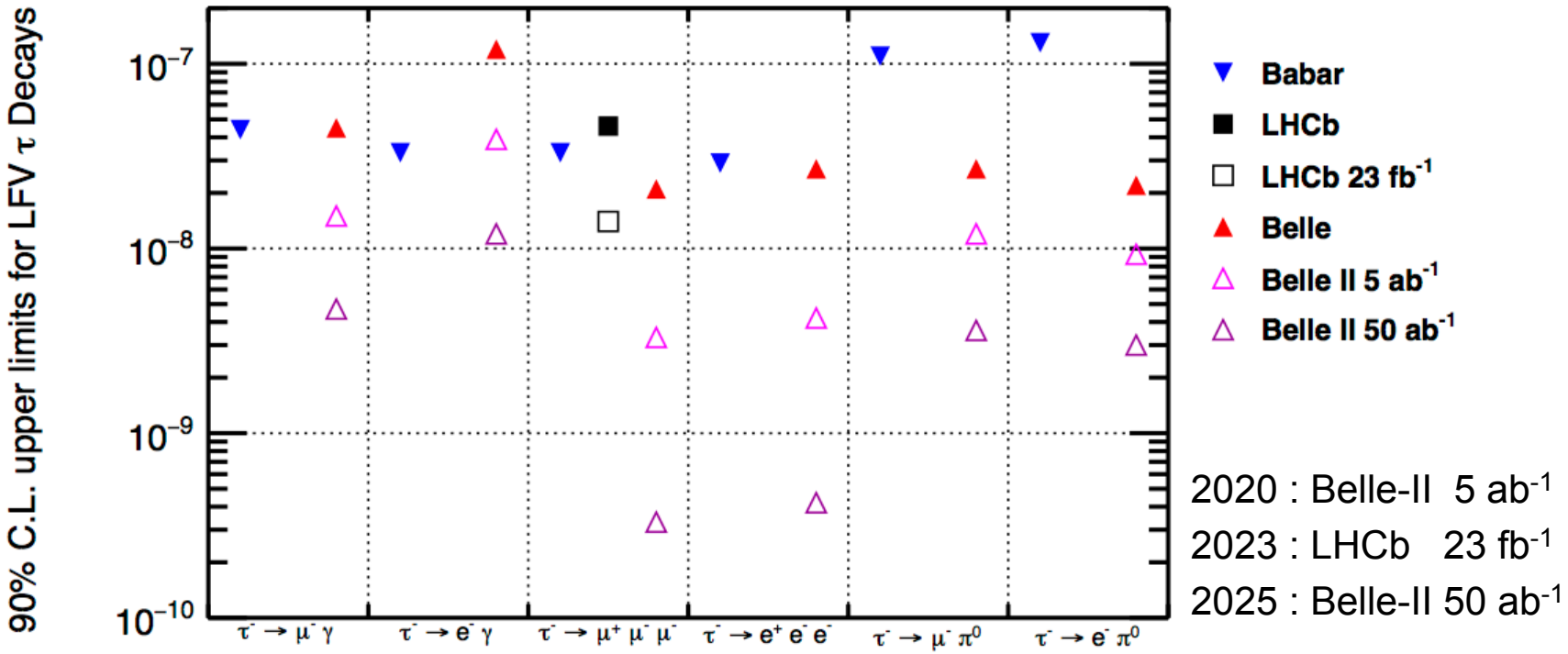

Expect 1-2 orders of magnitude improvement <10y

cLFV at CMS & ATLAS

Constraints from μ→e Experiments

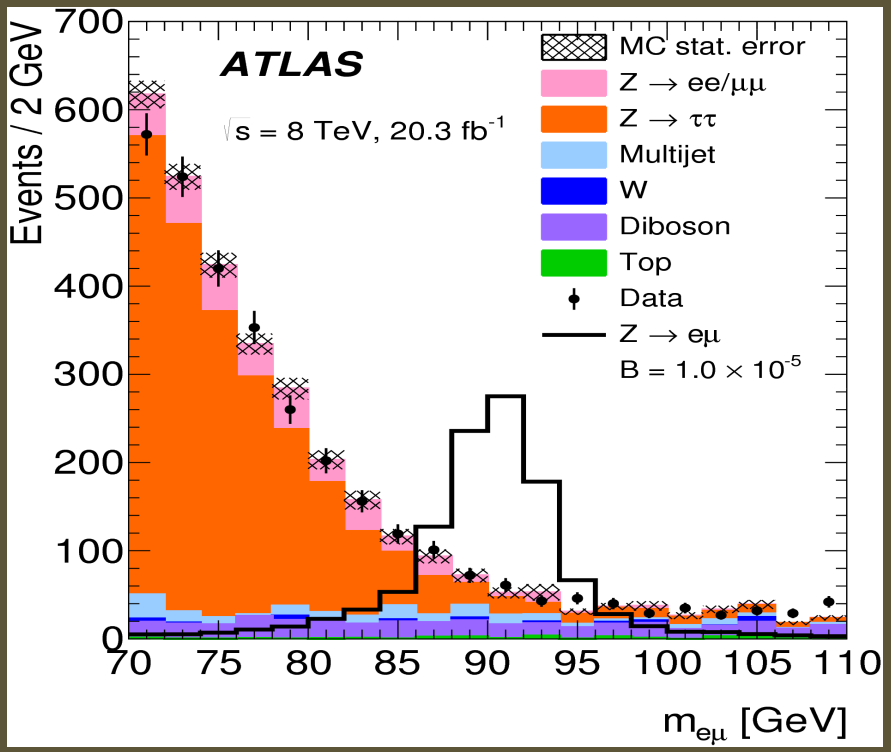

Constraints on LFV Z couplings

μ→eee: B(Z→μe) <5x10^{-13}* (now)

CMS : B(Z→μe) < 7.3 x 10^{-7}

ATLAS: B(Z→μe) < 7.5 x 10^{-7} (now)

* S. Nussinov, R.D. Peccei, and X.M. Zhang, Phys. Rev. D63 (2001) 016003 (arXiv:0004153 [hep-ph]).

Constraints from μ→e Experiments

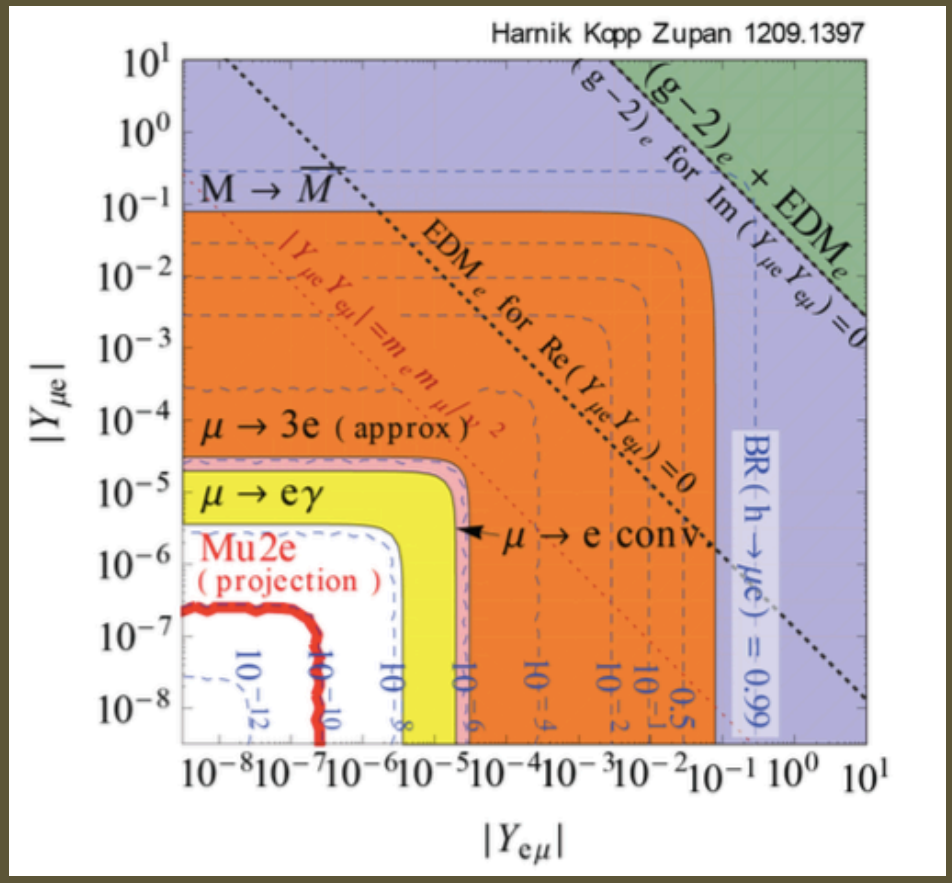

Constraints on LFV Yukawa couplings

μ→eγ : B(h→μe) < 10^{-8}* (now)

μN→eN : B(h→μe) < 10^{-10} (future)

Collider reach
LHC : B(h→μe) < 10^{-2} -10^{-3}

* R. Harnik, J. Kopp, and J. Zupan, JHEP 03 (2013) 026 (arXiv:1209.1397 [hep-ph]).

Constraints from τ→e,μ Experiments

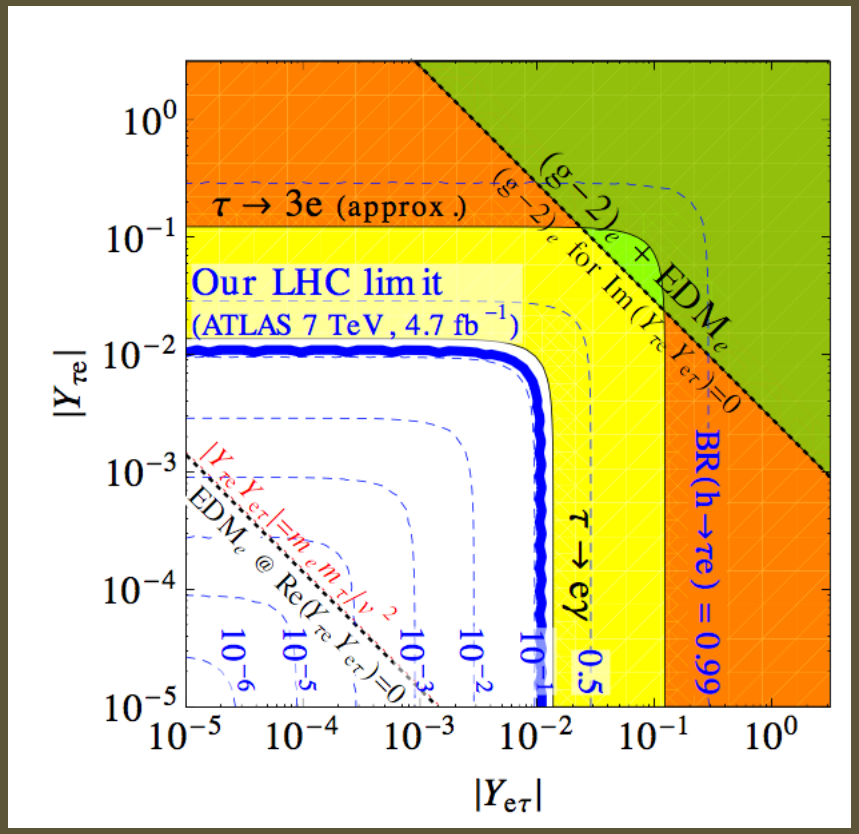

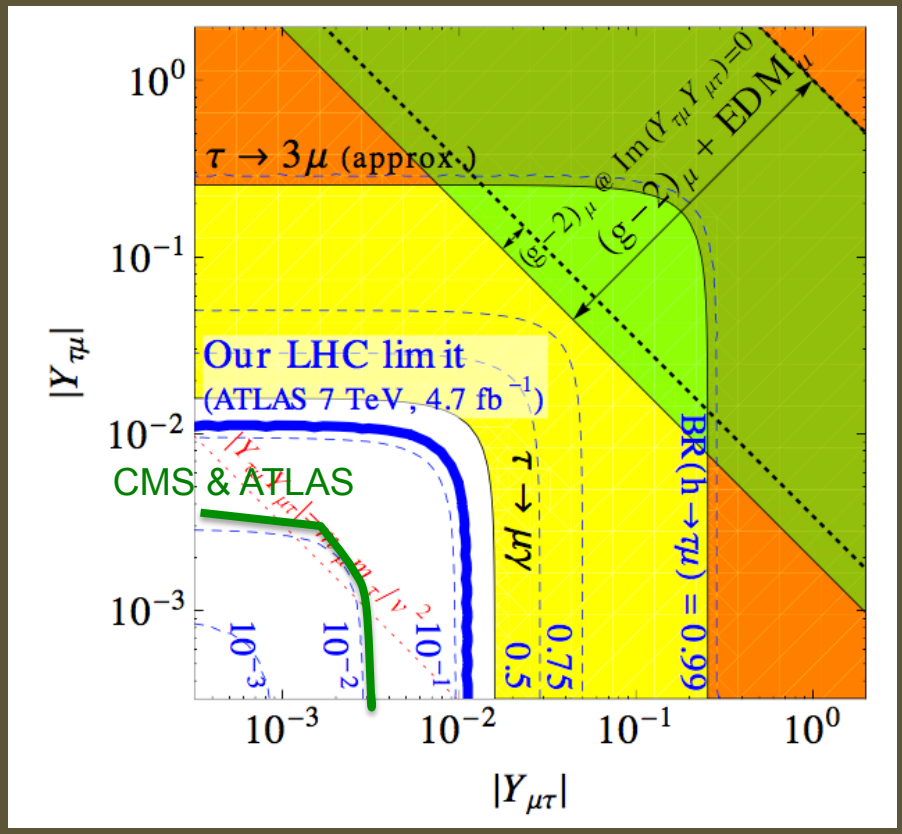

- cLFV using τ correspond to B(h→τe, τμ) ~ 10%
- CMS and ATLAS already exploring B(h→τμ) ~ 1%

h→τ constraints from μ→e cLFV

τμ-τe couplings can contribute to μ→e transitions. As an example:

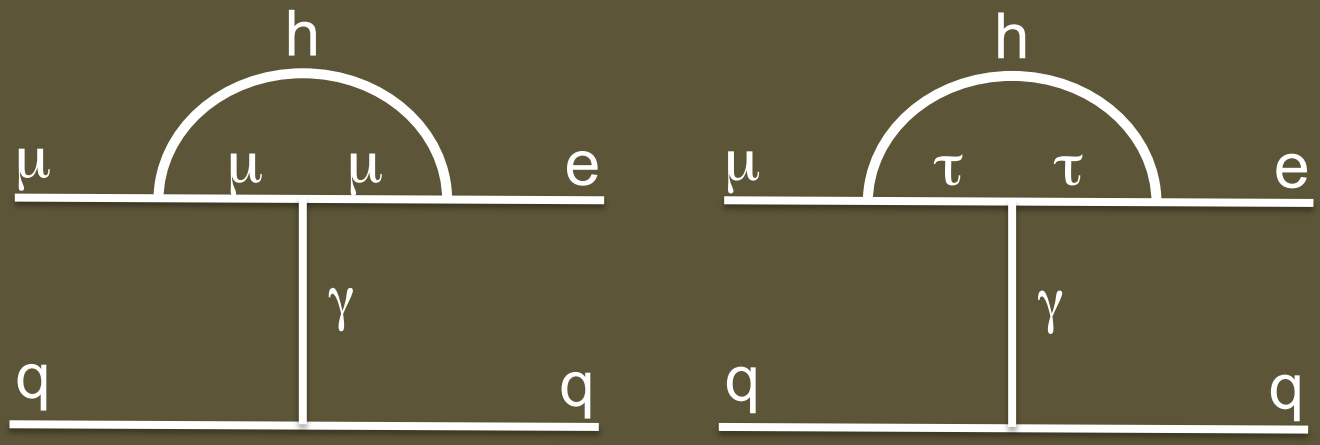

- μ→eγ constrains dipole contributions
- $\mu^- N \rightarrow e^- N$ constrains vector contributions
- Future improvements in $\mu^- N \rightarrow e^- N$ will probe $B(h\rightarrow\tau\mu)B(h\rightarrow\tau e) < 10^{-7}$

cf. I.Dorsner, S. Fajfer, A. Greljo, J. Kamenik, N, Kosnik, I. Nisandzic (1502.07784)
R. Harnik, J. Kopp, J. Supan (1209.1397)

Direct Searches for cLFV h decays

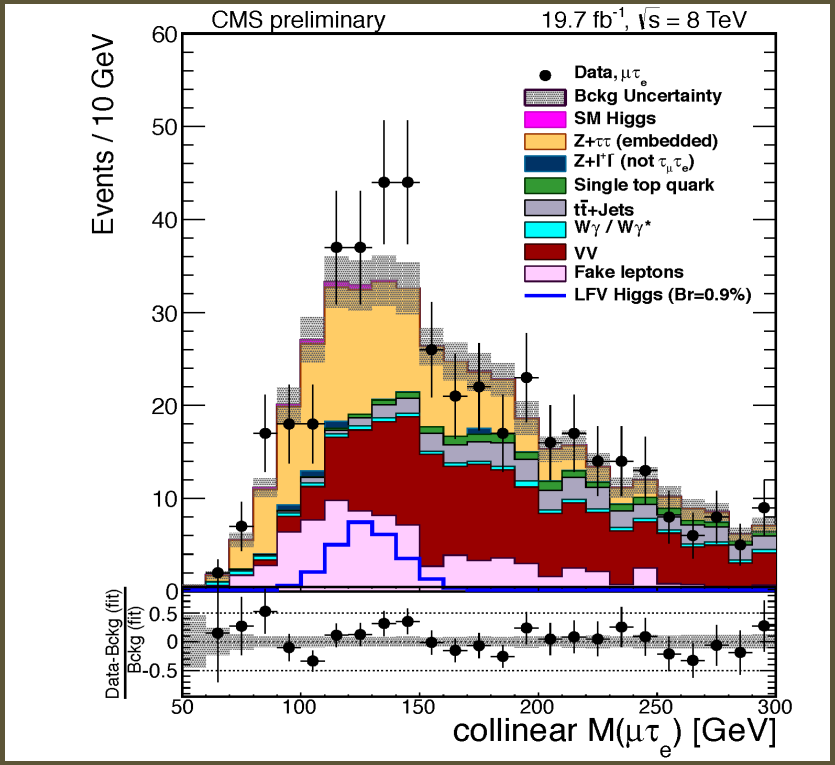

CMS

$B(h \rightarrow \tau\mu) < 1.51 \times 10^{-2}$

Best fit : (0.84 +/- 0.40)%

ATLAS

$B(h \rightarrow \tau\mu) < 1.43 \times 10^{-2}$

Best fit : (0.53 +/- 0.51)%

- Looking forward to more data…

Summary

- cLFV experiments provide deep, broad probes of New Physics parameter space
  - Will probe Λ_{NP} ~ O(10^3- 10^4) TeV >> LHC
- Near future experiments have compelling discovery sensitivity over a broad range of NP models (SUSY, GUT, ED, LHT, 2HDM,…)
- Combining information from >1 cLFV channels can allow a determination of underlying NP mechanism
- cLFV experiments probe NP in a manner that's complementary to the global HEP program

Acknowledgements

- Many thanks to
  - Christophe, Aurelio, Gilad, Frederic
  - D. Asner, S. Banerjee, Y. Kuno, M. Lancaster, J. Miller, T. Mori, A. Schoening, B. Tschirhart

Backup Slides

If an Observation is made?

Can determine details of underlying NP with

- Angular distributions
  - $\mu \rightarrow e\gamma$, eee, τ chnls

Changing stop target

- $\mu N \rightarrow eN$

Ratio of rates

- All

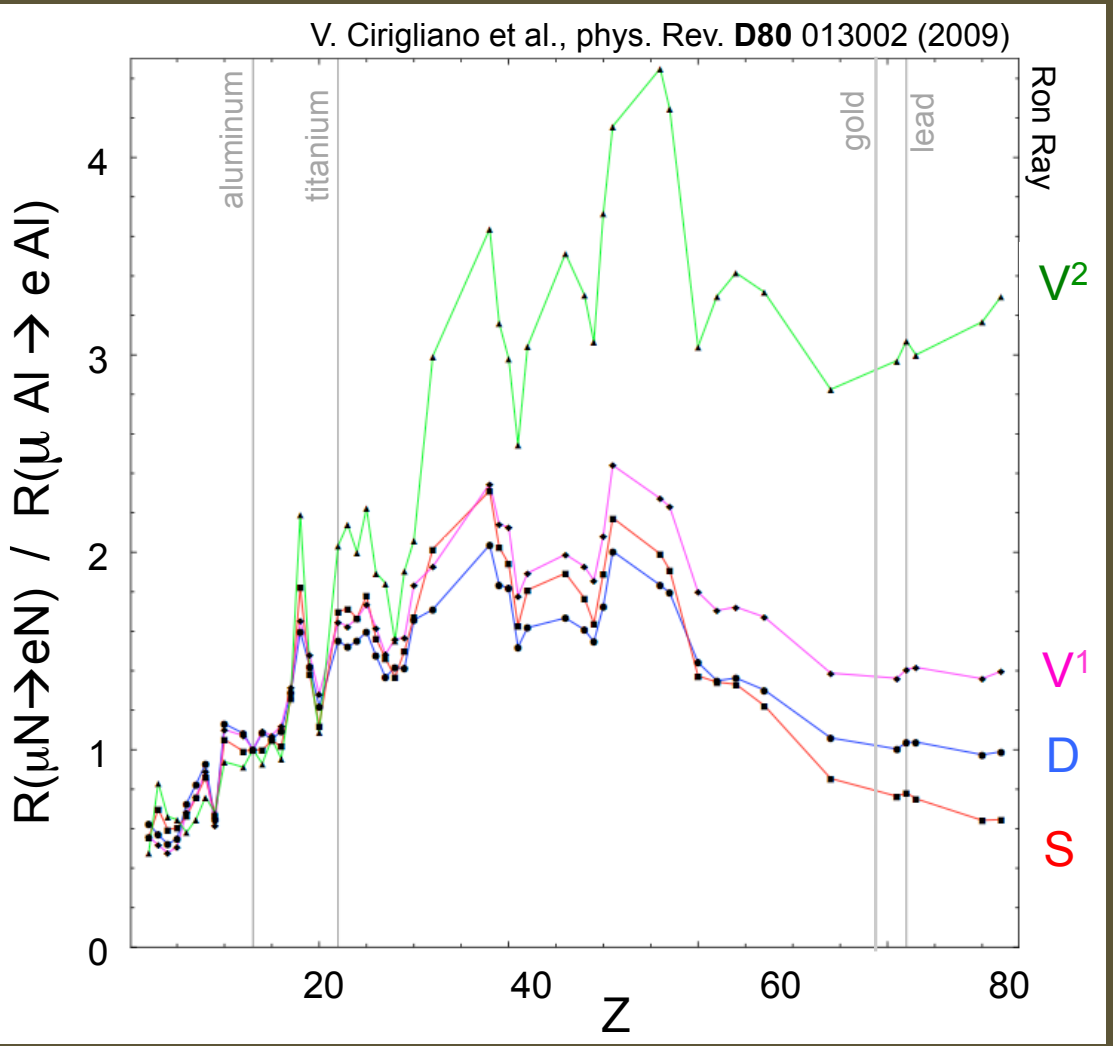

Ratio of Tau LFV decay BF: discrimination of NP models
JHEP 0705, 013(2007), PLB54 252 (2002)

	SUSY+GUT (SUSY+Seesaw)	Higgs mediated	Little Higgs	non-universal Z' boson
$\left(\frac{\tau \to \mu\mu\mu}{\tau \to \mu\gamma}\right)$	~2×10^{-3}	0.06~0.1	0.4~2.3	~16
$\left(\frac{\tau \to \mu ee}{\tau \to \mu\gamma}\right)$	~1×10^{-2}	~1×10^{-2}	0.3~1.6	~16
Br(τ→μγ)	$<10^{-7}$	$<10^{-10}$	$<10^{-10}$	$<10^{-9}$

C. Cecchi @Max

μ→eγ, μ→eee, μN→eN have different sensitivities to new physics

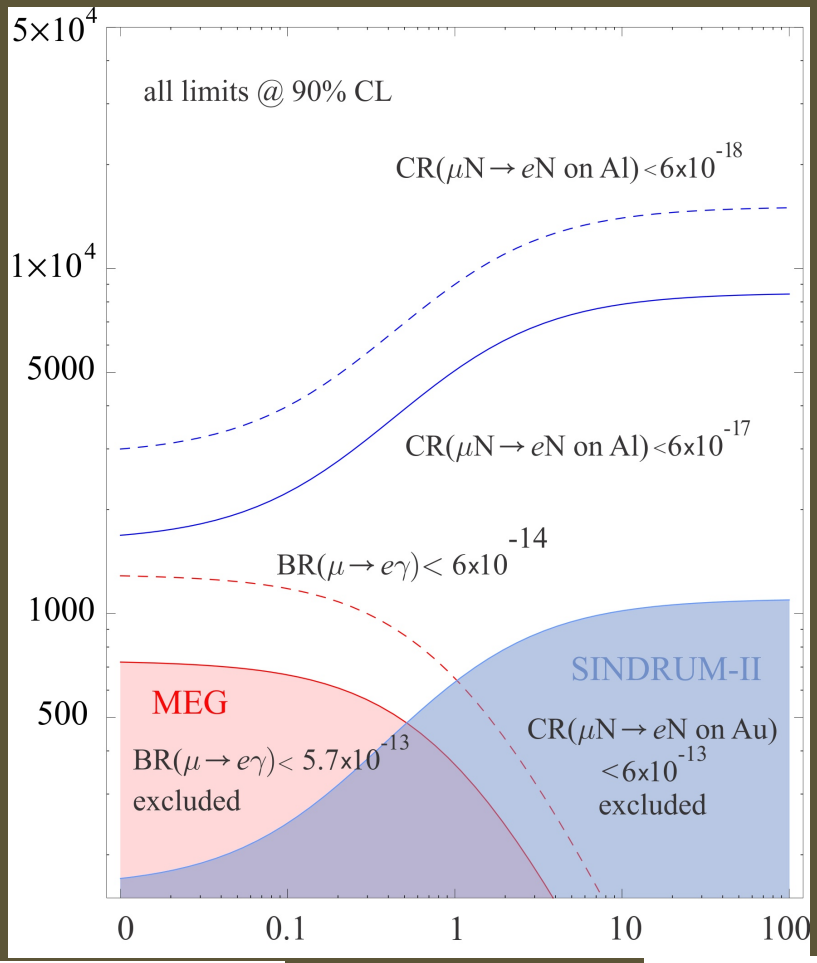

Courtesy A. de Gouvea , B. Bernstein, D. Hitlin

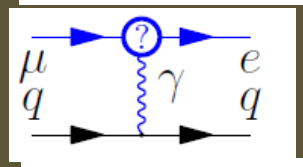

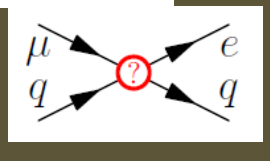

$$L_{CLFV} = \frac{m_\mu}{(1+\kappa)\Lambda^2}\bar{\mu}_R\sigma_{\mu\nu}e_L F^{\mu\nu} + \frac{\kappa}{(1+\kappa)\Lambda^2}\bar{\mu}_L\gamma_\mu e_L(\bar{u}_L\gamma^\mu u_L + \bar{d}_L\gamma^\mu d_L)$$

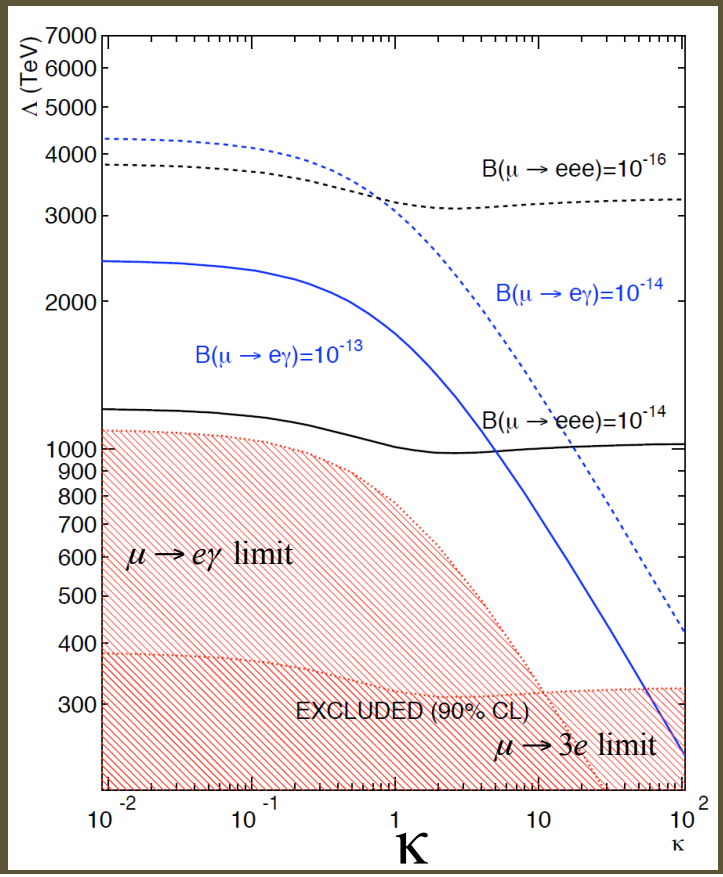

$$L_{CLFV} = \frac{m_\mu}{(1+\kappa)\Lambda^2}\bar{\mu}_R\sigma_{\mu\nu}e_L F^{\mu\nu} + \frac{\kappa}{(1+\kappa)\Lambda^2}\bar{\mu}_L\gamma_\mu e_L(\bar{e}\gamma^\mu e)$$

From deGouvea and Vogel

New Physics Contributions to μN→eN

Loops

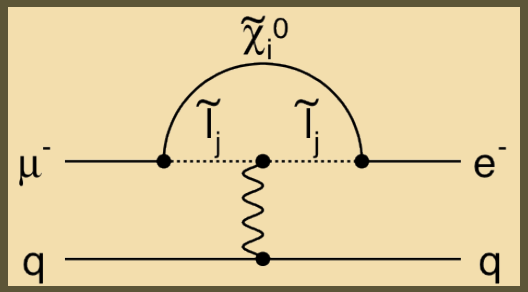

Supersymmetry

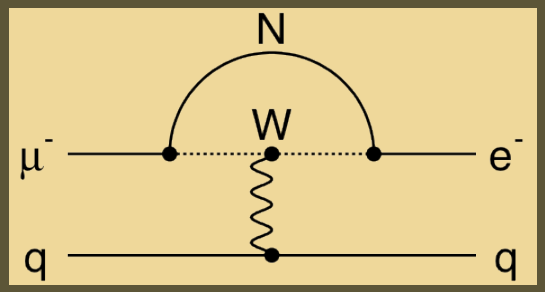

Heavy Neutrinos

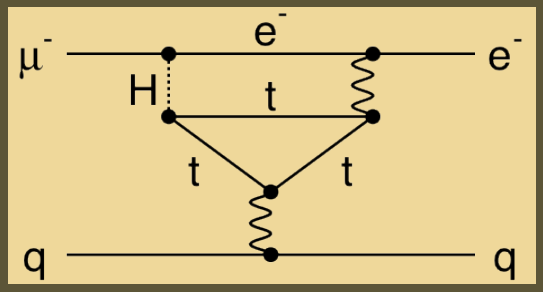

Two Higgs Doublets

Contact Terms

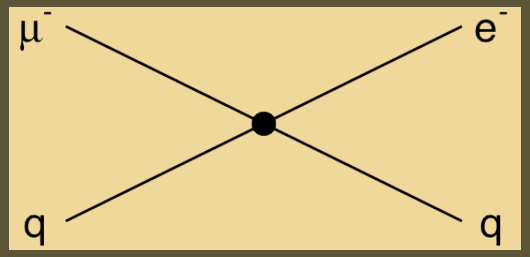

Compositeness

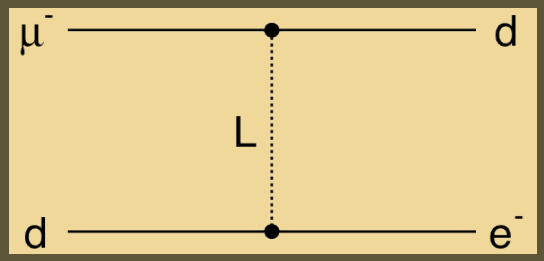

Leptoquarks

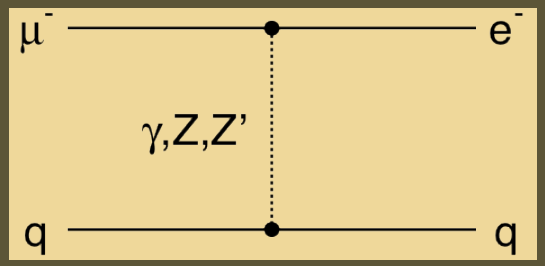

New Heavy Bosons / Anomalous Couplings

μN→eN sensitive to wide array of New Physics models

cLFV Sensitivity

★★★ = Discovery Sensitivity

W. Altmannshofer, A.J.Buras, S.Gori, P.Paradisi, D.M.Straub

	AC	RVV2	AKM	δLL	FBMSSM	LHT	RS
$D^0 - \bar{D}^0$	★★★	★	★	★	★	★★★	?
ϵ_K	★	★★★	★★★	★	★	★★	★★★
$S_{\psi\phi}$	★★★	★★★	★★★	★	★	★★★	★★★
$S_{\phi K_S}$	★★★	★★	★	★★★	★★★	★	?
$A_{\rm CP}(B \to X_s\gamma)$	★	★	★	★★★	★★★	★	?
$A_{7,8}(B \to K^*\mu^+\mu^-)$	★	★	★	★★★	★★★	★★	?
$A_9(B \to K^*\mu^+\mu^-)$	★	★	★	★	★	★	?
$B \to K^{(*)}\nu\bar{\nu}$	★	★	★	★	★	★	★
$B_s \to \mu^+\mu^-$	★★★	★★★	★★★	★★★	★★★	★	★
$K^+ \to \pi^+\nu\bar{\nu}$	★	★	★	★	★	★★★	★★★
$K_L \to \pi^0\nu\bar{\nu}$	★	★	★	★	★	★★★	★★★
$\mu \to e\gamma$	★★★	★★★	★★★	★★★	★★★	★★★	★★★
$\tau \to \mu\gamma$	★★★	★★★	★	★★★	★★★	★★★	★★★
$\mu + N \to e + N$	★★★	★★★	★★★	★★★	★★★	★★★	★★★
d_n	★★★	★★★	★★★	★★	★★★	★	★★★
d_e	★★★	★★★	★★	★	★★★	★	★★★
$(g-2)_\mu$	★★★	★★★	★★	★★★	★★★	★	?

Table 8: "DNA" of flavour physics effects for the most interesting observables in a selection of SUSY and non-SUSY models ★★★ signals large effects, ★★ visible but small effects and ★ implies that the given model does not predict sizable effects in that observable.

arXiv:0909.1333[hep-ph]

AC	U(1) flavor symmetry
RVV2	Non-abelian SU(3)-flavored MSSM
AKM	SU(3)-flavored SUSY
δLL	LH CKM-like currents
FBMSSM	Flavor-blind MSSM
LHT	Little Higgs w/T parity
RS	Randall-Sundrum

Neutrino Mass Hierarchy

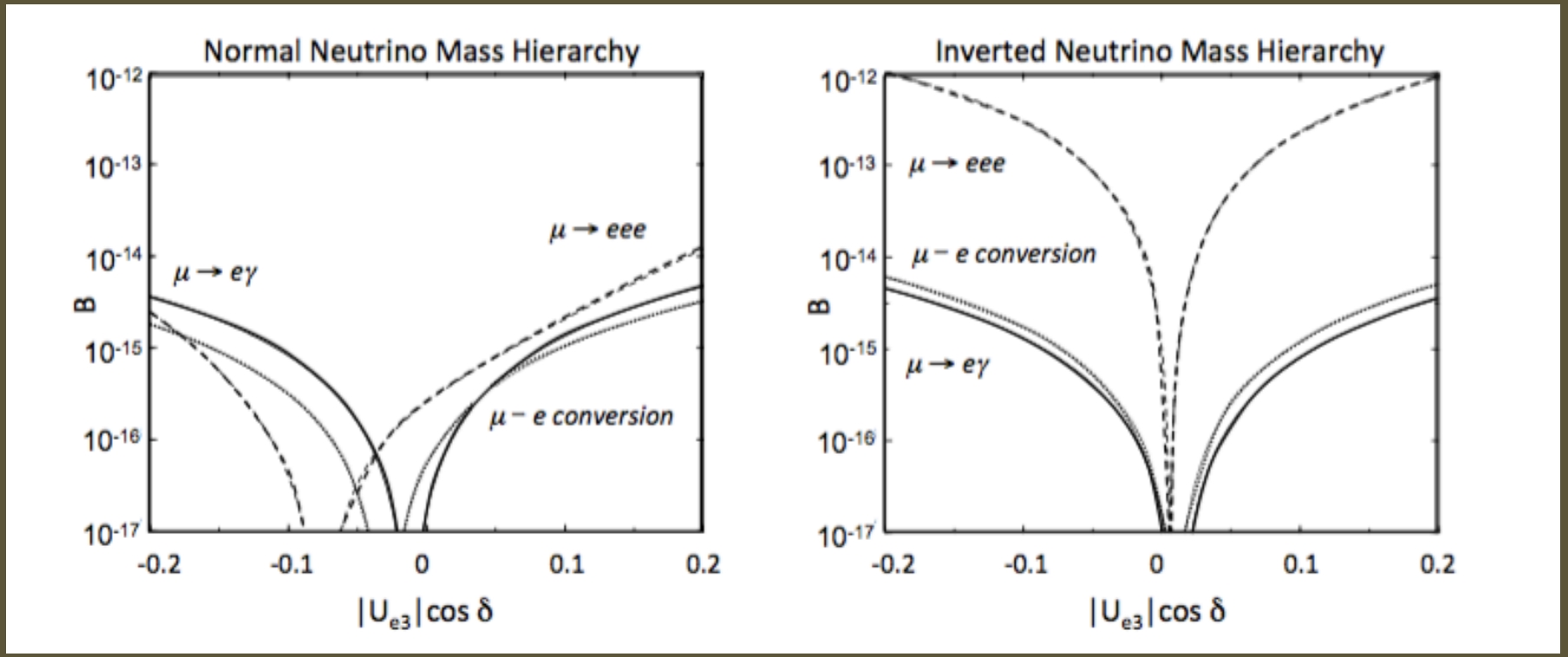

- Majorana neutrino mass from SU(2) triplet higgs field
  M. Kakizaki, et al, Phys. Lett. **B566**, 210 (2003)

Split SUSY

Sfermions not at TeV scale but: 100 – 1000 TeV with gauginos at a few TeV

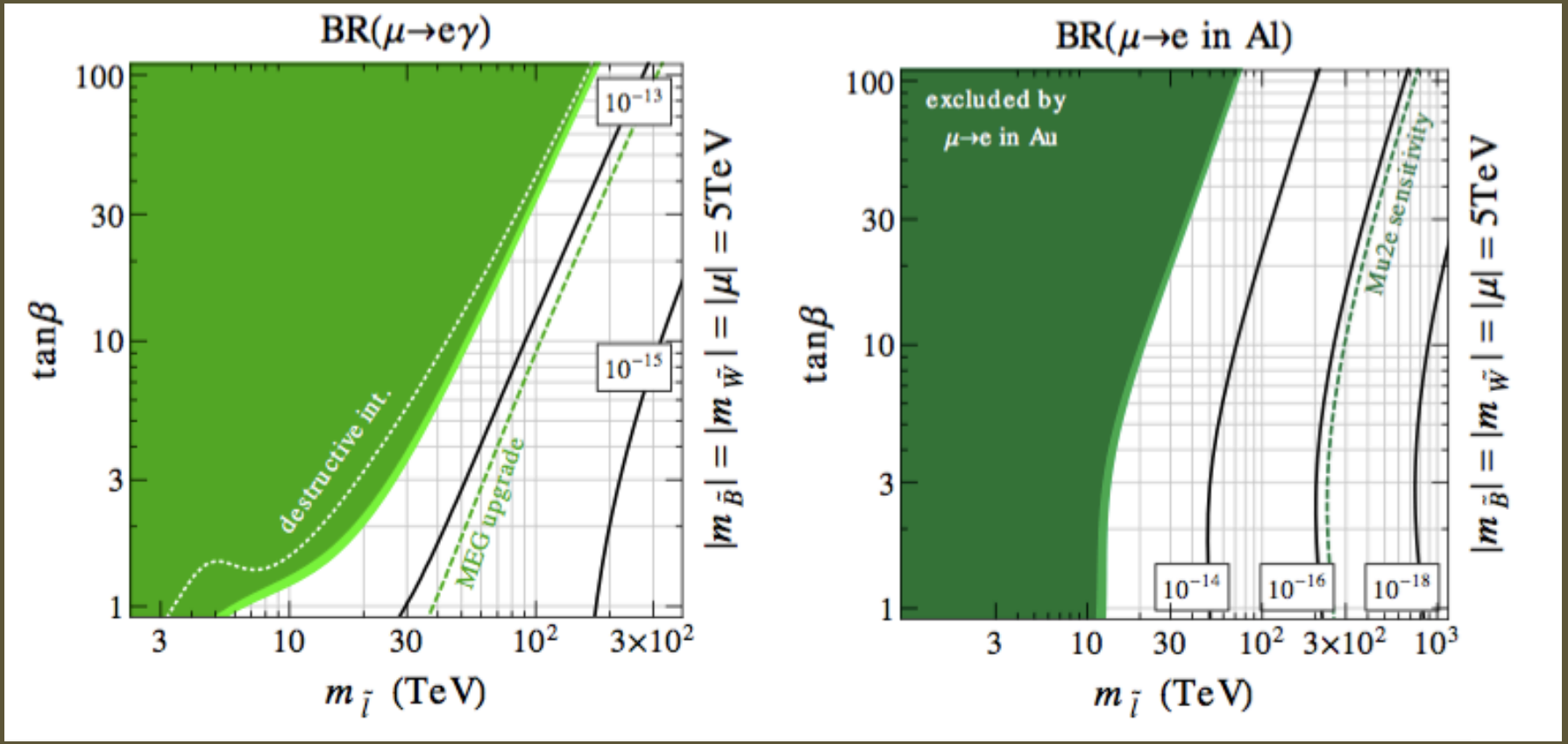

cLFV experiments probe slepton mass scales >>1 TeV/c^2

MEG Detector

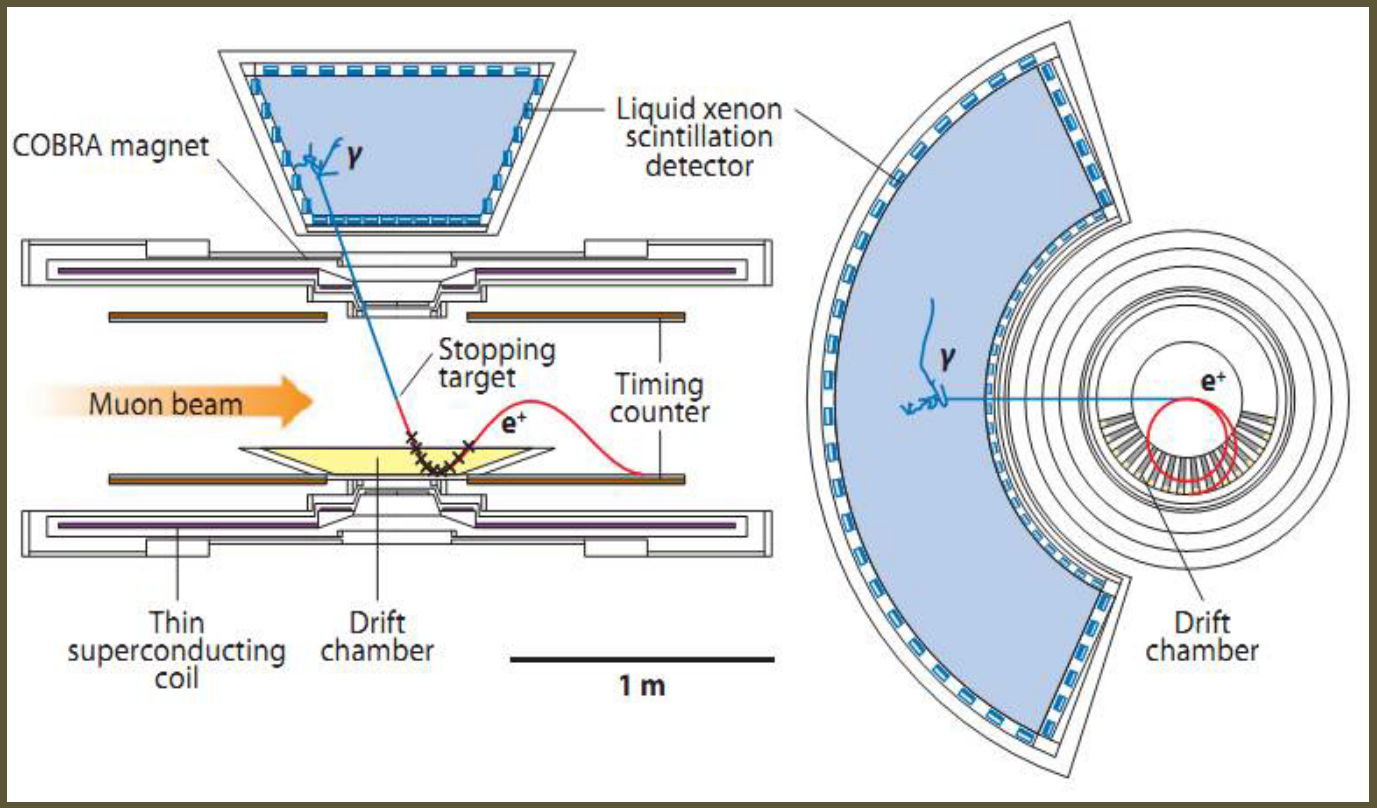

- Diameter of COBRA clear bore = 71 cm

MEG Calibration

- E_e calibrated using Michel edge
- E_γ calibrated during special runs using a liquid hydrogen target
  - π^- p → π^0 n → $\gamma\gamma$ n (pion charge exchange)
  - Tag opposite side γ using a small movable BGO array dedicated to this calibration
  - The angle and energy of the opposite side tag can be used to define a mono-energetic source of γ in the LXe (~55 MeV)

MEG Calibration

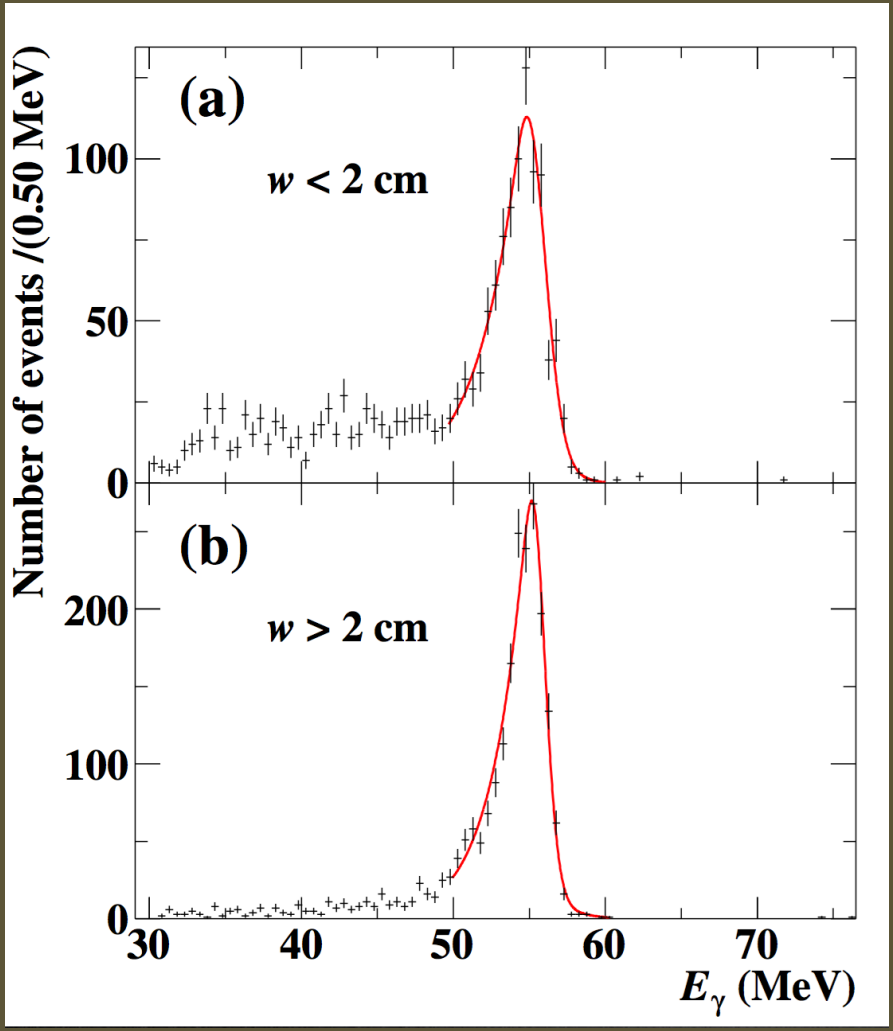

- Photon energy scale determined to <1%
- Monitor stability of Eγ with short special runs that use a <1 MeV proton beam and a $Li_2B_4O_7$ target to produce photons at 18, 12, & 4 MeV

MEG Calibration

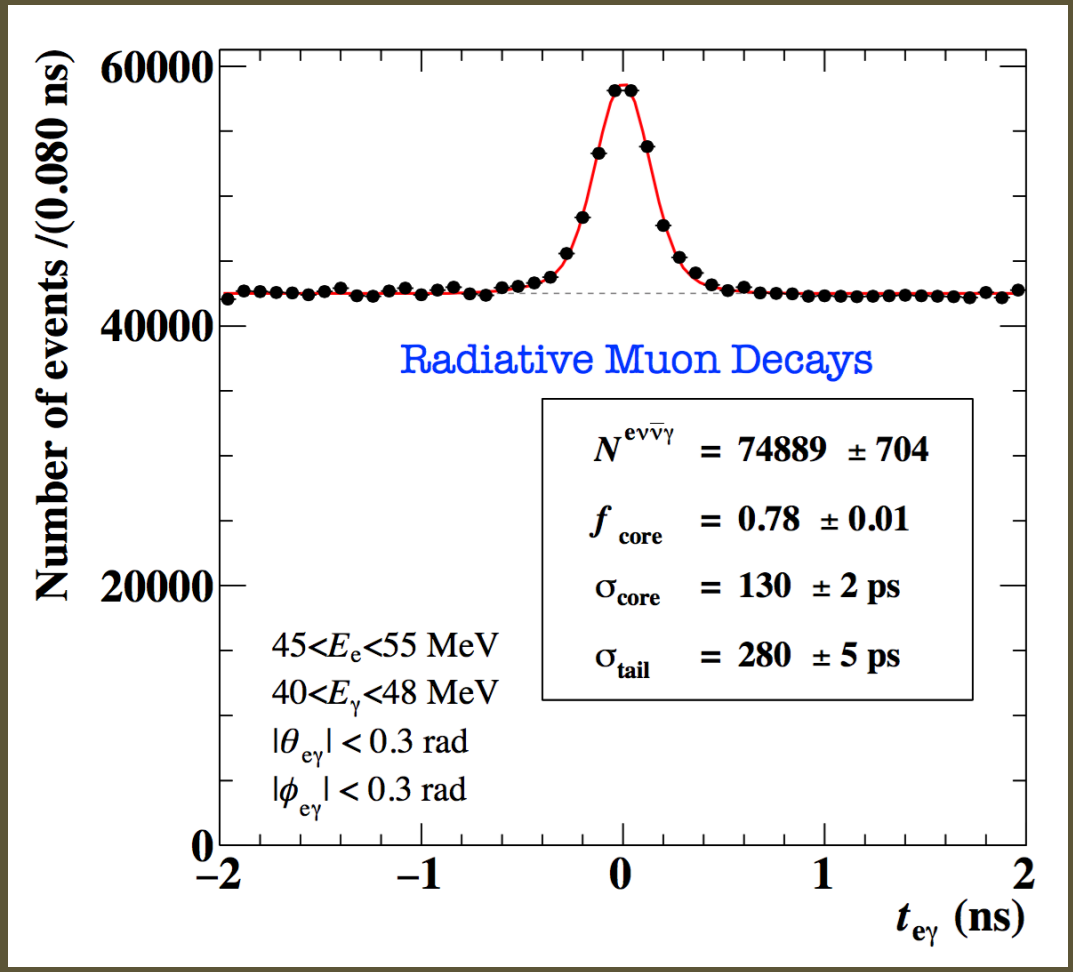

- Relative e-γ timing calibrated using radiative muon decays

MEG Backgrounds

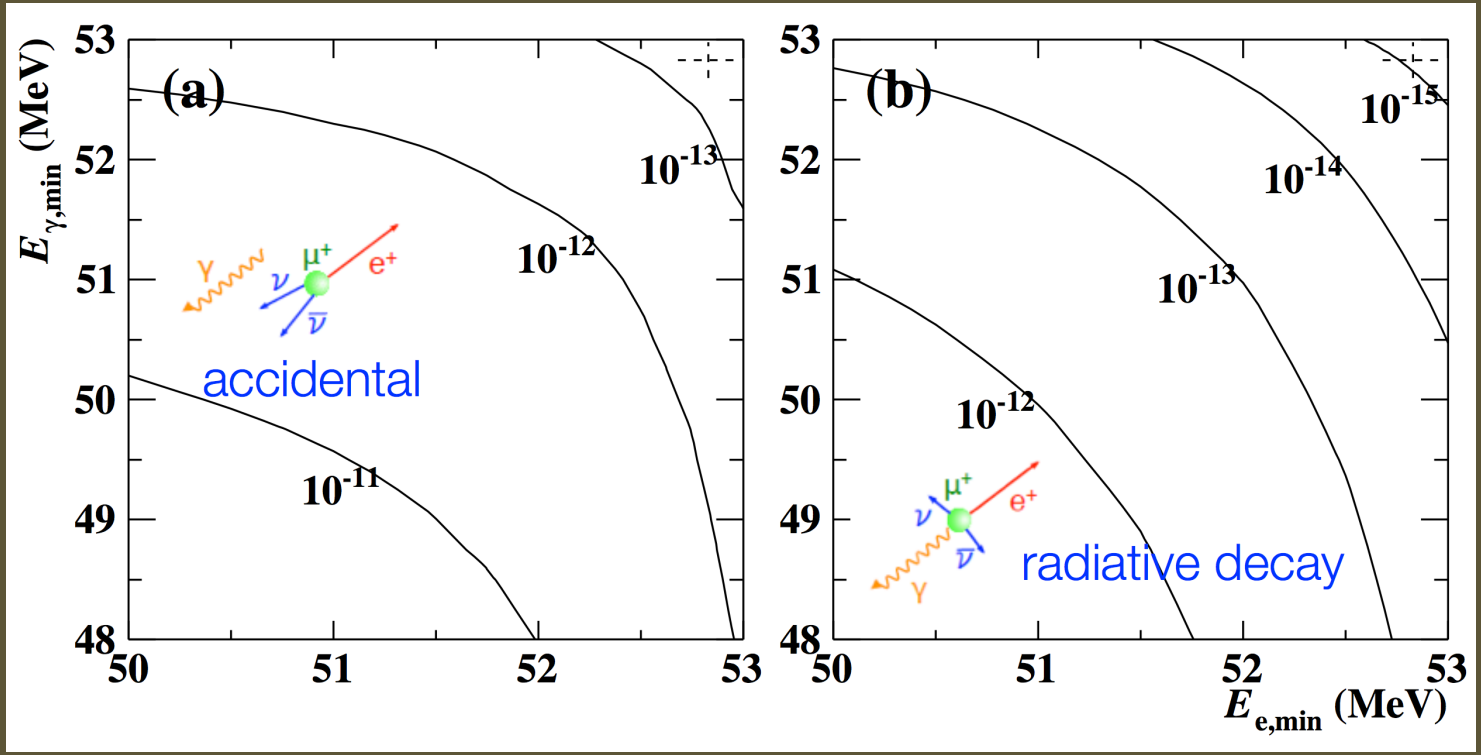

- Accidental backgrounds dominate.

MEG Accidental Background

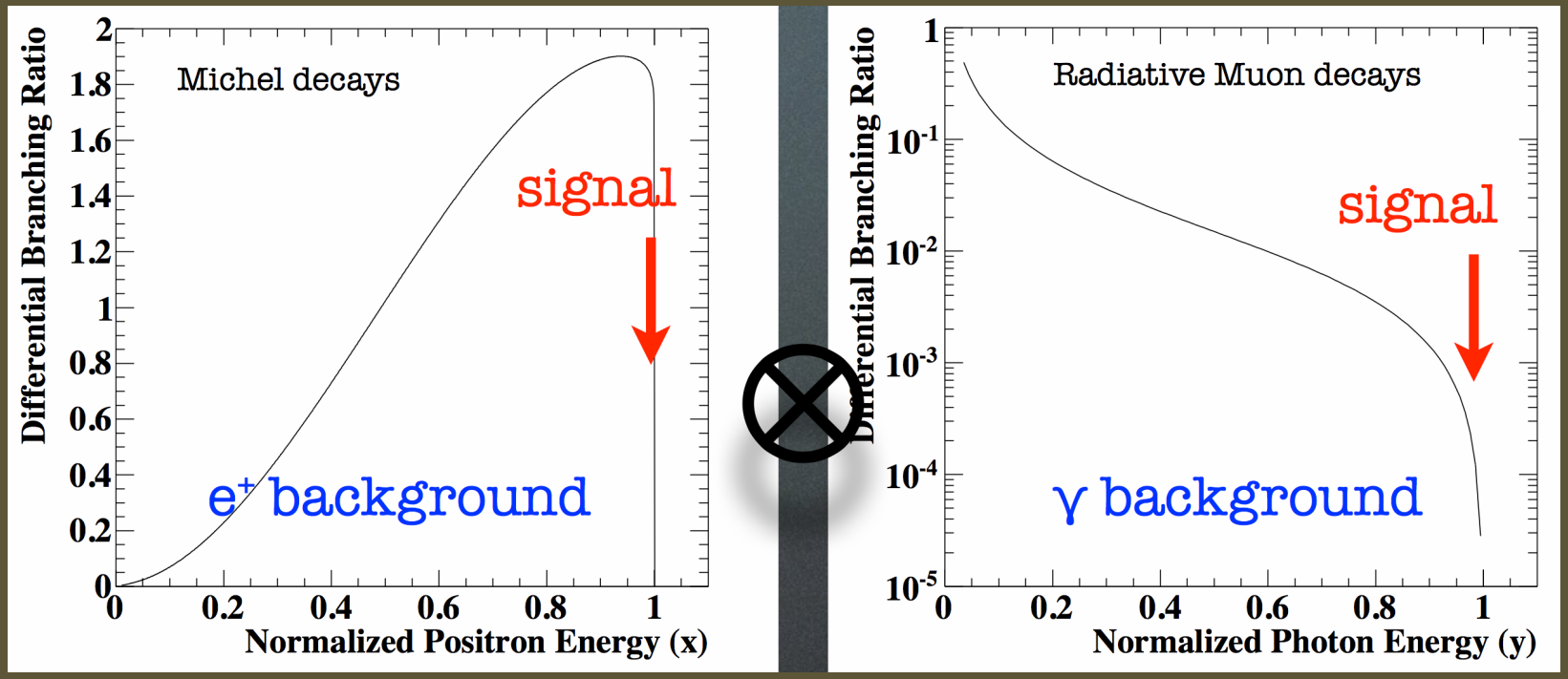

- Both curves are steeply falling in region of interest… sensitivity strong function of σ_E

DeeMee ($\mu^-N \rightarrow e^-N$)

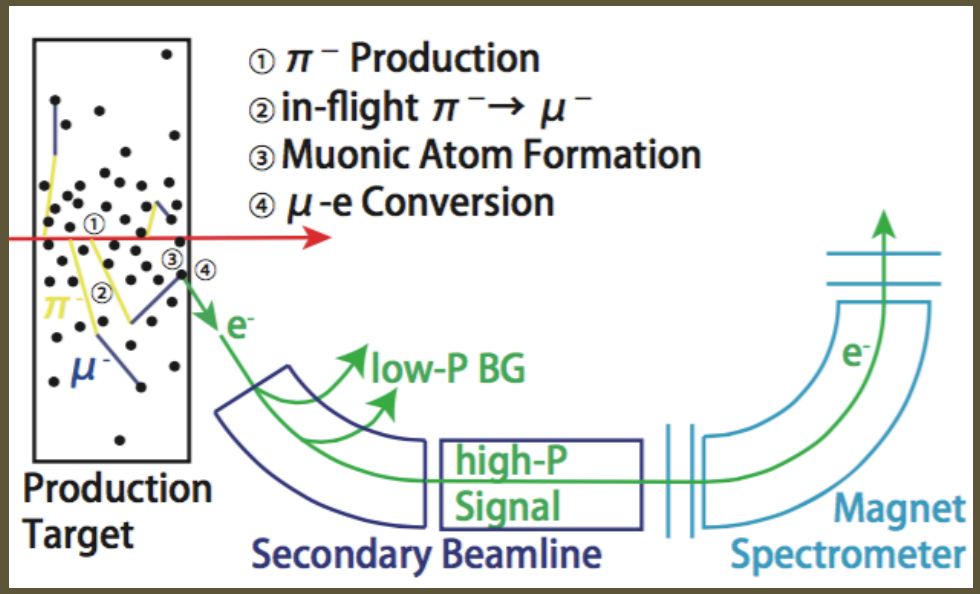

- New concept at JPARC
- Use thick target as production, deay, and stopping volumes
- Customize beam line to select momentum bite near $E_{\mu e} \sim m_{\mu}$ so that you're sensitive to $\mu N \rightarrow eN$ that occurs near the target surface
- Goal: $R_{\mu e} < 2 \times 10^{-14}$ @ 90%CL

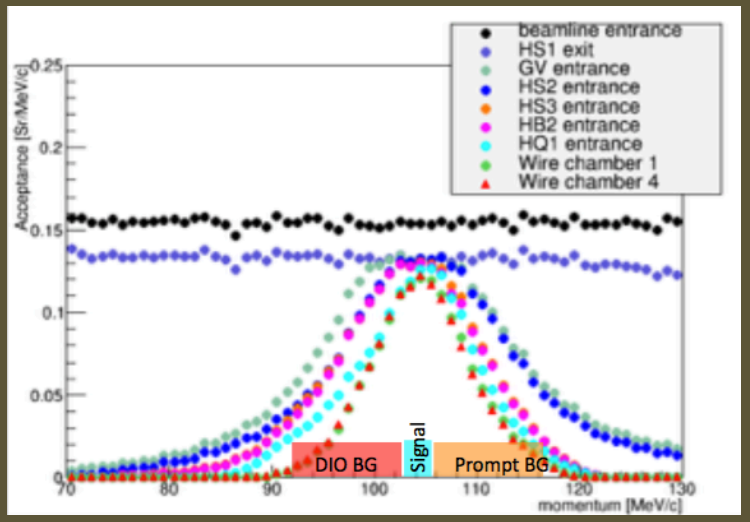

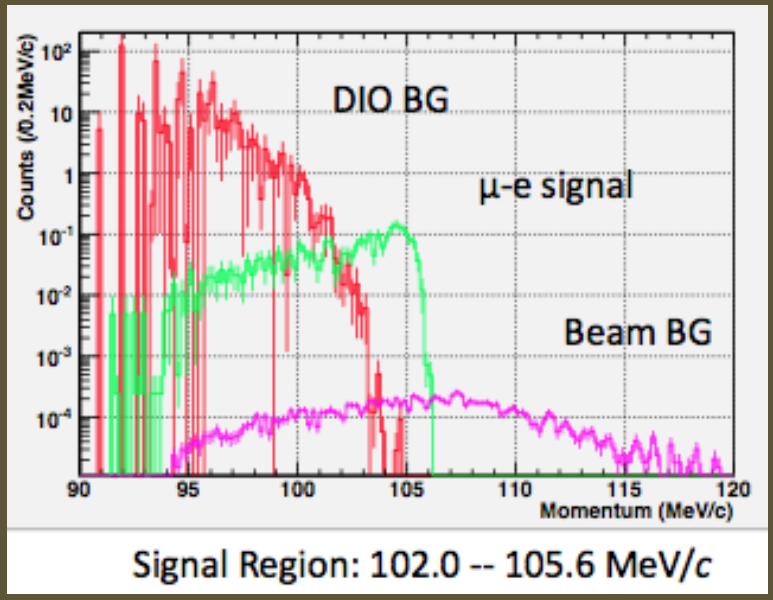

COMET Phase I & II

28

Summary of COMET phase-I/II

	COMET-Phase-I	COMET-Phase-II
experiment starts (*)	2019	2021
beam intensity	3.2kW (8GeV)	56kW (8GeV)
running time	1.5×10^{6} (sec)	2.0×10^{7} (sec)
# of protons	3.8×10^{18}	8.5×10^{20}
# of muon stops	8.7×10^{15}	2.0×10^{18}
muon rate	5.8×10^{9}	1.0×10^{11}
# of muon stops / proton	0.0023	0.0023
# of BG	0.03	0.3
S.E.S.	3.1×10^{-15}	2.6×10^{-17}
U.L. (90%CL.)	7.0×10^{-15}	6.0×10^{-17}

(*) Engineering runs and Physics runs

H.Nishiguchi(KEK) Project of Muon LFV at J-PARC Tau2012, Nagoya

Mu2e Backgrounds

Category	Source	Events
Intrinsic	μ Decay in Orbit	0.20
	Radiative μ Capture	<0.01
Late Arriving	Radiative π Capture	0.02
	Beam electrons	<0.01
	μ Decay in Flight	<0.01
	π Decay in Flight	<0.01
Miscellaneous	Anti-proton induced	0.05
	Cosmic Ray induced	0.10
Total Background		0.37

(assuming 6.8E17 stopped muons in 6E7 s of beam time)

- Designed to be nearly background free

Mu2e Intrinsic Backgrounds

Once trapped in orbit, muons will:

1) Decay in orbit (DIO): $\mu^- N \rightarrow e^- \nu_\mu \nu_e N$
   - For Al. DIO fraction is 39%
   - Electron spectrum has tail out to 104.96 MeV
   - Accounts for ~55% of total background

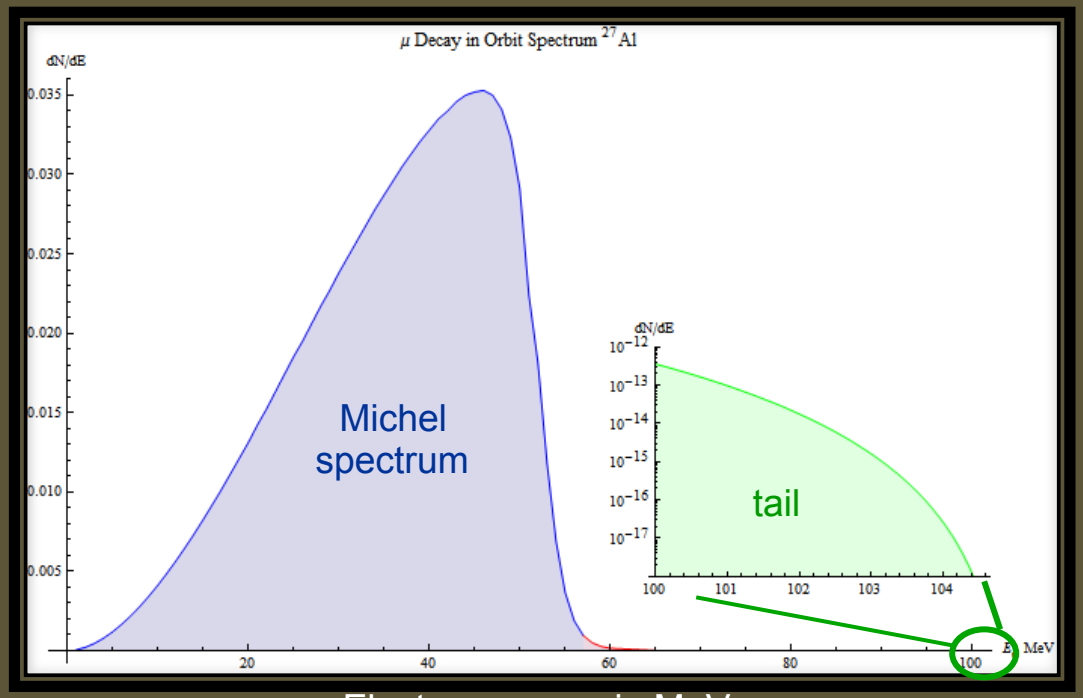

Electron energy in MeV

The Mu2e Proton Beam

Quantity	Value	Units
MI-RR Cycle Time	1400.0	msec
Number of Spills per MI-RR Cycle	8	
Spill Duration	43.12	msec
Reset (Beam Off) Time Between Spills	5	msec
Number of Pulses per Spill	25.4k	
Pulse Spacing	1695	ns
Protons on Target (POT) Per Pulse	39×10^{6}	POT
Instantaneous Rate	24×10^{12}	POT/s
Average Rate	6×10^{12}	POT/s
Duty Factor	25%	
Proton Beam Energy	8	GeV

- Mu2e will use 8kW of 8 GeV proton beam

Mu2e Solenoid Summary

	PS	TS	DS
Length (m)	4	13	11
Diameter (m)	1.7	0.4	1.9
Field @ start (T)	4.6	2.5	2.0
Field @ end (T)	2.5	2.0	1.0
Number of coils	3	52	11
Conductor (km)	10	44	15
Operating current (kA)	10	3	6
Stored energy (MJ)	80	20	30
Cold mass (tons)	11	26	8

- PS, DS will be built by General Atomics
- TS will be ASG + Fermilab

The Mu2e Tracker

- Will employ straw technology
  - Low mass
  - Can reliably operate in vacuum
  - Robust against single-wire failures

- 5 mm diameter straw
- Spiral wound
- Walls: 12 μm Mylar + 3 μm epoxy + 200 Å Au + 500 Å Al
- 25 μm Au-plated W sense wire
- 33 – 117 cm in length
- 80/20 Ar/CO2 with HV < 1500 V

The Mu2e Tracker

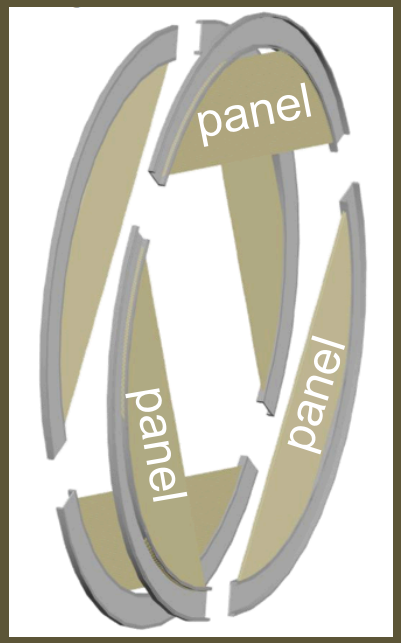

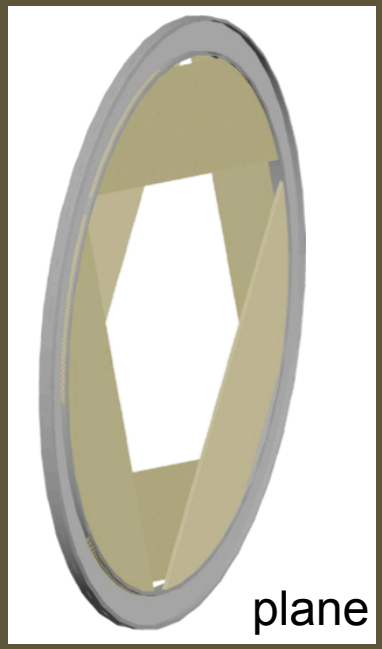

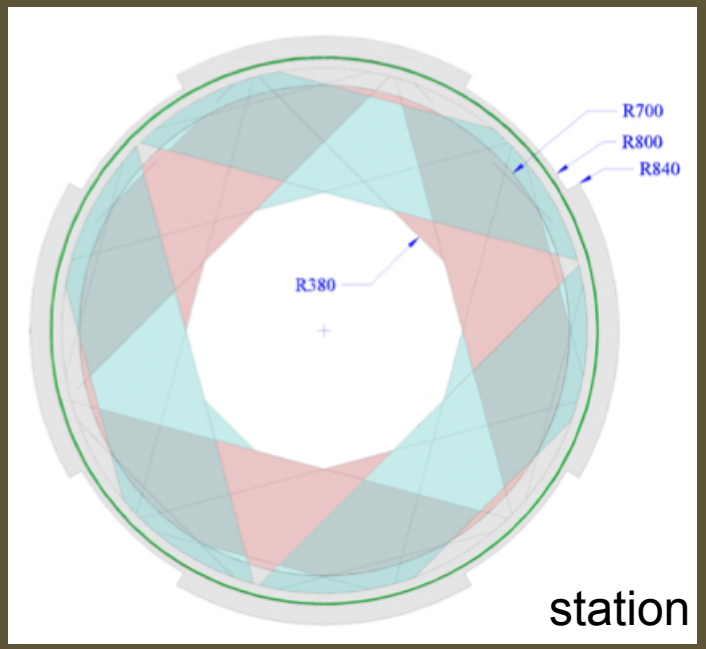

- Self-supporting “panel” consists of 100 straws
- 6 panels assembled to make a “plane”
- 2 planes assembled to make a “station”
- Rotation of panels and planes improves stereo information
- >20k straws total

The Mu2e Tracker

- 18 “stations” with straws transverse to the beam
- Naturally moves readout and support to large radii, out of the active volume

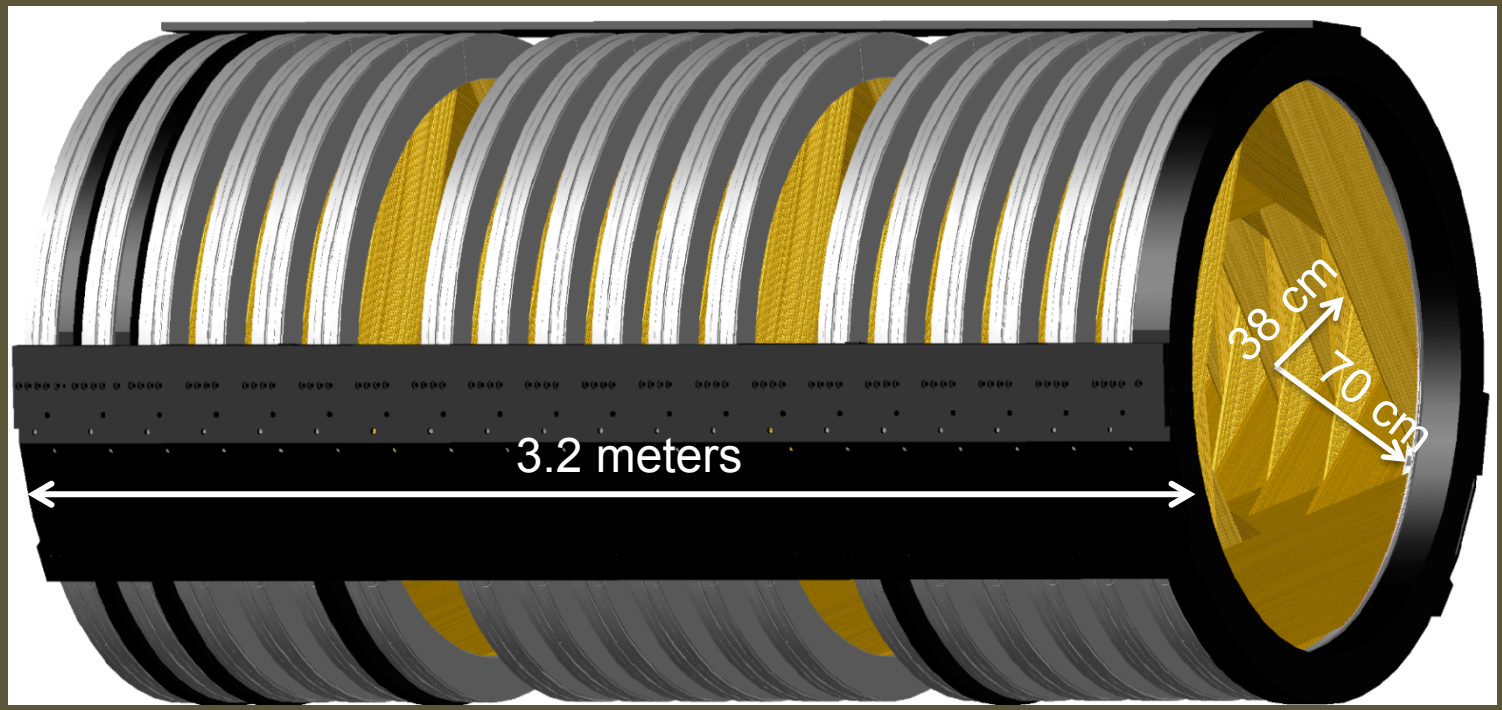

The Mu2e Tracker

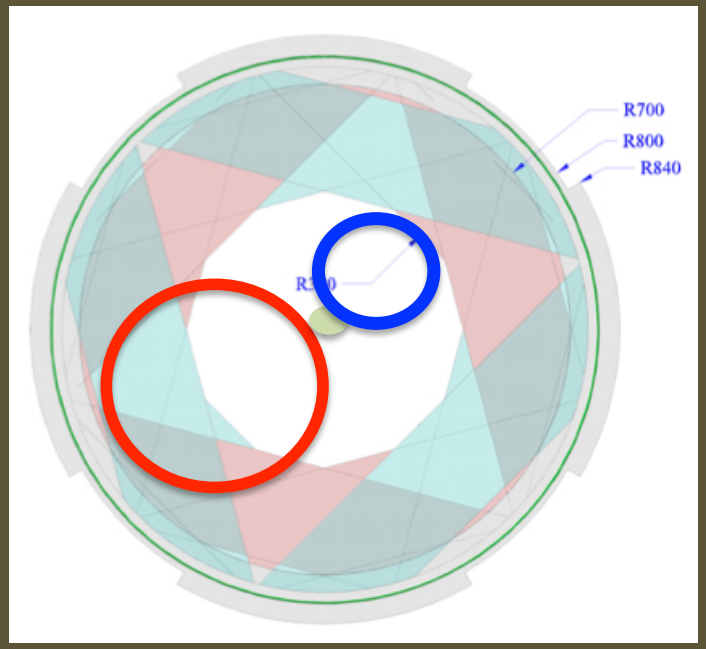

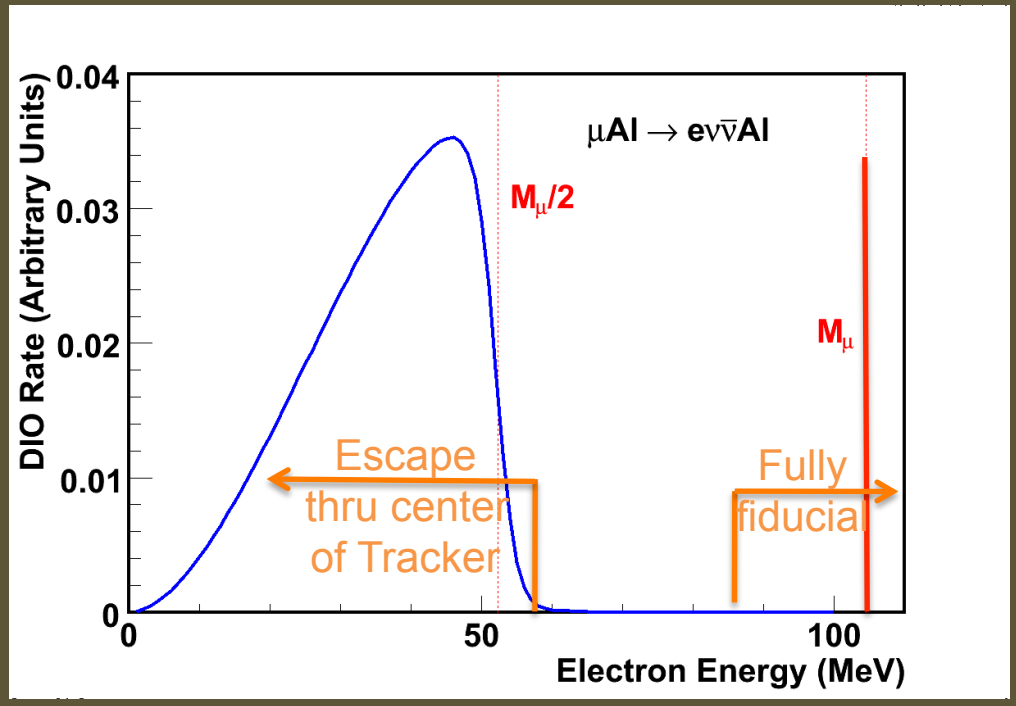

- Inner 38 cm is purposefully un-instrumented
  - Blind to beam flash
  - Blind to >99% of DIO spectrum

Mu2e Spectrometer Performance

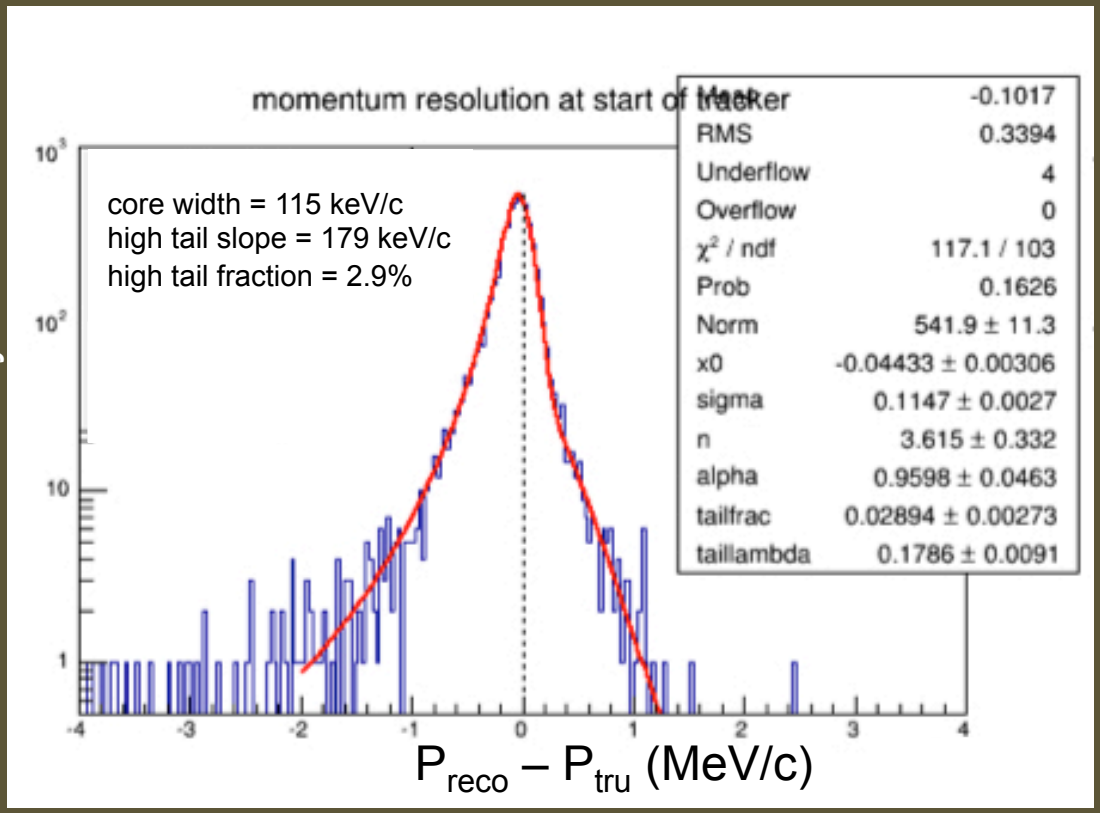

- Performance well within physics requirements

After all analysis requirements

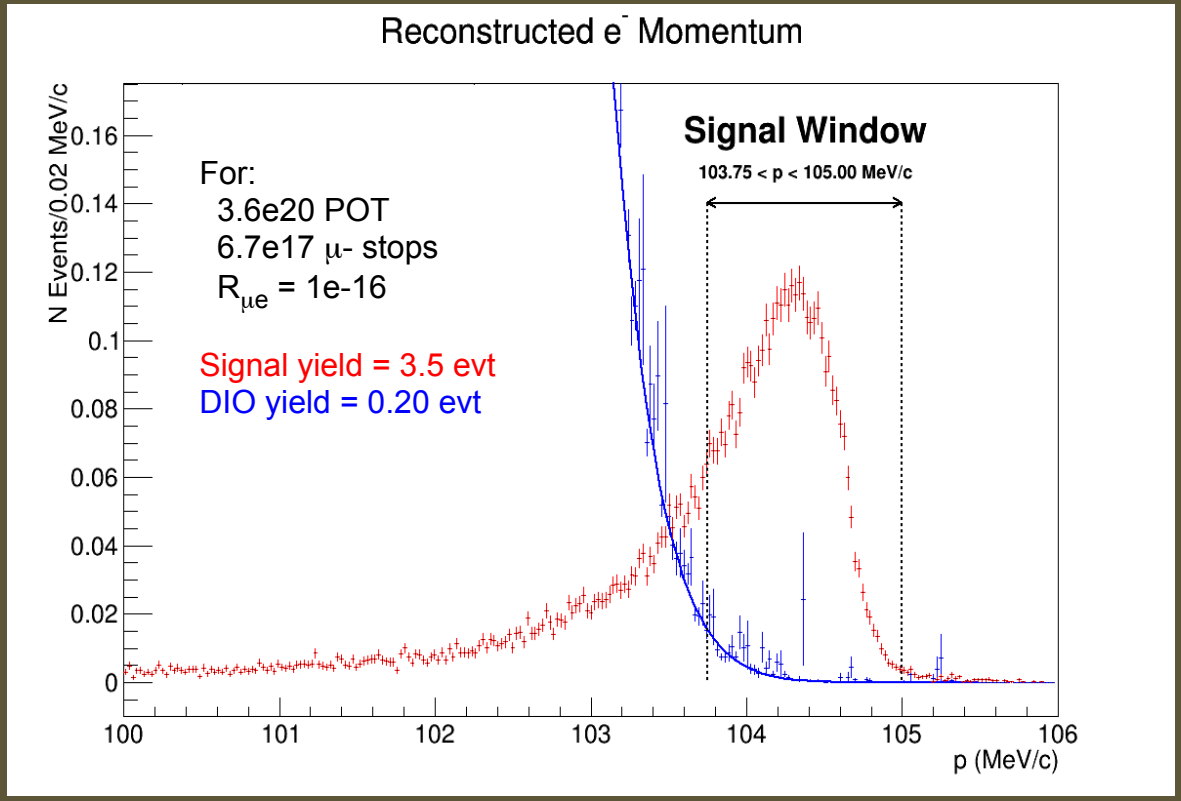

- Single-event-sensitivity = 2.9 x 10^{-17} (SES goal 2.4 x 10^{-17})
- Total background < 0.5 events

Track Reconstruction and Selection

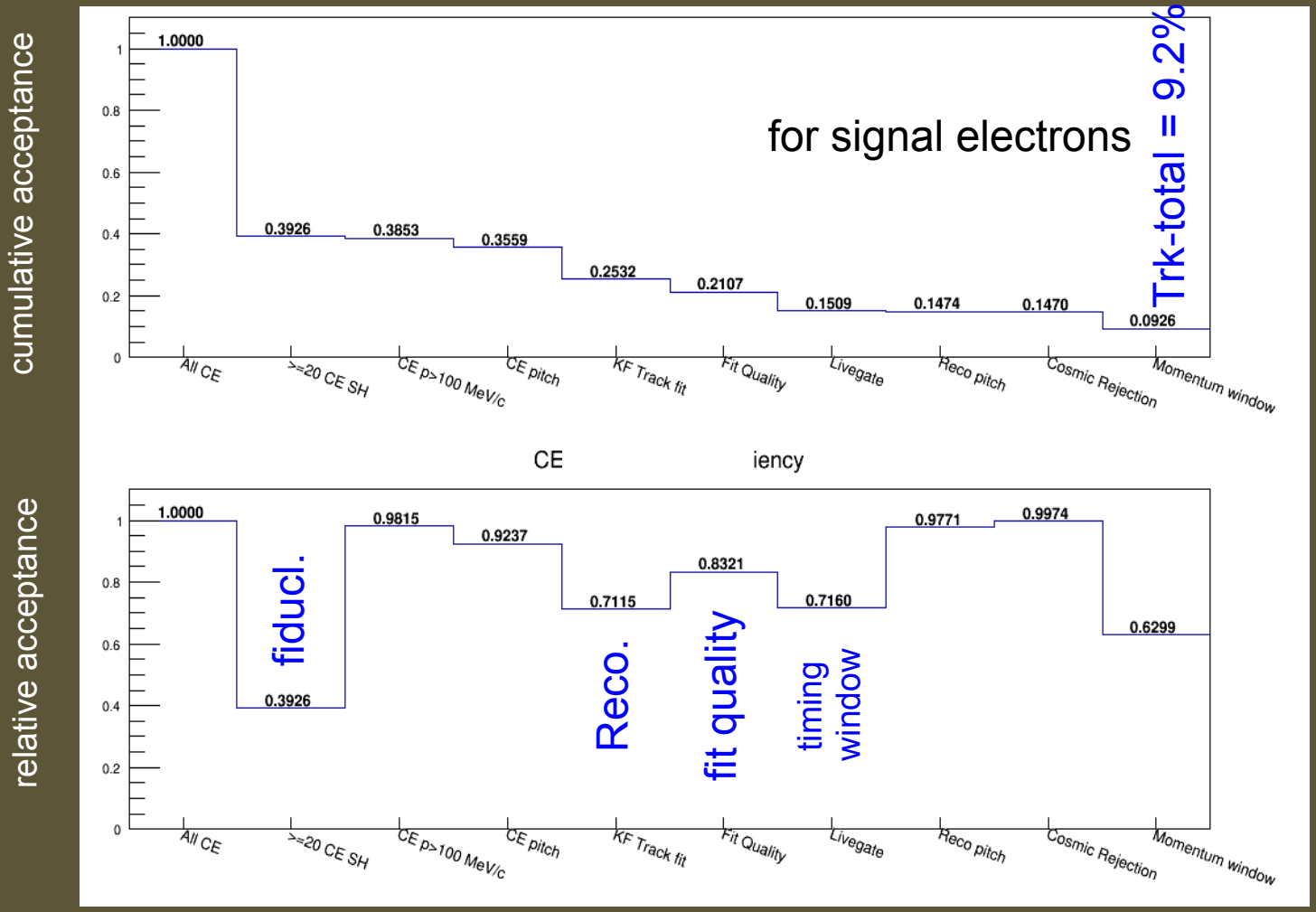

Inefficiency dominated by geometric acceptance

After calorimeter PID and CRV deadtime, Total = 8.5%

Mu2e Performance

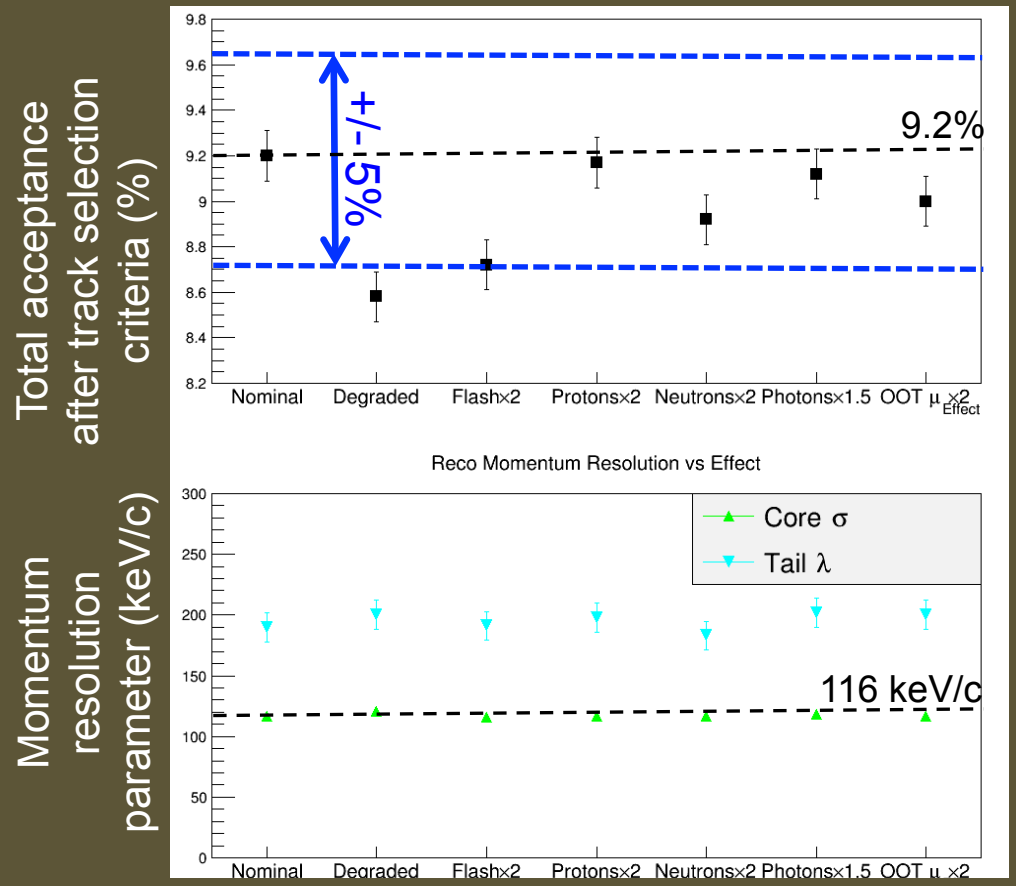

- Robust against increases in rate

Mu2e Calorimeter

- Baseline design : Cesium Iodine (CsI)
  - Radiation hard, fast, non-hygroscopic

	CsI
Density (g/cm3)	4.51
Radiation length (cm)	1.86
Moliere Radius (cm)	3.57
Interaction length (cm)	39.3
dE/dX (MeV/cm)	5.56
Refractive index	1.95
Peak luminescence (nm)	310
Decay time (ns)	26
Light yield (rel. to NaI)	3.6%
Variation with temperature	-1.4% / deg-C

Mu2e Calorimeter

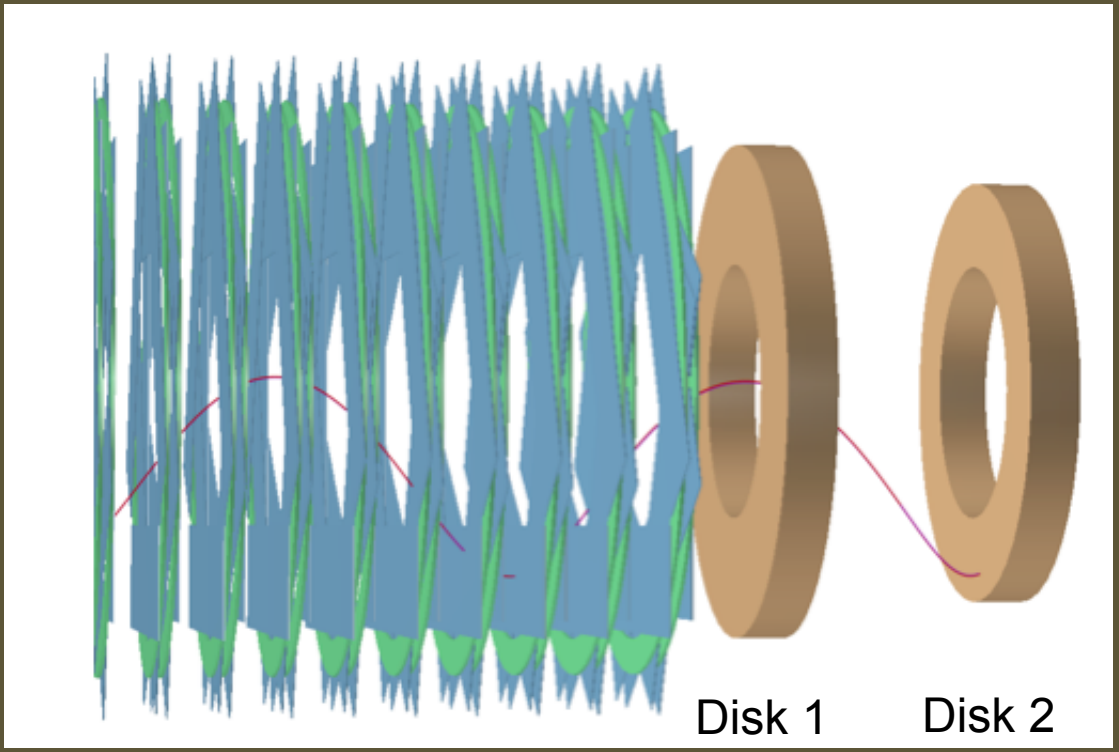

- Will employ 2 disks (radius = 36-70 cm)
- ~1900 crystals with square cross-section
  - ~3 cm diameter, ~20 cm long (10 X_0)
- Two photo-sensors/crystal on back (SiPMs)

Mu2e Calorimeter

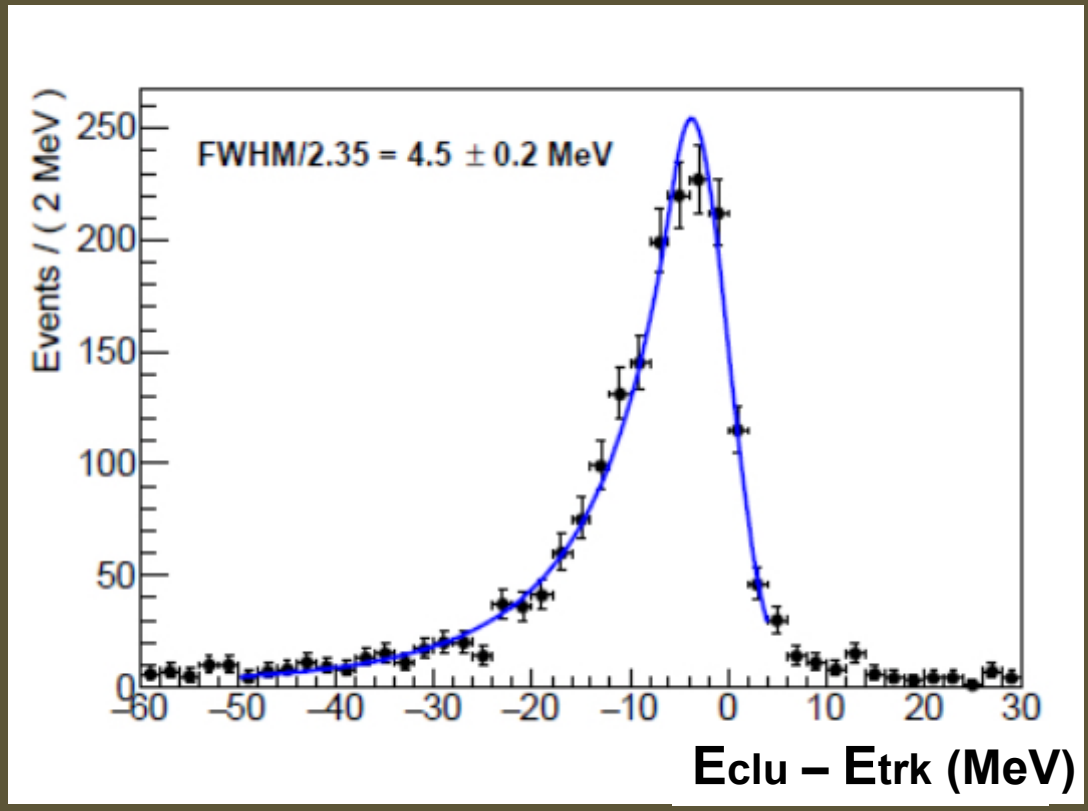

- With 60 ns integration, expect to achieve an energy resolution ~5% for 105 MeV electrons
  - Performance a weak function of rate in relevant range

Calorimeter Particle ID

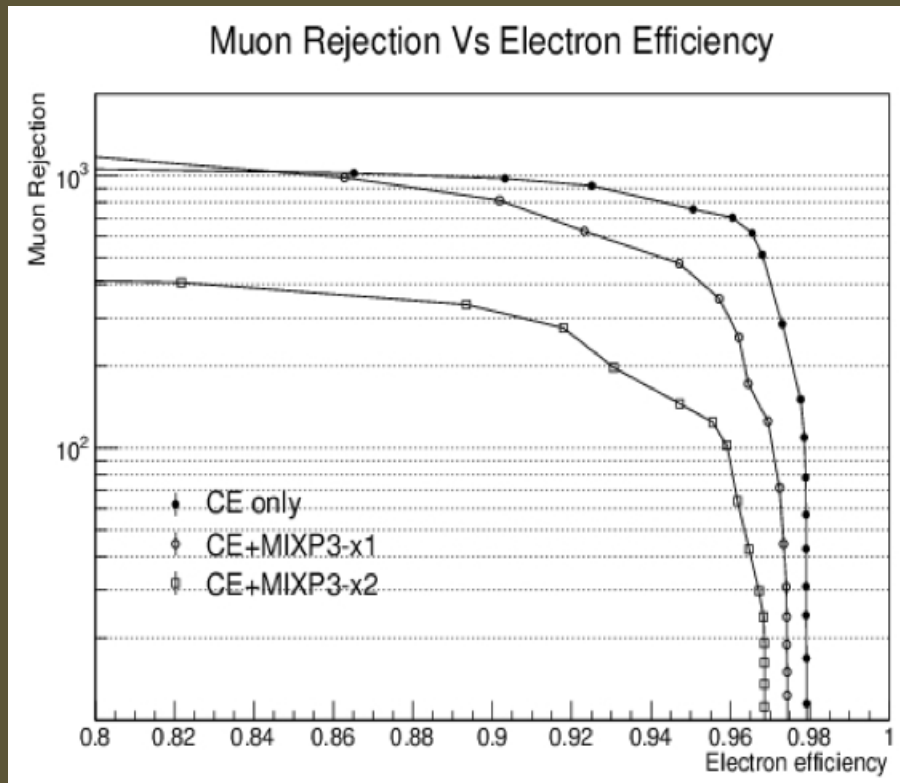

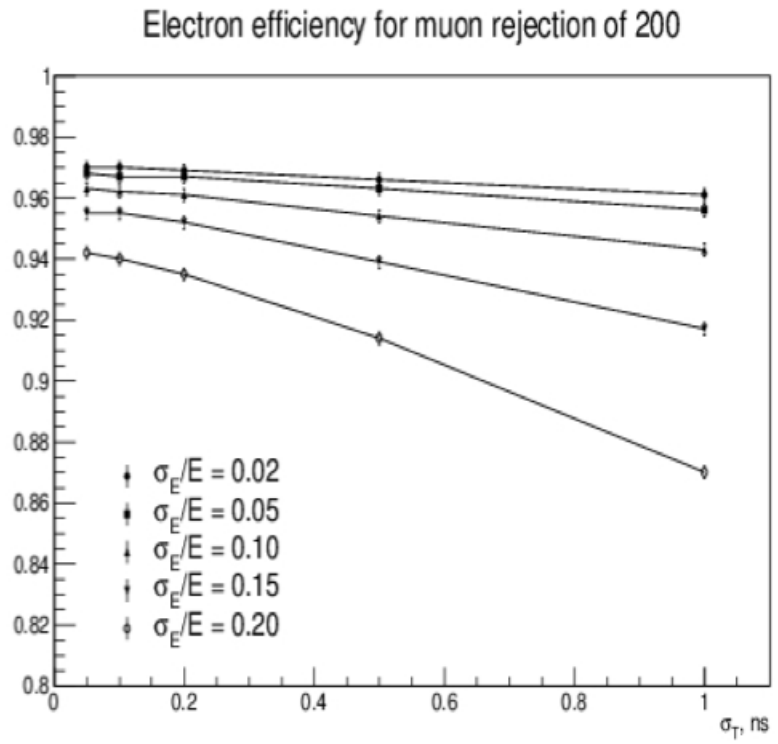

- Combine TOF and E/P information in LLR
  - 96% electron efficiency for muon rejection x200

Mu2e Cosmic-Ray Veto

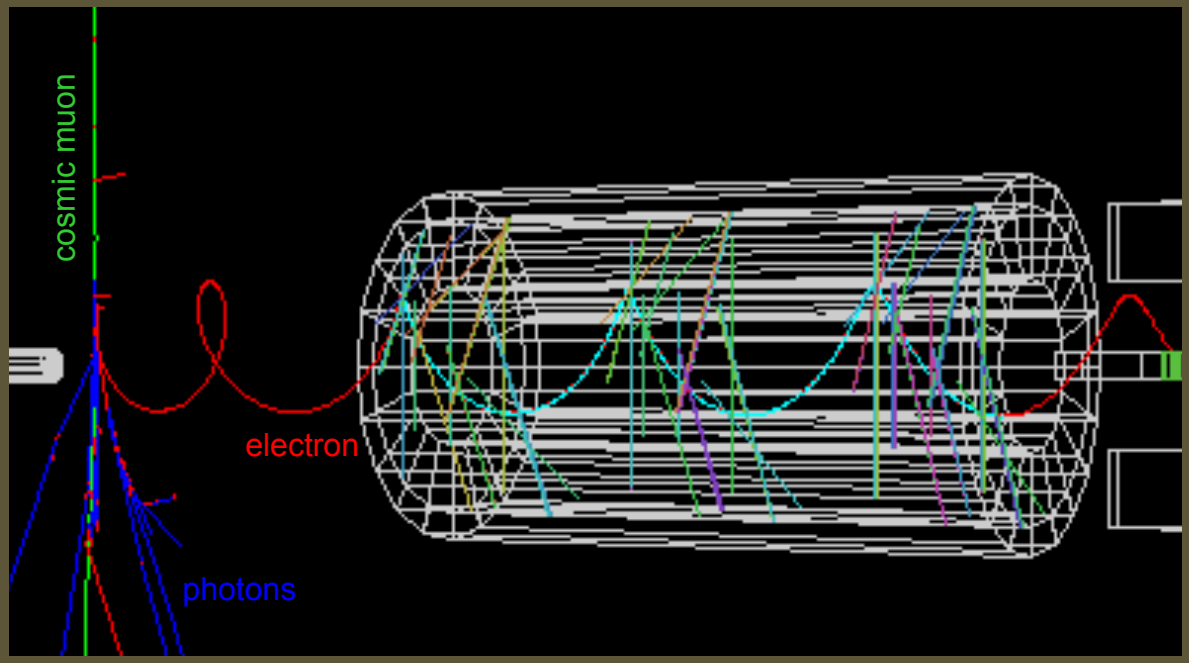

- Cosmic μ can generate background events via decay, scattering, or material interactions

Mu2e Cosmic-Ray Veto

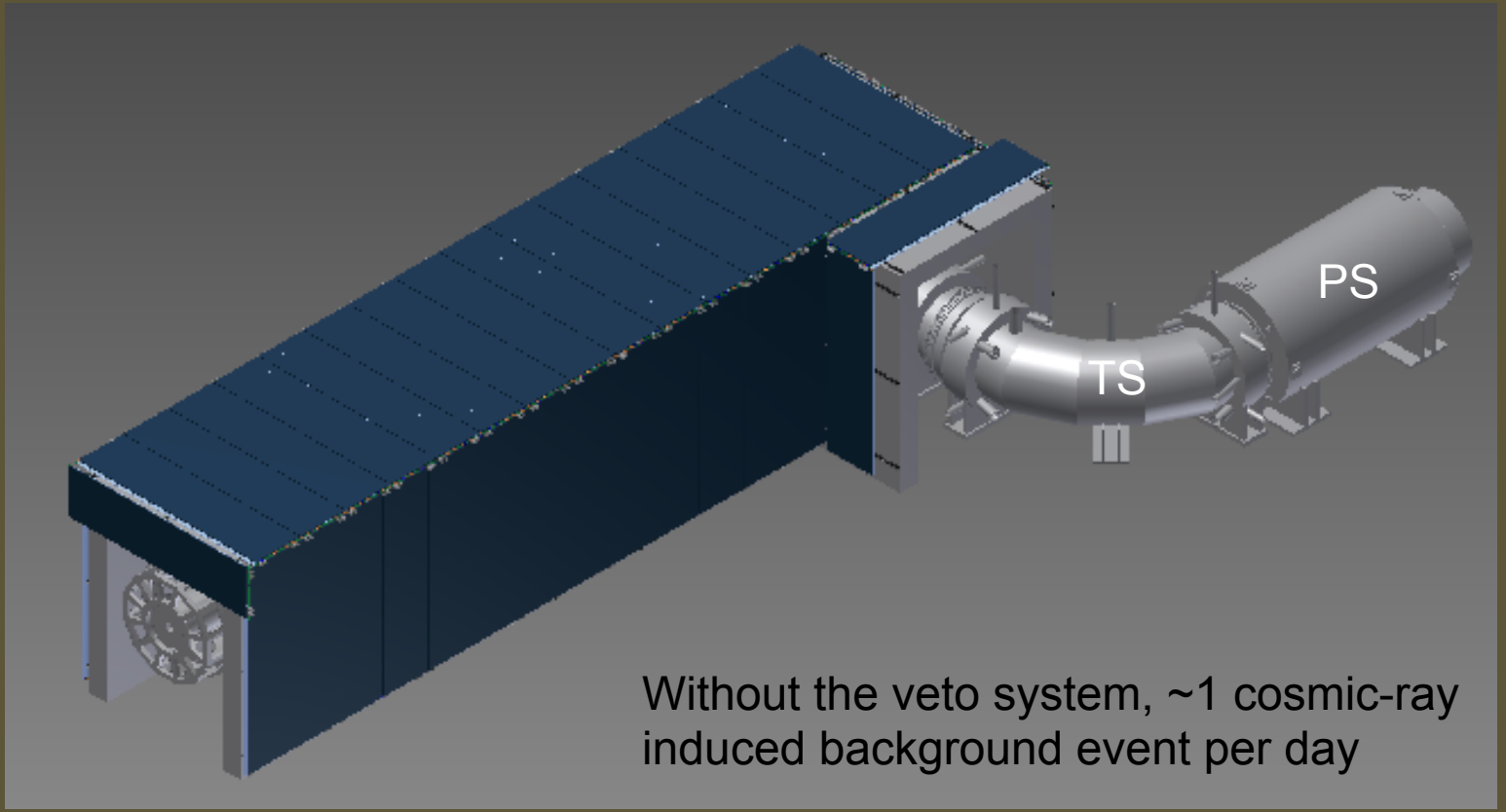

- Veto system covers entire DS and half TS

Mu2e Cosmic-Ray Veto

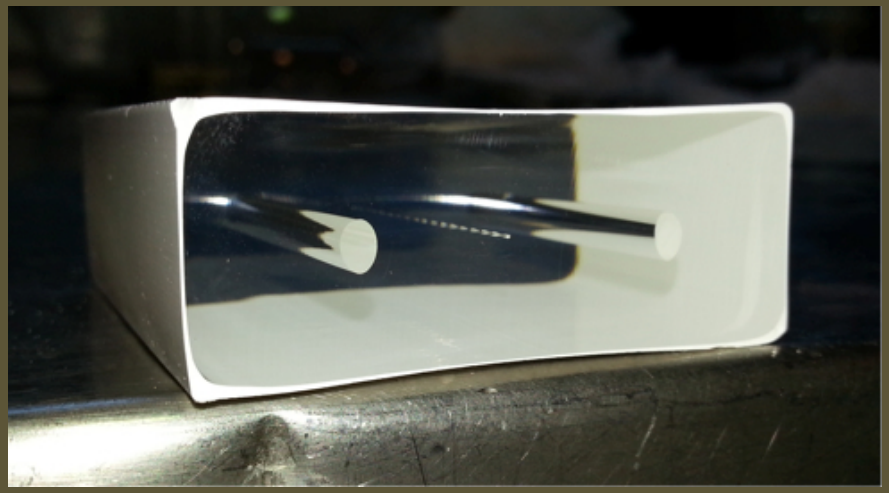

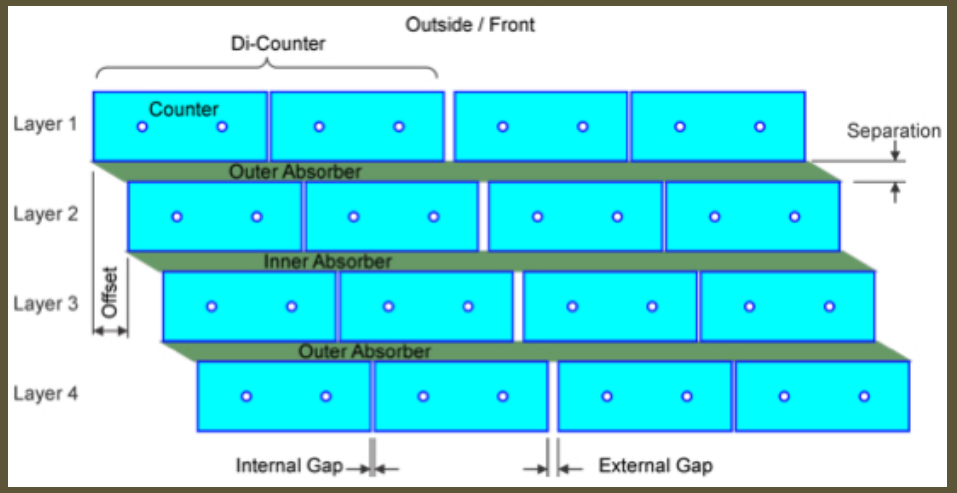

- Will use 4 overlapping layers of scintillator
  - Each bar is 5 x 2 x ~450 cm^3
  - 2 WLS fibers / bar
  - Read-out both ends of each fiber with SiPM
  - Have achieved $\varepsilon > 99.4\%$ (per layer) in test beam

Cosmic Ray Veto

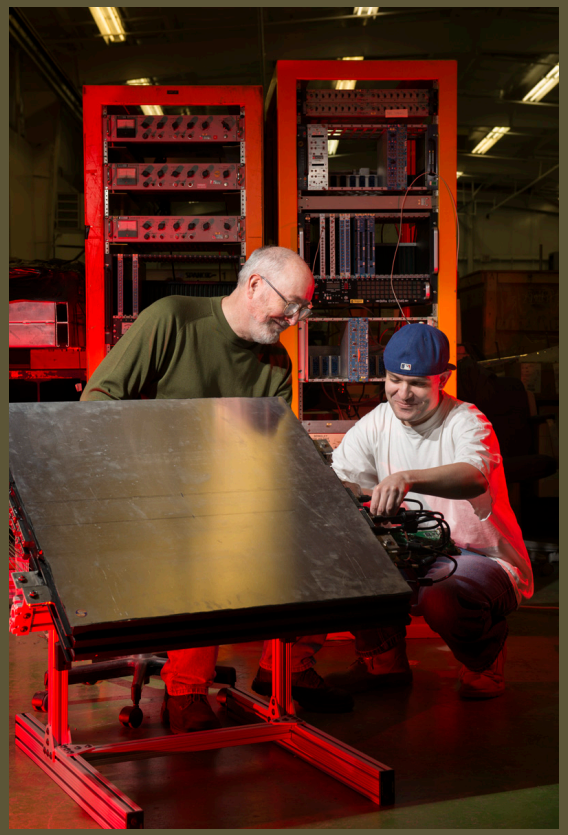

Typical light yield from CRV counter prototype – 20 cm from RO end

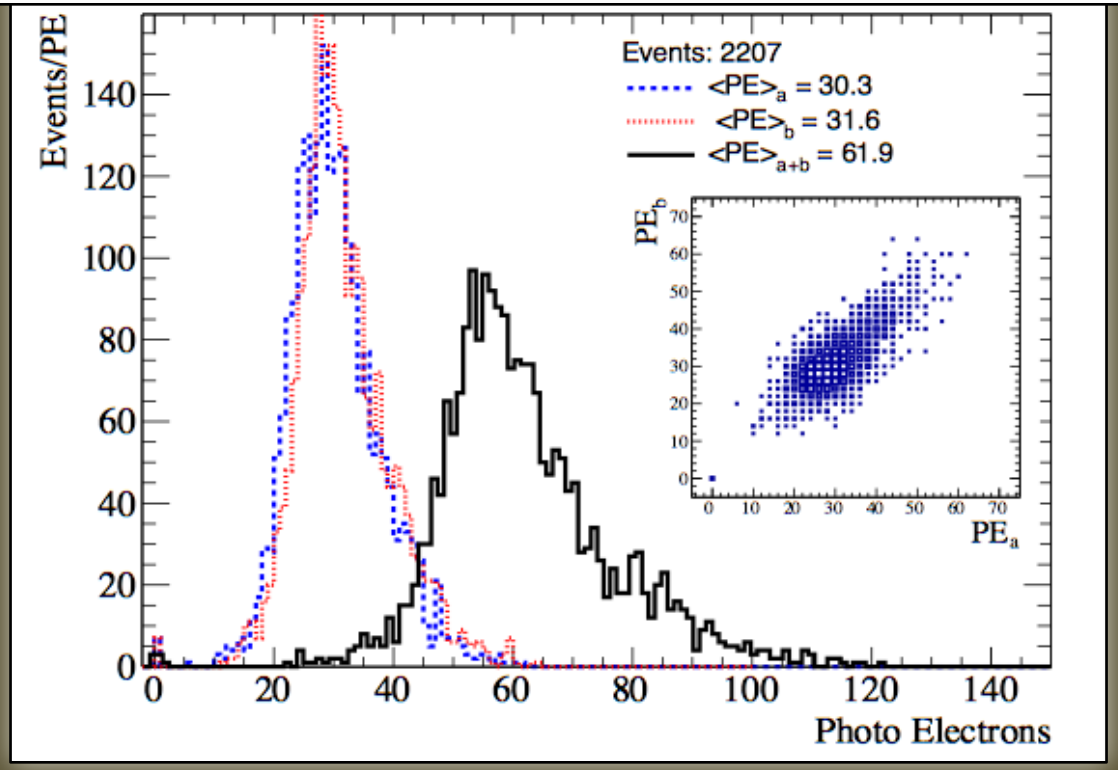

- Test beam data to vet design/performance

Selection Requirements

Parameter	Requirement
Track quality and background rejection criteria	
Kalman Fit Status	Successful Fit
Number of active hits	$N_{active} \geq 25$
Fit consistency	$\chi 2$ consistency $> 2 \times 10^{-3}$
Estimated reconstructed momentum uncertainty	$\sigma_p < 250$ keV/c
Estimated track t_0 uncertainty	$\sigma_t < 0.9$ nsec
Track t_0 (livegate)	700 ns $< t_0 <$ 1695 ns
Polar angle range (pitch)	$45° < \theta < 60°$
Minimum track transverse radius	-80 mm $< d_0 <$ 105 mm
Maximum track transverse radius	450 mm $< d_0 + 2/\omega <$ 680 mm
Track momentum	103.75 $< p <$ 105.0 MeV/c
Calorimeter matching and particle identification criteria	
Track match to a calorimeter cluster	$E_{cluster} > 10$ MeV $\chi 2$ (track-calo match) < 100
Ratio of cluster energy to track momentum	$E/P < 1.15$
Difference in track t_0 to calorimeter t_0	$\Delta t = \lvert t_{track} - t_{calo} \rvert < 3$ ns from peak
Particle identification	$\log(L(e)/L(\mu)) < 1.5$

- Full set of selection criteria employed to estimate backgrounds and sensitivity reported in TDR (Summer 2014)

Systematic Uncertainties

Effect	Uncertainty in DIO background yield	Uncertainty in CE single-event-sensitivity ($\times 10^{-17}$)
MC Statistics	±0.02	±0.07
Theoretical Uncertainty	±0.04	-
Tracker Acceptance	±0.002	±0.03
Reconstruction Efficiency	±0.01	±0.15
Momentum Scale	+0.09, -0.06	±0.07
μ-bunch Intensity Variation	±0.007	±0.1
Beam Flash Uncertainty	±0.011	±0.17
μ-capture Proton Uncertainty	±0.01	±0.016
μ-capture Neutron Uncertainty	±0.006	±0.093
μ-capture Photon Uncertainty	±0.002	±0.028
Out-Of-Target μ Stops	±0.004	±0.055
Degraded Tracker	-0.013	+0.191
Total (in quadrature)	+0.10, -0.08	+0.35, -0.29

- Evaluated for all background sources

Mu2e Proton Timing

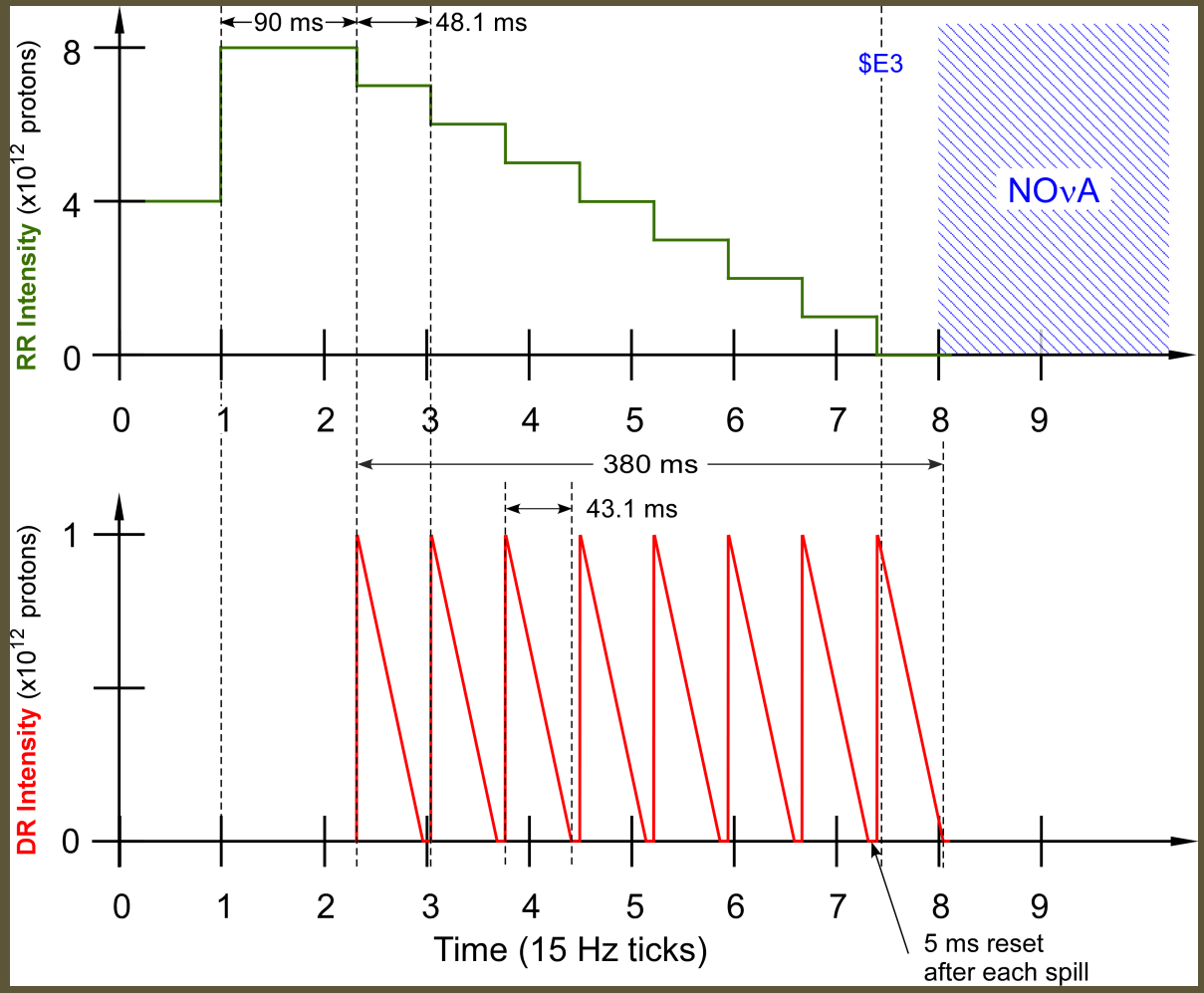

- Mu2e will run simultaneously with NOvA, BNB, etc.

Tracker Occupancy

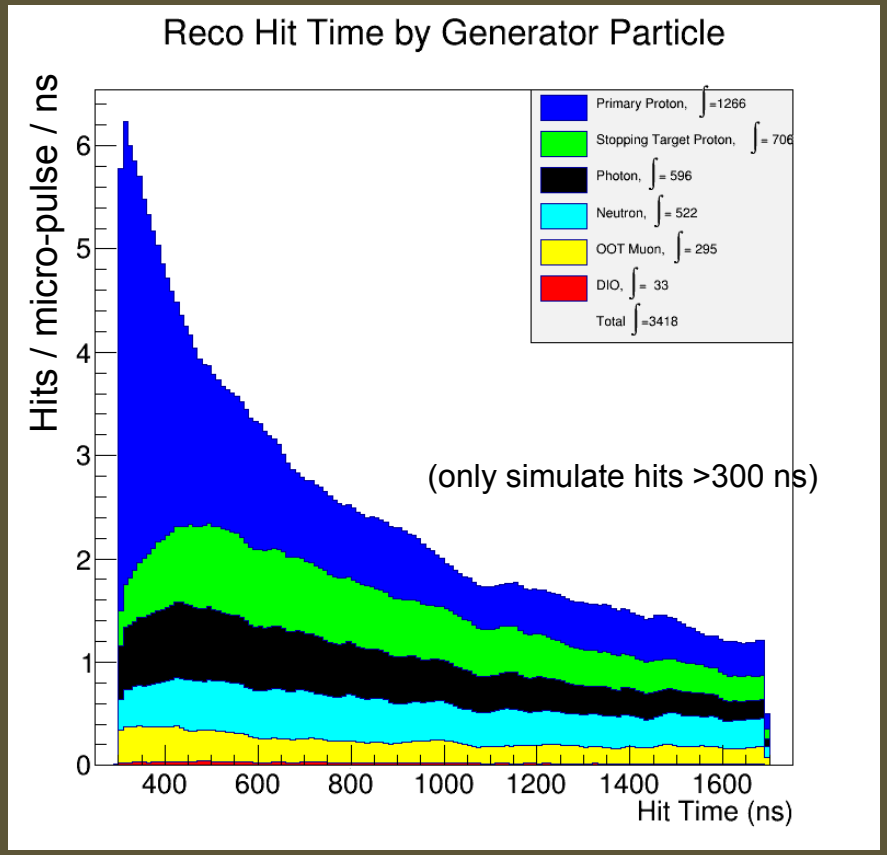

- Accidental occupancy from beam flash, μ capture products, out-of-target μ stops, etc.

Signal Momentum Spectrum

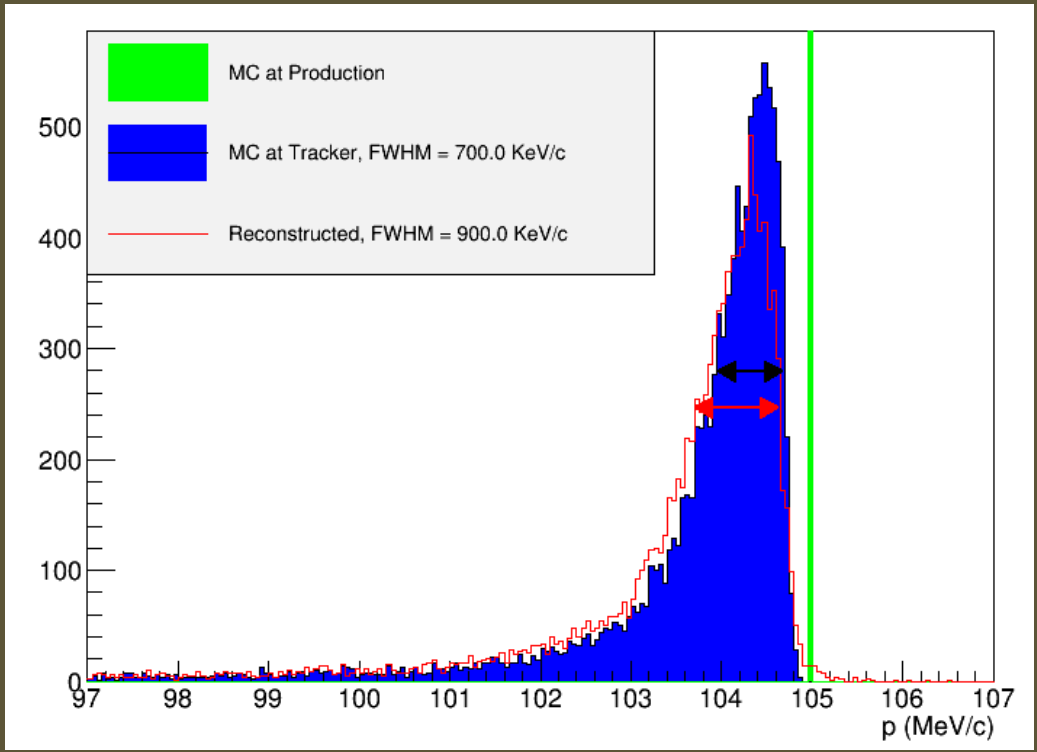

- Smearing dominated by interactions in stopping target and in (neutron/proton) absorbers upstream of tracker

False vetoes in CRV

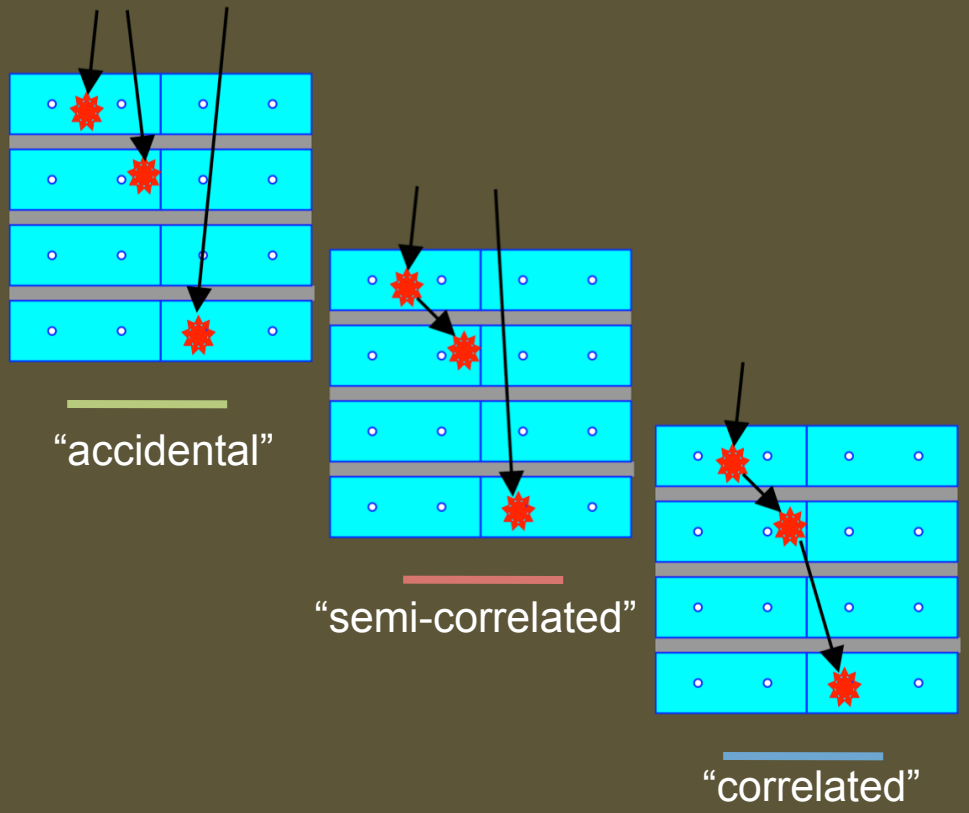

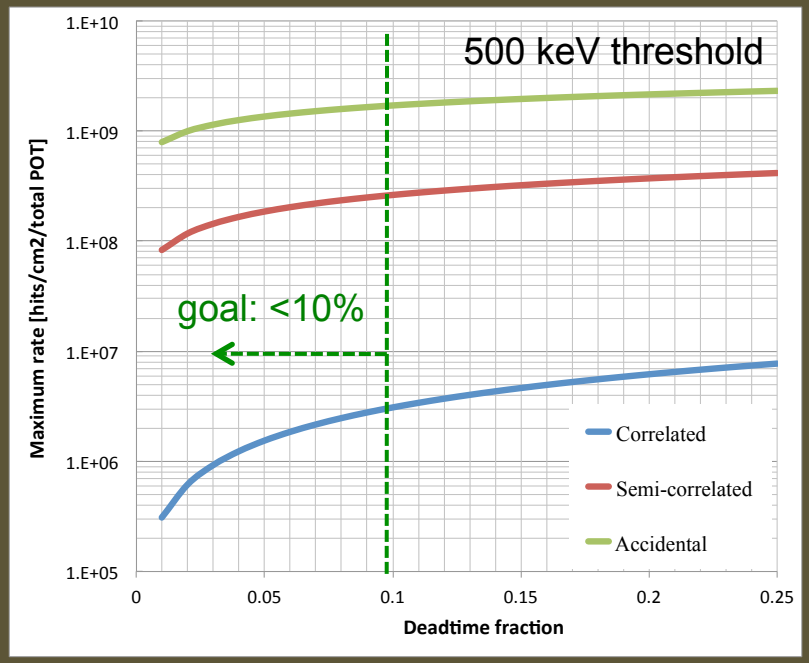

- We need to understand contributions from accidentals and correlated-accidentals
  - For neutrons and photons as a function of time, energy, timing resolution, and read-out threshold

Estimated dead time from CRV vetos – dominated by n/γ background

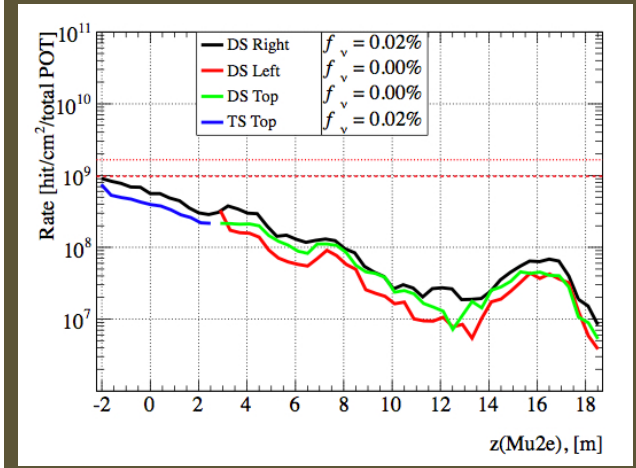

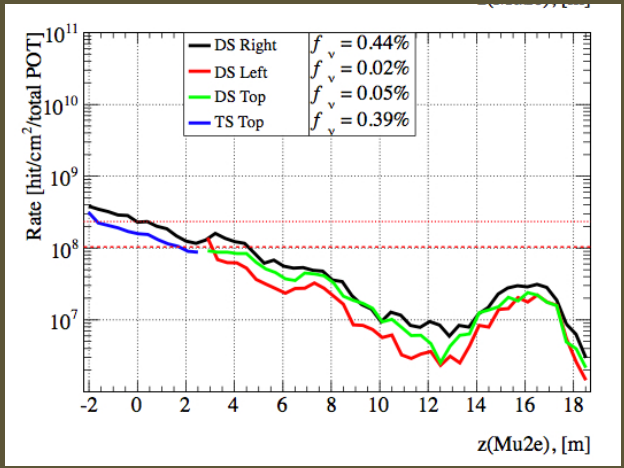

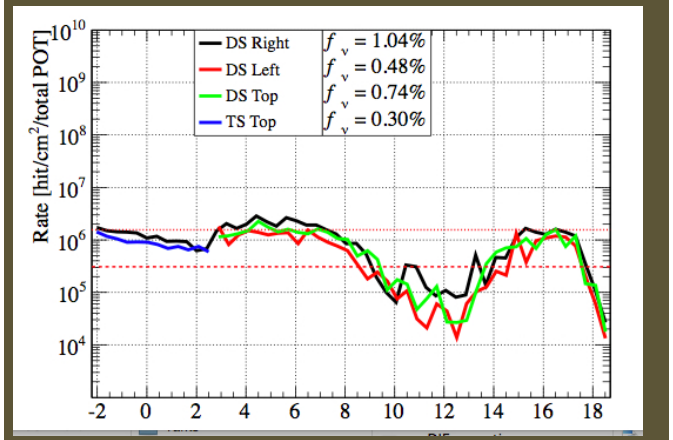

accidental semi-correlated correlated

- Total dead time from neutron/photon "noise" = 5%
  - For 500 keV readout threshold
  - Increasing to 1 MeV reduces to 2%
  - Cross-check with a separate physics generator (MARS) yields dead time within 50%

Muon momentum distribution

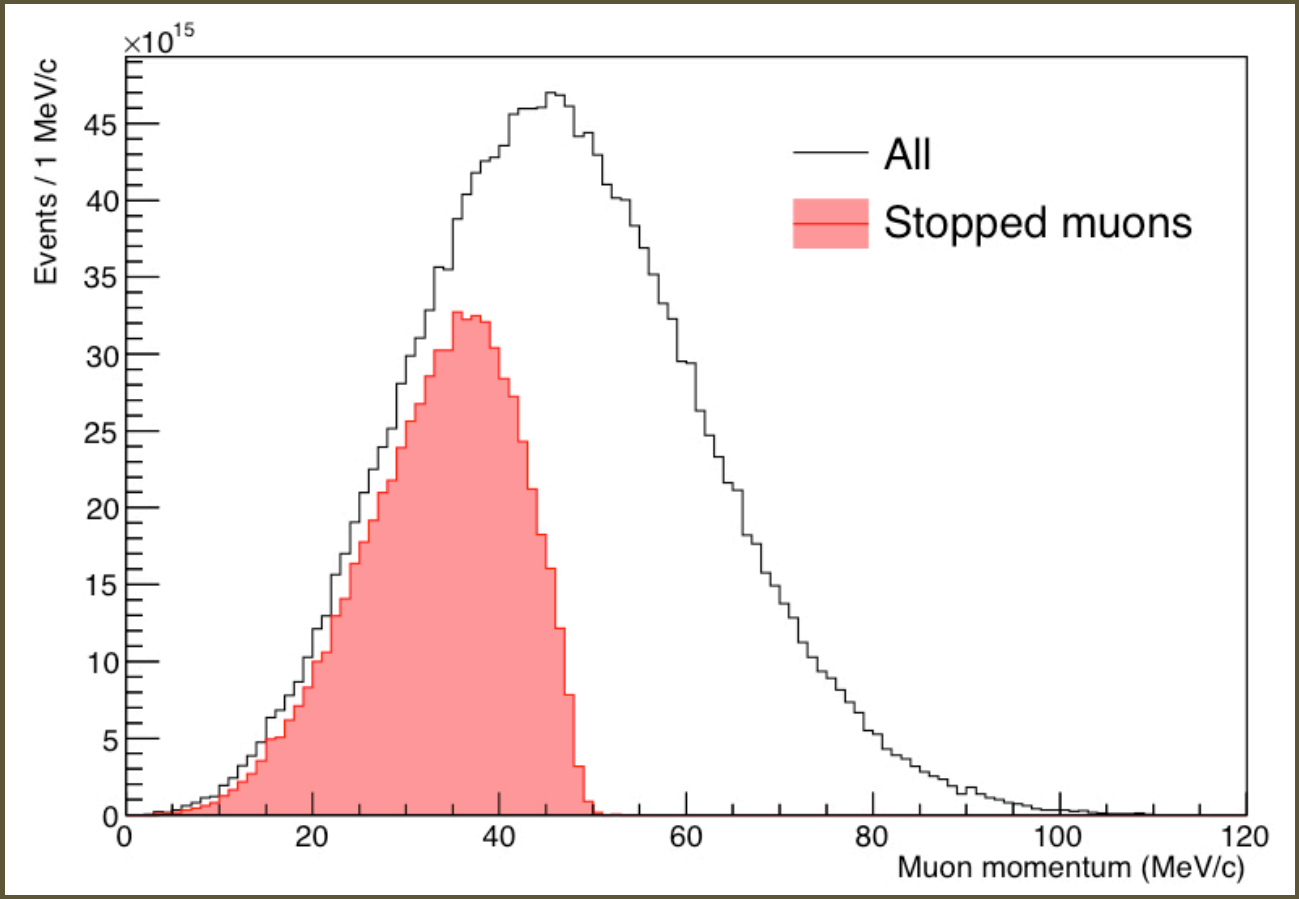

- The muons that stop are low momentum

As a function of Z

- Things change

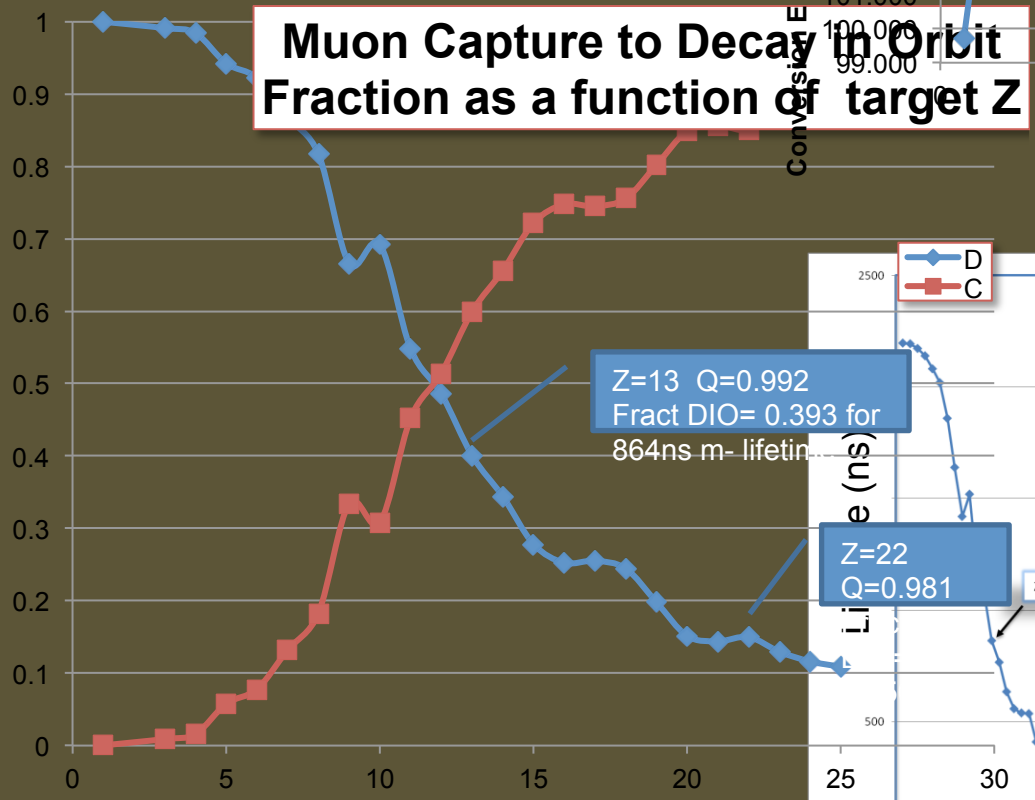

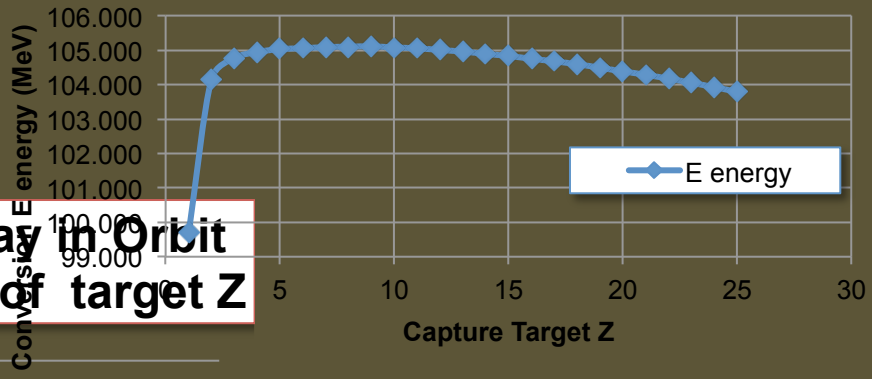

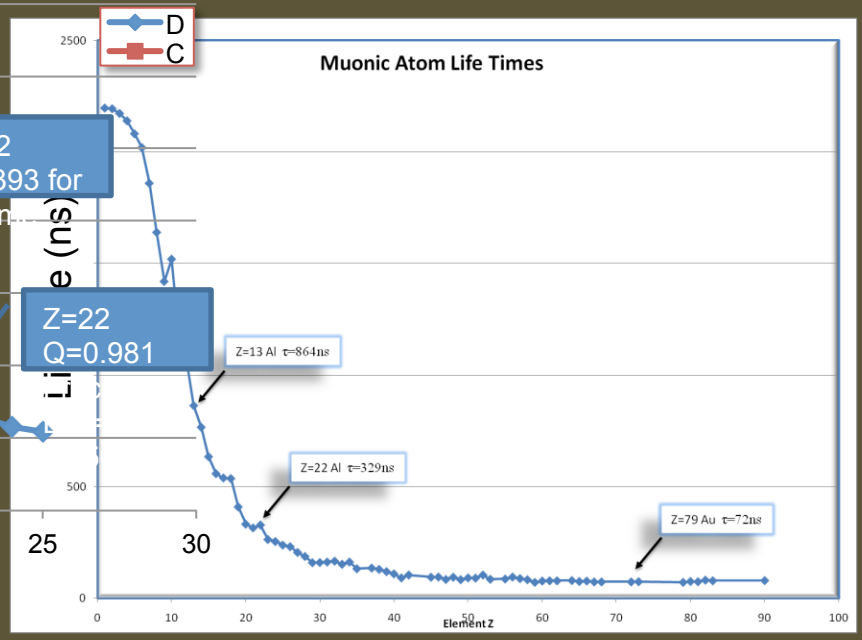

LHCb $\tau \to \mu\mu\mu$ Results

Table 1: Terms entering into the normalisation factors, α, and their combined statistical and systematic uncertainties.

	7 TeV	8 TeV
$\mathcal{B}(D_s^- \to \phi(\mu^+\mu^-)\pi^-)$	$(1.32 \pm 0.10) \times 10^{-5}$	
$\mathcal{B}(D_s^- \to \tau^-\bar{\nu}_\tau)$	$(5.61 \pm 0.24) \times 10^{-2}$	
$f_\tau^{D_s}$	0.78 ± 0.04	0.80 ± 0.03
$\epsilon_{\rm cal}{}^{\rm R}/\epsilon_{\rm sig}{}^{\rm R}$	0.898 ± 0.060	0.912 ± 0.054
$\epsilon_{\rm cal}{}^{\rm T}/\epsilon_{\rm sig}{}^{\rm T}$	0.659 ± 0.006	0.525 ± 0.040
$N_{\rm cal}$	$28\,200 \pm 440$	$52\,130 \pm 700$
α	$(7.20 \pm 0.98) \times 10^{-9}$	$(3.37 \pm 0.50) \times 10^{-9}$

$$\mathcal{B}(\tau^- \to \mu^-\mu^+\mu^-) = \frac{\mathcal{B}(D_s^- \to \phi(\mu^+\mu^-)\pi^-)}{\mathcal{B}(D_s^- \to \tau^-\bar{\nu}_\tau)} \times f_\tau^{D_s} \times \frac{\epsilon_{\rm cal}^{\rm R}}{\epsilon_{\rm sig}^{\rm R}} \times \frac{\epsilon_{\rm cal}^{\rm T}}{\epsilon_{\rm sig}^{\rm T}} \times \frac{N_{\rm sig}}{N_{\rm cal}} \equiv \alpha N_{\rm sig} ,$$

Table 3: Expected background candidate yields in the 8 TeV data set, with their uncertainties, and observed candidate yields within the τ^- signal window in the different bins of classifier response. The classifier responses range from 0 (most background-like) to +1 (most signal-like). The first bin in each classifier response is excluded from the analysis.

$\mathcal{M}_{\text{PID}}$ response	$\mathcal{M}_{\text{3body}}$ response	Expected	Observed
	0.26 – 0.34	39.6 ± 2.3	39
	0.34 – 0.45	32.2 ± 2.1	34
	0.45 – 0.61	28.7 ± 2.0	28
0.40 – 0.54	0.61 – 0.70	9.7 ± 1.2	5
	0.70 – 0.83	11.4 ± 1.3	7
	0.83 – 0.94	7.3 ± 1.1	6
	0.94 – 1.00	6.0 ± 1.0	0
	0.26 – 0.34	13.6 ± 1.4	8
	0.34 – 0.45	12.1 ± 1.3	12
	0.45 – 0.61	8.3 ± 1.0	13
0.54 – 0.61	0.61 – 0.70	2.60 ± 0.62	1
	0.70 – 0.83	1.83 ± 0.60	5
	0.83 – 0.94	2.93 ± 0.72	6
	0.94 – 1.00	2.69 ± 0.63	3
	0.26 – 0.34	13.5 ± 1.4	7
	0.34 – 0.45	10.9 ± 1.2	11
	0.45 – 0.61	9.7 ± 1.2	12
0.61 – 0.71	0.61 – 0.70	3.35 ± 0.69	2
	0.70 – 0.83	4.60 ± 0.89	5
	0.83 – 0.94	4.09 ± 0.81	4
	0.94 – 1.00	2.78 ± 0.68	1
	0.26 – 0.34	7.8 ± 1.1	6
	0.34 – 0.45	7.00 ± 0.99	8
	0.45 – 0.61	6.17 ± 0.95	6
0.71 – 0.80	0.61 – 0.70	1.57 ± 0.56	2
	0.70 – 0.83	2.99 ± 0.72	0
	0.83 – 0.94	3.93 ± 0.81	0
	0.94 – 1.00	3.22 ± 0.68	1
	0.26 – 0.34	5.12 ± 0.86	3
	0.34 – 0.45	4.44 ± 0.79	6
	0.45 – 0.61	3.80 ± 0.78	5
0.80 – 1.00	0.61 – 0.70	2.65 ± 0.68	2
	0.70 – 0.83	3.05 ± 0.67	2
	0.83 – 0.94	1.74 ± 0.54	2
	0.94 – 1.00	3.36 ± 0.70	3

LHCb $\tau \to \mu\mu\mu$ Results ($2fb^{-1}$ @ 8TeV)

Data are consistent with Background expectations

Table 2: Expected background candidate yields in the 7 TeV data set, with their uncertainties, and observed candidate yields within the τ^- signal window in the different bins of classifier response. The classifier responses range from 0 (most background-like) to +1 (most signal-like). The first bin in each classifier response is excluded from the analysis.

$\mathcal{M}_{\rm PID}$ response	$\mathcal{M}_{\rm 3body}$ response	Expected	Observed
0.40 – 0.45	0.28 – 0.32	3.17 ± 0.66	4
	0.32 – 0.46	9.2 ± 1.1	6
	0.46 – 0.54	2.89 ± 0.63	6
	0.54 – 0.65	3.17 ± 0.66	4
	0.65 – 0.80	3.64 ± 0.72	2
	0.80 – 1.00	3.79 ± 0.80	3
0.45 – 0.54	0.28 – 0.32	4.22 ± 0.78	6
	0.32 – 0.46	8.3 ± 1.1	10
	0.46 – 0.54	2.3 ± 0.57	4
	0.54 – 0.65	2.83 ± 0.63	8
	0.65 – 0.80	2.72 ± 0.69	5
	0.80 – 1.00	4.83 ± 0.90	7
0.54 – 0.63	0.28 – 0.32	2.33 ± 0.58	6
	0.32 – 0.46	8.3 ± 1.1	8
	0.46 – 0.54	2.07 ± 0.53	1
	0.54 – 0.65	3.29 ± 0.68	1
	0.65 – 0.80	2.96 ± 0.65	4
	0.80 – 1.00	3.11 ± 0.69	3
0.63 – 0.75	0.28 – 0.32	2.69 ± 0.62	1
	0.32 – 0.46	7.5 ± 1.0	5
	0.46 – 0.54	2.06 ± 0.53	3
	0.54 – 0.65	2.00 ± 0.55	5
	0.65 – 0.80	3.16 ± 0.66	2
	0.80 – 1.00	4.67 ± 0.84	2
0.75 – 1.00	0.28 – 0.32	2.19 ± 0.55	2
	0.32 – 0.46	3.38 ± 0.76	5
	0.46 – 0.54	1.52 ± 0.46	3
	0.54 – 0.65	1.28 ± 0.47	1
	0.65 – 0.80	2.78 ± 0.65	1
	0.80 – 1.00	4.42 ± 0.83	7

LHCb $\tau \to \mu\mu\mu$ Results ($1fb^{-1}$ @ 7TeV)

Data are consistent with Background expectations